Role of miR-592 and miR-204 in medulloblastoma pathogenesis

By

Raikamal Paul

LIFE09201304012

Tata Memorial Centre, Mumbai

A thesis submitted to the

Board of Studies in Life Sciences

In partial fulfillment of requirements
for the Degree of

DOCTOR OF PHILOSOPHY

Of

HOMI BHABHA NATIONAL INSTITUTE

December, 2020

Homi Bhabha National Institute

Recommendations of the Viva Voce Committee

As members of the Viva Voce Committee, we certify that we have read the dissertation prepared by Ms. Raikamal Paul entitled "**Role of miR-592 and miR-204 in medulloblastoma pathogenesis** " and recommend that it may be accepted as fulfilling the thesis requirement for the award of Degree of Doctor of Philosophy.

Chairperson – Dr. Rajiv Sarin Date: 30/12/2020

Guide/Convener – Dr. Neelam Shirsat Date: 30/12/2020

30/12/2020

External Examiner – Dr. Suvendra N. Bhattacharyya Date:

30/12/2020

Member – Dr. Abhijit De Date:

Member -Dr Rukmini Govekar Date: 01/01/2021

Final approval and acceptance of this thesis is contingent upon the candidate's submission of the final copies of the thesis to HBNI.

I hereby certify that I have read this thesis prepared under my direction and recommend that it may be accepted as fulfilling the thesis requirement.

Date:

Place: Navi Mumbai

Dr. .....

Guide

STATEMENT BY AUTHOR

This dissertation has been submitted in partial fulfillment of requirements for an advanced degree at Homi Bhabha National Institute (HBNI) and is deposited in the Library to be made available to borrowers under rules of the HBNI.

Brief quotations from this dissertation are allowable without special permission, provided that accurate acknowledgement of source is made. Requests for permission for extended quotation from or reproduction of this manuscript in whole or in part may be granted by the Competent Authority of HBNI when in his or her judgment the proposed use of the material is in the interests of scholarship. In all other instances, however, permission must be obtained from the author.

Raikamal Paul

DECLARATION

I, hereby declare that the investigation presented in the thesis has been carried out by me. The work is original and has not been submitted earlier as a whole or in part for a degree / diploma at this or any other Institution / University.

Raikamal Paul

Publications from the study:

1. Published (joint first author): Downregulation of miR-204 expression defines a highly aggressive subset of Group 3 / Group 4 medulloblastomas .Harish Shrikrishna Bharambe[#], Raikamal Paul[#], Pooja Panwalkar[#], Rakesh Jalali, Epari Sridhar, Tejpal Gupta, Aliasgar Moiyadi, Prakash Shetty, Sadaf Kazi, Akash Deogharkar, Shalaka Masurkar, Kedar Yogi, Ratika Kunder, Nikhil Gadewal, Atul Goel, Naina Goel, Girish Chinnaswamy, Vijay Ramaswamy[*] and Neelam Vishwanath Shirsat[*] Acta Neuropathol Commun. 2019 Apr 3;7(1):52. doi: 10.1186/s40478-019-0697-3.

2. Published: Autophagy inhibition impairs the invasion potential of medulloblastoma cells. Raikamal Paul, Harish Shrikrishna Bharambe, Neelam Vishwanath Shirsat. Mol Biol Rep. 2020 Jul;47(7):5673-5680. doi: 10.1007/s11033-020-05603-3

3. Manuscript under preparation: MiR-592, a Group 4 specific microRNA, activates mTOR kinase by targeting DEPTOR in medulloblastoma. Raikamal Paul, Akash Deogharkar, Sadaf Kazi, Tejpal Gupta, Rakesh Jalali, Epari Sridhar, Aliasgar Moiyadi, Prakash Shetty, Neelam Vishwanath Shirsat.

Conferences Presented:

1. Presented a poster entitled 'Role of miR-592 in medulloblastoma biology' at the 8th Annual Conference of Indian Society of Neuro-Oncology held at HICC Hyderabad from 1 – 3 April, 2016.

2. Presented a poster entitled 'Role of microRNAs differentially expressed in Group 3, Group 4 medulloblastomas' at International Congress of Cell Biology 2018 organized by CCMB, Hyderabad from Jan 27-31st,2018.

3. Presented a poster entitled 'Role of differentially expressed microRNAs in Group 3, Group 4 medulloblastomas' at AACR Annual Meeting 2018 held at McCormick Place, Chicago, IL from 14th to 18th April, 2018.

4. Platform presentation on 'Role of microRNAs differentially expressed in non-WNT, non-SHH medulloblastomas' at the 14th National Research Scholars Meet organized by ACTREC and held at ACTREC on 3rd-4th December, 2018.

This thesis is dedicated to my lovely family and dear friends who I am blessed to have in my life.

Acknowledgement

I believe the journey of PhD is not just about acquiring a degree, but it is a self- development process that moulds you into a person with grit and perseverance to fulfil all your life goals and career aspirations. Therefore, I take this opportunity to thank everyone who has made me a better person and also played an instrumental role in making this journey fruitful and memorable.

First and foremost, I would like to sincerely thank my supervisor Dr. Neelam Shirsat for her support and guidance throughout the tenure. Her critical analysis, scientific thinking, 'eye for detail' and love for science is something I will always be in awe of. I wish I could have even half of her zeal and vigour. I thank her for always pushing me to do better and for always being there in times of difficulties. If ever I am able to do good science, it will be for Ma'am.

I would like to thank Dr. Sudeep Gupta (Director, ACTREC), Dr. Rajiv Sarin and Dr. S.V. Chiplunkar (Ex-Directors, ACTREC) for providing us excellent research and academic infrastructure. I would like to thank Dr. Prasanna Venkatraman (Deputy-Director, CRI) for her caring and supportive nature towards students. I would like to acknowledge my Doctoral committee members, Dr. Rajiv Sarin (Chairperson), Dr. Abhijit De and Dr. Rukmini Govekar for their intellectual insights, guidance and support throughout the tenure. I express my sincere thanks to our clinical collaborators Dr. Sridhar, Dr. Tejpal Gupta and Dr. Rakesh Jalali for providing us with the medulloblastoma tumour samples and also to the patients and their families for participating in the study.

I would like to specially acknowledge ACTREC for providing me with the fellowship and Department of Biotechnology (DBT) and Tata Memorial Centre (TMC) for providing the funds for the research work. I am grateful to Homi Bhabha National Institute (HBNI), Sam Mistry and Patel fellowship for providing me the financial support to present my work at an international conference.

This research work would not have been possible without the help and expertise of so many people. I would like to thank Mr. Uday Dandekar and all the CIR staff members. I would like to thank the staff and physicist of the radiation department, Vaishali ma'am, Tanuja ma'am and Jayraj sir of microscopy facility and all the personnel of the Laboratory Animal Facility for their help. I also thank Mr. Anand (IT facility), Mr. Munnoli, Ms. Swati and Ms. Mughda (Library), Ms. Aparna Bagwe, Ms. Ojaswini and Ms. Prema (SCOPE) for their assistance. Special thanks to Maya ma'am and Sharwari ma'am for efficiently handling all the administrative work.

These seven years of PhD wouldn't have been half as fun if not for the people of Shirsat Lab. They have really been a 'Family away from home'. I express my sincere gratitude to Anandji, Umesh ji and Sadaf for their excellent technical assistance. Anand ji has helped me with the RNA and protein extraction from the tumour tissues. Umesh ji has collected tumour tissues and made the tissue culture

resources available to us on time. Sadaf, my ‘bench-neighbour’ and dear friend has helped me with the molecular profiling of the medulloblastoma tumour tissues. She also taught me the basic cell culture assays with utmost precision. It was great to have wonderful seniors like Dr. Ratika Kunder, Dr. Kedar Yogi, Dr. Pooja Panwalkar, Dr. Satish Singh and Dr. Vijay Padul in the lab who helped me whenever I required it. A special thanks to Kedar for standardising the Boyden chamber invasion assay and orthotopic tumorigenicity experiments in the lab and showing us how to work methodically and in an organised manner. Pooja di has been of utmost help with the miR-204 study.

This journey has been all the more cherishable thanks to my colleagues in the lab. Shalaka, my batchmate and labmate, has contributed to this journey in ways I cannot thank enough. With her contagious enthusiasm and positivity, she has always been my guardian, dearest friend and a rock-solid support. Harish, the voracious worker, has also contributed significantly to this journey not only with his help with the experiments but also with his meticulous skills in making figures. As much as I look up to him as a colleague, I must say his fights and tantrums have been an absolute entertainment. Akash is an amazing colleague with his fine wit and keen intelligence and has wonderful teaching skills. I totally commend his way of handling the animals and thank him for carrying out the orthotopic tumorigenicity experiments. Purna, with her logical reasoning and rational thinking (which makes it impossible to win any arguments against her), is my forever go-to-person and never let me miss my sister back at home. I have also cherished every moment spent with Shweta, who is a composed and lovely person. Dr. Aditi and Dr. Annada also deserves special credit to maintain a cheerful environment in the lab. I would love to thank the trainees Sailee, Shivali, Rohan, Roshni, Sahana, Harshika, Shruti and Srilekha for their help and also for adding up to the fun quotient in the lab. I am going to miss everything about this lab including the sharing of dabba, evening chai, lab parties and discussing anything and everything under the sun. The way we have stood beside each other as a team is something I will always be proud of.

My batch JRF 2013 is one of a kind and I feel so blessed to meet them here. It is full of vibrant people from all over India and each one of them is unique in their own way. Ajay, Anuja, Asmita, Burhan, Dhanashree, Mahalaxmi, Mythreyi, Prathamesh, Pravin, Raghav, Raghupathi, Rahul, Rajashree, Shalaka, Shalini and Vasudha each of them has a special place in my heart. Special shout out to Ajay and Shalini for making my hostel days fun and always helping me lift my mood and enjoy the process. I will cherish my special bond with Burhan who has been a great companion all through this journey. I have always looked forward to our conversations about life and philosophy. I hope to keep in touch with all of them and cherish this friendship forever. My heartfelt thanks to Pratik, Asim and all the lab members of Prasanna lab, Teni lab, Bhattacharya lab, Gupta lab and Waghmare lab for lending reagents and equipments whenever in need.

My family have been my biggest strength throughout all these years. I thank Maa for loving me as much as she loves her own work and teaching me the values of commitment and sincerity. Baba has always shown me the spiritual side of life and by mere power of his words, he has given me the strength required to carry on this journey of PhD. I thank my younger sister Raadhika for bearing my absence and taking care of Maa, Baba and Dia all these years. I miss being with her during her growing up years but none the less it is an absolute joy to see what she has grown up to! My uncle and aunty whom I lovingly call Bunima and Mesho have been the source of joy during my initial years of PhD when I could visit them often in Borivali. My grandma Dia, has always kept herself updated with the progress of my work and has asked me when I will be going home at the end of every phone call! I am blessed to have in-laws who are extremely supportive and take pride in everything I do. I sincerely thank Baapi and Mamoni for being my saviour during the national lockdown imposed due to the pandemic. Last but not the least, words will fall short to thank my best friend and dear husband Sayantan, who has given me all kinds of support and always made sure that I have a lovely world outside the lab. He has pushed me to work harder and always been the pillar of strength. For all the cancelled plans and compromises he has made for me in this journey, I promise to live up to it and never let him down. All I am today is because of the love, prayers and blessings of my family.

I thank my friends Adrija, Snehasish, Pritha, Paulami, Ekta, Subhamoy and Mitali have always been there by my side and trusted me even when I lost faith in myself. I also thank Tania di and Bibaswan Sir who have made me love the subject and showed me how research was done long before I actually started doing it.

My sincere gratitude to the almighty God for keeping my loved ones safe and healthy in all these years and enabling me to carry out this entire journey with patience and enthusiasm.

- Raikamal Paul

Content

Summary and Conclusions

The role of two microRNAs, miR-592 and miR-204, that are differentially expressed in the two non-WNT, non-SHH medulloblastomas was investigated in detail. Group 3 and Group 4 subgroups share genetic alterations and expression profiles but are distinct in their clinical behavior. Despite the extensive genomic analysis of these two subgroups, the molecular mechanism underlying the pathogenesis of these two tumor types is poorly understood, and there is a paucity of prognostication markers for accurate risk stratification.

The expression profiles of miR-592 and miR-204 were studied in a large cohort of 260 medulloblastomas from the Tata Memorial Centre and correlated with the clinical parameters: metastasis and overall survival. These findings were validated in an independent large western cohort of 763 medulloblastomas. Furthermore, the functional role of the two microRNAs was investigated by studying the effect of their expression on growth and malignant behavior of multiple medulloblastoma cell lines. The molecular mechanism underlying their tumor-suppressive effect on medulloblastoma cells was deciphered by identifying the genes and signaling pathways targeted by the two microRNAs. The salient findings of the study are given below.

- MiR-592 is overexpressed in 95% of the Group 4 medulloblastomas, which is almost 100-fold higher than the expression in the other subgroups and normal cerebellar tissues. Thus, it acts as a surrogate marker for Group 4 tumors, which have much better survival than Group 3 tumors.

- The expression of miR-592 brought about a reduction in the anchorage-independent growth, invasion potential, and tumorigenic potential of the Group 3 medulloblastoma cell lines, although it did not affect their proliferation, radiation sensitivity, or chemosensitivity.

- DEPTOR and EML1 genes were identified as novel direct targets of miR-592. Consistent with this finding, these genes are expressed at lower levels in Group 4 medulloblastomas as compared to Group 3 tumors, as analyzed in a large cohort of medulloblastomas.

- DEPTOR is an endogenous inhibitor of mTOR kinase. MiR-592 mediated downregulation of DEPTOR upregulated the activities of both mTORC1 and mTORC2 complexes in medulloblastoma cells. This finding is consistent with a recent phosphoproteomic study showing activation of mTOR signaling pathway in Group 4 medulloblastomas. Thus, miR-592 could contribute to the activation of mTOR pathway by targeting DEPTOR in Group 4 tumors, thereby contribute to their pathogenesis.

- MiR-592 also activated the feedback loop of mTORC1 that inhibited the activity of AKT kinase as judged by the reduction in the levels of the active form of AKT kinase and its target protein. The reduction in the AKT kinase activity is likely to decrease the malignant potential of the tumors, as is evident from the tumor-suppressive activity of miR-592 in medulloblastoma cells. MiR-592, thus, is likely to contribute to the indolent nature and much better survival rates of Group 4 medulloblastomas.

- Interestingly, miR-592 expression resulted in the upregulation of several neuronal differentiation-related genes, a characteristic of Group 4 tumors, in Group 3 medulloblastoma cell lines. MiR-592 distinguishes Group 4 tumors from Group 3 tumors, the two tumor types that overlap in expression profile and genetic alterations. The expression of miR-592 giving Group 4 characteristics to Group 3 cell lines is consistent with the continuum of Group 3, Group 4 tumors, as has now been accepted universally.

- MiR-592 mediated activation of mTOR signaling, and MAPK signaling was found to be instrumental in upregulating neuronal differentiation-related genes in Group 3

medulloblastoma cell lines as evident from the loss of their expression upon treatment with inhibitors of mTOR and MAPK signaling.

- Thus, miR-592, a Group 4 specific microRNA, plays a crucial role in pathogenesis by targeting DEPTOR, EML1, by upregulating mTOR and MAPK kinase activity and by imparting characteristic neuronal differentiation signature to Group 4 medulloblastomas.

- MiR-204, a known tumor-suppressive microRNA, is differentially expressed in Group 3, Group 4 tumors, and downregulation of its expression correlated with poor survival in a combined cohort as well as in individual Group 3 and Group 4 medulloblastomas. These findings were validated in a large western cohort of 763 medulloblastomas as well. Thus, miR-204 is a useful prognostication marker in the non-WNT, non-SHH medulloblastomas, particularly in Group 4, which lacks markers for accurate risk stratification.

- Restoration of MiR-204 expression inhibited the anchorage-independent growth, invasion potential, and increased radiation sensitivity of medulloblastoma cells. Downregulation of miR-204 expression correlating with poor survival, therefore, is likely to be due to higher malignant potential and poor response to treatment.

- The tumor-suppressive effect of miR-204 was found to be accompanied by inhibition of basal autophagy in medulloblastoma cells by targeting LC3B, an autophagy regulator. Inhibition of autophagy upon shRNA mediated downregulation of ATG5, a key upstream regulator of autophagy, did not affect proliferation or anchorage-independent growth of medulloblastoma cells. Autophagy inhibition, however, resulted in the reduction in the invasion potential of medulloblastoma cells. Thus, miR-204 mediated inhibition of invasion potential of medulloblastoma cells is likely to be due to autophagy inhibition.

- The study, for the first time, showed the role of autophagy in the invasion potential of medulloblastoma cells and indicated the therapeutic potential of autophagy inhibitors in the treatment of medulloblastomas.

Significance of the study

- This is the first study that has correlated microRNA expression with survival in a molecularly classified two large cohorts of medulloblastomas.

- MiR-592 was identified as a molecular marker for Group 4 medulloblastoma that can be included in the routine clinical practice of molecular classification of medulloblastomas.

- The study delineated the role of miR-592 in the pathogenesis of Group 4 tumors identifying the crucial role of mTOR signaling and MAPK signaling in the biology of this tumor type.

- MiR-204 was identified as a prognostication marker for accurate risk-stratification in Group 3, Group 4 medulloblastomas, based on the clinical correlation study done on an Indian cohort and an independent large western cohort.

- The tumor-suppressive effect of restoration of miR-204 expression accompanied by inhibition of autophagy in medulloblastoma cells indicates the therapeutic potential of miR-204 and autophagy inhibitors in the treatment of medulloblastomas.

टाटा स्मारक केंद्र
TATA MEMORIAL CENTRE

26692

कैंसर उपचार, अनुसंधान एवं शिक्षा का प्रगत केन्द्र
ADVANCED CENTRE FOR TREATMENT RESEARCH & EDUCATION IN CANCER

- CANCER RESEARCH INSTITUTE
- CLINICAL RESEARCH CENTRE
- CENTRE FOR CANCER EPIDEMIOLOGY

प. ऊ. वि.भारत सरकार का एक सहायता अनुदान प्राप्त संस्थान
A GRANT-IN-AID INSTITUTION OF THE DEPARTMENT OF ATOMIC ENERGY, GOVT OF INDIA

Date: 30.12.2020

To,
Dean HBNI,
B.A.R.C., Anushakti Nagar,
Mumbai – 400085

Sub: Certification for the Award of Ph.D. degree.

Dear Sir,

Ms. Raikamal Paul, (ACTREC, Enrollment No. LIFE09201304012; Year-2013) has been working under my guidance for HBNI Ph.D. program in Life Sciences. The topic of her thesis is "Role of miR-592 and miR-204 in medulloblastoma pathogenesis". Please find attached copies of the thesis evaluation reports received from the two external referees of the thesis. Both the examiners have recommended award of the Ph.D. degree. As there were no suggestions for any change in the thesis examined, the final thesis retains the same presentation details. The final Ph.D. *viva voce* of Ms. Raikamal Paul was held on 30.12.2020 in presence of the Doctoral Committee members and External Examiner Prof. Suvendra N. Bhattacharyya, Indian Institute of Chemical Biology (IICB), Kolkata over skype. The committee recommended the award of HBNI Ph.D. degree in Life Sciences to Ms. Raikamal Paul.

Recommendation of the viva voce committee with report of the final viva voce examination, thesis evaluation reports from the approved examiners, one hard copy and two soft copies (CDs) of the thesis and Abstract are included herewith for your kind perusal.

We request you to award HBNI Ph.D. degree in Life Sciences to Ms. Raikamal Paul

Dr. 30.12.2020
Neelam Shirsat
Guide & Convener)

Dr. .....
Rajiv Sarin
(Chairperson, Doctoral Committee)

Forwarded Through:

S. N. Dalal 4/1/2021
Dr. Sorab N Dalal,
Chairperson, Academic &
Training Programme, ACTREC

6/1/2021
Dr. S. D. Banavali,
Dean (Academics)
T.M.C.

PROF. S. D. BANAVALI, MD
DEAN (ACADEMICS)
TATA MEMORIAL CENTRE
MUMBAI – 400 012.

Cc: Dr. V. Prasanna – **Convener, Board of studies in** Life Sciences, HBNI
Email: **vprasanna@actrec.gov.in**

खारघर, नवी मुंबई - ४१० २१०, भारत.
दूरभाष : +९१-२२-२७४० ५०००
+९१-२२-३९२४ ५०००
फैक्स : +९१-२२- २७४० ५०८५

जल्द इलाज होने पर कैंसर ठीक हो सकता है।

E-mail : mail@actrec.gov.in
Website : www.actrec.gov.in

Kharghar,
Navi Mumbai - 410 210. INDIA.
Phone : +91-22-2740 5000
+91-22-3924 5000
Fax : +91-22-2740 5085

Cancer is curable, if detected early.

Chapter 1: INTRODUCTION

Medulloblastoma is the most common childhood brain tumor, occurring in the cerebellar region of the brain [1]. It accounts for almost 20% of all cerebellar tumors occurring in children below 18 years of age [2]. Although medulloblastoma is a childhood tumor, 30% of medulloblastomas occur in the adult [3]. In 2007, WHO histologically classified medulloblastoma as Grade 4, the grade with the highest degree of malignancy [4]. Later on, in 2016, medulloblastoma was further classified on the basis of genetically defined identities [5]. Medulloblastoma is initially diagnosed by magnetic resonance imaging or computed tomography scans. Post-surgery, the final diagnosis is made by the histopathological analysis and further molecular classification is performed on the tumor tissues. This tumor has the potential to spread into the leptomeningeal space or the spinal cord through the cerebrospinal fluid. Risk stratification of medulloblastoma is primarily based upon clinical features like age at diagnosis, residual disease after surgical resection, and the dissemination of the disease [1]. The current treatment modality for medulloblastoma includes a combination of surgery, cranio-spinal irradiation and chemotherapy. Although this strategy has improved the overall survival of almost 70% patients, those who survive have a poor quality of life and often have neurocognitive disabilities, neuro-endocrine disturbances, and in some cases secondary malignancies [6, 7]. Integrated genomic analyses by different research groups across the world have reported that medulloblastoma is not a single disease, it comprises of four distinct molecular subgroups that vary in their genetic profile, demographic as well as clinical outcome. The molecular classification of medulloblastomas is now used in clinics for risk stratification [8]. The four subgroups are named WNT, SHH, Group 3, and Group 4. The pathogenesis of the WNT and SHH subgroup is driven by the WNT and SHH signaling pathway,

respectively. Genomic studies have not identified any signaling pathway as a major driver associated with the pathogenesis of Group 3, Group 4 medulloblastomas. Further, there is an overlap in the genetic profiles of these two non-WNT, non-SHH subgroups. They are characterized by the overexpression of transcription factors involved in neuronal development such as *FOXG1B*, *EOMES* [9]. They also share chromosomal level alterations like isochromosome 17q [10]. The distinguishing features of Group 3 medulloblastomas are the overexpression of the proliferation-related and retina-specific genes [11]. Group 3 is the worst prognosis subgroup of medulloblastoma and shows the highest incidence of metastasis at diagnosis [12]. Most Group 3 tumors overexpress MYC oncogene, and some even have amplification of the gene. Group 4 is characterized by the expression of neuronal differentiation-related genes like those encoding synaptic proteins, neurotransmitter receptors, and axonal guidance proteins [13]. Despite these distinguishing features of Group 3, Group 4 medulloblastomas, some tumors are difficult to classify having characteristics intermediate between Group 3 and Group 4. Thus, a deeper understanding of the biology of these two subgroups is required so that they can be accurately risk-stratified and appropriate treatment strategies can be designed. The four subgroups of medulloblastoma not only differ in their molecular characteristics, but also differ in clinical features like incidence, age distribution, sex ratio, incidence of metastasis at diagnosis and importantly their overall survival rates. The WNT subgroup is the best prognosis subgroup with almost 95% long-term survival [12]. SHH subgroup has a moderate outcome for the children with the 5-year and 10-year survival of 68% and 55%, respectively) and in the case of adults, it has a poor outcome (5-year and 10-year survival of 75 and 37%) [12]. Group 3 has the worst outcome of ~50% five-year survival while

Group 4 has an intermediate survival of 75% that is similar to the SHH subgroup [12]. Group 3 and Group 4 medulloblastomas have the highest prevalence of metastasis at diagnosis (40% - 45% and 35% - 40% for Group 3 and Group 4, respectively). Thus, Group 3 and Group 4 medulloblastomas that have an overlap in their gene expression profile have similar rates of metastasis incidence, but Group 4 tumors have a much better outcome. It is thus extremely important to understand the molecular mechanism underlying this distinct clinical behavior of the two non-WNT, non-SHH medulloblastoma subgroups in order to design appropriate treatment strategies.

The four molecular subgroups of medulloblastomas also differ in the expression profile of microRNAs. MicroRNAs are small, 22 to 25 nucleotide long non-coding RNAs that regulate gene expression at the post-transcriptional level by binding to complementary sequences in the 3' UTR region of the protein-coding genes, leading to their cleavage or translational repression [14]. Cancer is a complex genetic disease carrying multiple genetic alterations. Thus, targeting a single gene at a time may not prove to be effective. MicroRNAs, on the other hand, are known to regulate the expression of several genes at a time thereby regulating vital cellular processes like proliferation, differentiation, survival, and also cell fate determination [15]. The deregulation of microRNAs has been implicated in various benign and malignant diseases [16]. MicroRNAs being natural regulators of vital genes involved in essential cellular processes are promising candidates for biomarkers and novel therapeutics. MiRNA profiling of medulloblastomas carried out in our lab showed a characteristic profile of each of the four molecular subgroup of medulloblastomas. [13]. The expression profile of a set of 12 genes and 9 microRNAs were used to develop a real-time PCR based assay that could classify medulloblastomas into the four molecular

subgroups with 97% accuracy [17]. This assay is now routinely used at the Tata Memorial Centre for the molecular subgrouping of medulloblastomas. The WNT subgroup medulloblastomas, which have an excellent survival rate, have the most distinctive microRNA profile that includes overexpression of several microRNAs like miR-193a, miR-148a, miR-224, miR-204, miR-365. The functional role of miR-193a, miR-148a, and miR-224 in medulloblastoma biology was investigated in detail that demonstrated their tumor-suppressive activity, indicating their role in better survival rates of the WNT subgroup tumors. The SHH subgroup is characterized by the downregulation of miR-135b, miR-204, and miR-153. MiR-135b, on the other hand, is overexpressed in Group 3 and Group 4 medulloblastomas [13, 18].

In the present study, the role of two microRNAs, miR-592 and miR-204 that are differentially expressed in Group 3, Group 4 medulloblastomas was investigated in detail. MiR-592 is a cerebellum enriched miRNA with a handful of reports on its functional role. It is reported to act both as a tumor-suppressive as well as an oncogenic miRNA in different cancers [19, 20]. MiR-204, on the other hand, is a well-known tumor-suppressive miRNA reported to belong to the top-most deleted family (miR-204, miR-211) of microRNAs in several cancers [21] . The expression of miR-592 and miR-204 was studied in a molecularly classified cohort of 260 medulloblastomas and was correlated with the clinical characteristics like incidence of metastasis at diagnosis and survival. The functional role of miR-592 and miR-204 in medulloblastoma cell biology was studied by exogenously expressing the microRNA in an inducible manner in the established medulloblastoma cell lines and studying the effect of the miRNA expression on cell growth and malignant

behavior. The underlying molecular mechanism was deciphered by identifying the protein-coding genes and biological pathways targeted by the microRNA in medulloblastoma cells.

Chapter 2: REVIEW OF LITERATURE

2.1 Medulloblastoma: history and clinical perspective

Medulloblastoma was identified by Bailey and Cushing as ‘Spongioblastoma cerebelli’ in 1925 [22]. It was described as the undifferentiated neuroepithelial neoplasm of the cerebellar vermis (midline) or rarely the cerebellar hemispheres (lateral) (Figure 2.1). Medulloblastoma was believed to arise from hypothetical precursor cells called ‘medulloblasts’ and it was classified as a primitive neuro-ectodermal tumor (PNET) owing to the histological similarity with PNETs occurring in cerebrum or spinal cord. The separate identity of medulloblastoma was postulated based on the differences in chromosomal level alterations in PNETs outside the posterior fossa and those inside it, which were classified as medulloblastoma, separately from other cerebral PNETs [23]. Later on in the year 2002 gene expression profiling studies proved that medulloblastoma is distinct from the PNETs, atypical teratoid/rhabtoid tumors (AT/ RTs), and the malignant gliomas in the posterior fossa region [24].

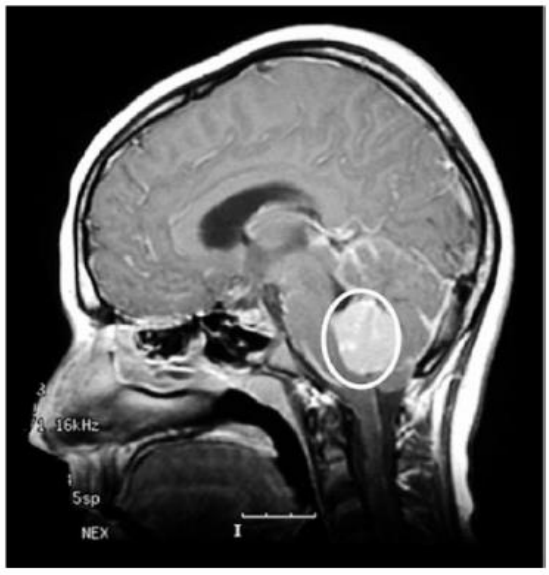

Figure 2.1 Sagittal MRI scan post gadolinium injection shows dense medulloblastoma tumor region marked in white [25].

2.2 Epidemiology, Risk stratification and Treatment:

Medulloblastoma is the most common pediatric, embryonal brain tumor that accounts for almost 20% of all pediatric brain tumors [26]. WHO classifies medulloblastoma as the Grade IV tumor owing to its aggressive behavior and histological characteristics like high mitotic activity and the presence of apoptotic cells and foci of necrosis [4]. 70% of all medulloblastomas occur in childhood (3-10 years of age), whereas 10-15% occur in the infants (< 3 years of age). About 12% medulloblastomas occur in adults [12]. The age of incidence is bimodal and peaks at around 3 - 4 years and again at 8 - 9 years of age, with the male: female ratio of about 1.5:1 [12].

Histologically, medulloblastomas are divided into three broad variants: i) The classic variant comprises almost 70% of medulloblastomas, having small round blue cells with minimal cytoplasm and dense basophilic nuclei that often display features of neuroblastic differentiation ii) Desmoplastic variant accounts for 16% medulloblastomas, wherein the cells in nodules often exhibit neurocytic differentiation, surrounded by more cellular inter-nodular zone containing a collagen-rich extracellular matrix iii) Large cell anaplastic (LCA) accounting for 10% medulloblastoma often has both large cells with abundant cytoplasm and anaplastic cells and correlates with worse prognosis and short survival [11, 27]. The frequency of these histological variants varies amongst the different age categories. In infants, the incidence of desmoplastic medulloblastoma is much higher (42%) than in children (9%). Adults have a very low (3%) frequency of the LCA variant of medulloblastoma [12].

2.3 Symptoms, Diagnosis, Risk stratification and Treatment

The time interval between the occurrence of the first symptoms to the diagnosis is about two months, but it can range from a few days to a possibly years. The symptoms mostly arise from cerebellar dysfunction and hydrocephalus (excessive accumulation of fluid in the brain). They include severe headache, vomiting, blurry vision, failure to achieve behavioral development in infants, ataxia, and cranial nerve palsy in the case of older patients [28]. Diagnosis of medulloblastoma is primarily carried out by the Computer Assisted Topography/Computed tomography (CAT/CT) scan or Magnetic Resonance Imaging (MRI) scan, which often shows a cerebellar tumor with a compression at the fourth ventricle due to the obstruction of cerebrospinal fluid (CSF) flow into it. The imaging is done for the entire craniospinal axis along with cytological tests in the CSF to diagnose metastastic disease. The final diagnosis relies on the histopathological analysis of the tumor tissues following surgical resection [28, 29].

Current methods for risk stratification classify medulloblastoma patients into two broad categories: i) Standard or average risk and ii) High risk. This method of risk stratification is based on the clinical factors - a) age at diagnosis, b) extent or resection, and c) Chang metastatic staging. Patients who are above 3 years of age or those whohave almost total surgical resection with no or minimal tumor residuals do not have a CSF metastasis, have non-anaplastic or non-large cell histology are considered to be ‘standard risk or average risk’ patients. Rest of the patients, including infants who are under 3 years of age are considered to be ‘High risk’ patients [28].

Medulloblastoma treatment follows a trimodal strategy in which surgery is the primary mode of treatment followed by the cranio-spiral irradiation (CSI) and adjuvant

chemotherapy[28]. A reduced dose of CSI of 23.4 Gy along with a localized boost to the posterior fossa to a total of 55.8 Gy is usually recommended for a 'Standard risk' patient. This CSI is combined with concurrent single drug and followed by multidrug chemotherapy. The introduction of adjuvant chemotherapy in the treatment protocol has lowered the CSI dose from 36.0 Gy to 23.4 Gy without a significant deterioration in survival, as observed by the progression-free survival of 67-81% at 5 years. Adjuvant chemotherapy also helped in preserving the neuro-cognitive abilities of the patients better [28]. The treatment strategy achieved a lot of improvement upon the addition of maintenance chemotherapy that includes vincristine, cisplatin, and cyclophosphamide. However, the complaint of loss of neurocognitive abilities still persists, particularly in younger children [28, 29]. In the case of the high-risk patients, a full CSI of 36.0 Gy is provided along with concurrent single drug therapy and is followed by a more aggressive adjuvant chemotherapy. In spite of this aggressive treatment, the high-risk medulloblastoma patients have a low survival rate of 43-70% progression-free survival at 5 years and compromised neuro-cognitive abilities [29]. A higher survival rate of 60-70% overall or progression-free survival may be achieved with the help of more intense chemotherapy and alternative radiation fractionation schedules. At present, the patients are hugely benefitted from the metronomic strategy of drug administration, in which the drugs are administered at lower doses and regular intervals over an extended period of time [30].

2.4 Shortcomings of the present risk stratification system

The present system for risk stratification has multiple caveats that need to be addressed immediately.

1. There is a recurrence of disease in almost 20- 40% of patients who are classified as standard risk, indicating that they are classified in a wrong manner, thus leading to the delay in the application of aggressive treatment.
2. A patient wrongly diagnosed as a high-risk patient would be unnecessarily exposed to high dose radiotherapy and aggressive chemotherapy, that would cause neurocognitive disabilities along with other side effects.
3. The current risk stratification system reduces the complexity of tumor behavior by simply classifying them into 'standard risk' and 'high risk' patients. This consequently hinders the efforts to design the treatment strategy more accurately [28].

Therefore, the greatest challenge in medulloblastoma right now is the accurate risk stratification of the patients so that the children having low risk of recurrence are spared from excessive radiation to the developing brain and the high-risk patients are treated aggressively. The advances in understanding the molecular heterogeneity of the disease is thus a step in the right direction and will definitely prove to be beneficial in understanding the disease biology and hence in better risk stratification and novel treatment strategies with the least side effects.

2.5 Molecular Genetics in medulloblastoma and deregulated signaling pathways

Unlike other cancers in which genetic alterations occur in common oncogenes or tumor suppressor genes like *TP53, EGFR, P16INK*^{4A}, medulloblastoma rarely have alterations in these common cancer-causing genes [31]. The most common chromosomal alteration reported in medulloblastoma is isochromosome 17q (i17q), an alteration that occurs by the

simultaneous loss of chromosome 17p and gain of 17q. i17q occurs in almost 40-50% of the tumors and is associated with an unfavorable prognosis [32, 33]. Amplification of *MYC* locus at 8q24 has also been reported in primary tumors and medulloblastoma cell lines [34, 35]. Medulloblastoma tissues show the presence of both glial and neuronal differentiation markers suggesting neural stem cells as the cell of origin of medulloblastoma [25]. This further suggested that the pathogenesis of medulloblastoma could be driven by the deregulation of cerebellar development. Moreover, the familial syndromes like Gorlin and Turcot syndrome provided the first indication that the WNT and SHH signaling pathways, which are crucial for cerebellar development, are deregulated in medulloblastoma. The patients with Gorlin and Turcot syndrome have a predisposition to medulloblastoma. Germline mutations in the *PTCH1* gene that encodes a membrane localized receptor of the Sonic Hedgehog (SHH) signaling pathway were identified in patients with Gorlin syndrome. Affected individuals often developed basal cell carcinoma, and in some cases developed medulloblastoma [36]. Subsequently, mutations in *PTCH1*, *SMO*, *SUFU* genes that are involved in the SHH signaling pathway were found in sporadic medulloblastoma [37, 38]. Individuals affected by the type II Turcot syndrome, were found to harbor germline mutations in *APC* (Adenomatous Polyposis Coli) gene, which is a tumor suppressor gene negatively regulating the expression of cytoplasmic β-catenin, a key regulator of the canonical WNT signaling pathway. The affected patients showed a predisposition towards developing colorectal cancers and medulloblastoma [39].

2.6 Evolution of the gene expression profiling studies in medulloblastoma

With the notion of involvement of development-related signaling pathways involved in the pathogenesis of medulloblastoma, the quest to understand the molecular biology of medulloblastoma was evident in several gene expression profiling studies carried out by different research groups across the globe. In 2006, Thompson *et. al* showed the existence of 5 molecular subgroups of medulloblastoma by studying 46 tumor tissues and observed that *CTNNB1* mutations and monosomy 6 were found to be mutually exclusive to *PTCH1* and *SUFU* mutations in medulloblastoma tumor tissues [40]. Kool *et al.* performed a study on 62 medulloblastoma tumor tissues and for the first time, suggested the existence of five unique medulloblastoma subgroups. Medulloblastomas driven by the WNT and SHH pathway deregulation were segregated as distinct subgroups, and the rest 3 subgroups were classified as non-WNT, non-SHH subgroups [11]. WNT and SHH subgroups also had a characteristic gene expression profile, whereas there was an overlap in the genetic signatures of the non-WNT, non-SHH subgroups. Kool *et al.* for the first time reported a higher incidence of metastasis to be associated with the non-WNT, non- SHH subgroups. Next, Northcott *et al.* performed a gene expression study in 103 tumors, and concluded that medulloblastoma with the highest confidence could be divided into 4 core molecular subgroups [9] and also reported that these subgroups were associated with different demographic and clinical characteristics like age, histology, chromosomal alterations, and survival. Cho and his colleagues came up with six molecular subgroups of medulloblastoma that included WNT, SHH, and four non-WNT, non-SHH subgroups [41]. Tumors with a retinal gene signature were mostly classified as the Group 3 tumors, and amongst them, the tumors harboring *MYC* amplification were associated with a worse prognosis. This classification of medulloblastoma helped greatly in the risk stratification

of the disease based on their molecular subgroup. In 2012, a consensus regarding the molecular subgroups was reached among the investigators, and they accepted the existence of four core molecular subgroups of medulloblastoma, namely WNT, SHH, Group 3, and Group 4 that differed in their demographics as well as clinical characteristics including prognosis and overall survival (Table 2.1) [12]. The subgroups were also believed to have a distinct cell of origin as they differed significantly in their expression profiles and underlying genetic alterations. Studies then focused on the mechanism of pathogenesis of the four subgroups and heterogeneity within each subgroup. The current understanding of the different subgroups including the gene expression signatures and chromosomal aberrations, is given in Table 2.1.

Subgroup	**WNT**	**SHH**	**Group 3**	**Group 4**
Frequency	10 %	28-30 %	25-28 %	40-45%
Age of incidence	Older children and adults	Infants, children and adults	Infants and younger children, rare in adults	Children and adults
Histology	Mostly classic with few cases of LC/A	Mostly nodular desmoplastic and classic, rarely LC/A	Mostly classic, LC/A	Mostly classic with few cases of LC/A
Anatomic location	Central, frequently Near the brainstem	Cerebellar hemispheres, rarely in midline vermis	Midline (filling fourth ventricle), rarely hemispheric	Midline (filling fourth ventricle)
Cell of origin	Progenitors in the lower rhombic lip/	Cerebellar granule neural	CGNPs in the cerebellar analage arising	Not defined

	dorsal midbrain	progenitors in the EGL	from upper rhombic lip	
Metastatic disease at diagnosis	10 %	18-20 %	35-40 %	40-45 %
Gender ratio **Male: Female**	1:1	1-1.2:1	2:1	2.3-3:1
Overall survival **(Five years)**	~90 %	~60-70 %	~50-70 %	~60-80 %
Expression signature	WNT signaling	SHH signaling	retinal signature MYC signature;	Neuronal differentiation, glutamatergic signature
Chromosomal aberrations (Gain +, Loss -)		3q+ (27%), 9p+	1q+ (35%), 7+ (55%), 17q+ (26%), 18+	4+, 7+ (47%), 17q+(66%), 18+
Gene mutations	6- (85%)	9q- (47%), 10q-, 14q-, 17p-	8p- (33%), 10q-, 11-, 16q- (50%), 17p-	8p- (41%), 10-, 11-, 17p-, X-
	CTNNB1 (90%), *DDX3X* (50%), *SMARCA4* (25%), *MLL2* (13%), *TP53* (13%)	*PTCH1 (*28%), *TP53 (11%), MLL2* (12%), *DDX3X* (11%), *BCOR*	*SMARCA4* (11%), *CTDNEP1* (5%), *MLL2* (5%)	*KDM6A* (12%), *KMT2C*, *ZMYM3*, *KDM1A*, *KDM4C* *MLL3* (5%) *ZMYM3* (5%)
Focal amplifications		*MYCN* (8%), *GLI2* (5%)	*MYC* (17%), *PVT1* (12%), *OTX2* (8%)	*SNCAIP* (10%), *MYCN* (6%), *OTX2*

				(6%), *CDK6* (5%)
Gene fusion			*MYC-PVT1*, *MYC-NDRG1*	
Rearrangement (enhancer hijacking)			*GFI1*/*GFI1B*	*GFI1*/*GFI1B* and *SNCAIP-PRDM6*

Table 2.1 Molecular and clinical characteristics of the four molecular subgroups of medulloblastoma: The table shows differential gene expression signature, chromosomal aberrations, gene mutations and focal amplifications in four different subgroups of medulloblastoma. The percentage values indicate the percentage of tumors displaying the particular abnormality within that subgroup [42, 43].

2.7 Refinement of the molecular classification of medulloblastoma

Genomics has greatly improved our understanding of medulloblastoma biology. It is now widely accepted that medulloblastoma is not a single tumor, it comprises of 4 different, molecularly distinct subgroups. However, the level of heterogeneity within each of the four molecular subgroups as well as the extent of overlap between the four subgroups remained to be elucidated. In 2017, 3 groups came up with further sub-classification of the 4 molecular subgroups based on the genome-wide DNA methylation profiling integrated with expression profiling and chromosomal level alterations. Schwalbe *et. al.* carried out comprehensive molecular profiling including DNA methylation microarray analysis and unsupervised class discovery in 428 primary medulloblastoma samples from the UK cohort and a validation cohort of 276 archival tumor samples [44]. They came up with seven robust and reproducible subgroups of medulloblastoma that were clinically relevant. WNT subgroup remained unchanged; SHH subgroup was divided into infant and childhood

patients based on their age differences. Both Group 3 and Group 4 were subclassified into high-risk and low-risk categories. The features of these novel subtypes with each core subgroup were predictive of their outcome, and hence they could help in the disease risk stratification. Next, Cavalli *et. al* carried-out Similarity Network Fusion (SNF) analysis of 763 primary medulloblastoma tissues [45]. SNF is a method of integrative clustering that analyzes multiple data types (both genetic and non-genetic), thus creating a unified view of patients based on multiple, heterogenous data sources. SNF thus provides superior results as compared to analysis of a single data type in isolation. Applying SNF to integrated gene expression and DNA methylation profile minimized the degree of overlap between Group 3, Group 4 subgroups, which was not apparent from analyzing the individual data sets. This analysis came up with a total 12 subtypes of medulloblastoma- 2 WNT subtypes, 4 SHH, 3 Group 3, and 3 Group 4 subtypes. The identified subtypes had distinct somatic copy number aberrations, activated pathways, as well as different clinical outcomes. In July 2017, Northcott *et. al* integrated the methylation subtypes of a sample with its matched genomic and transcriptome data that revealed enrichment of probable driver events in the specific subtypes [46]. They studied the somatic landscape across 491 sequenced medulloblastoma samples, and the molecular heterogeneity among 1256 epigenetically analyzed cases. They came up with 8 different subtypes amongst Group 3, Group 4 medulloblastomas. The four broad molecular subgroups of medulloblastoma and their respective subtypes will now be discussed in detail.

2.7.1 WNT subgroup medulloblastoma

The WNT subgroup medulloblastoma accounts for about 10% of all the medulloblastomas. This subgroup has its prevalence mostly in older children and adults and occurs only in 1%

infants [12]. The rate of incidence in the Indian cohort is almost 15% [17]. WNT subgroup medulloblastoma is mostly characterized by classic histology and has a male: female ratio of 1:1. WNT subgroup is the best prognosis subgroup with the long-term survival of more than 90% and rarely shows leptomeningeal spread [46]. The constitutive activation of the canonical WNT signaling is thought to be the driver of tumorigenesis in this subgroup. Several genes involved in the WNT signaling pathway like *WIF1, DKK2, LEF1, CCND1,* and *MYC* have a high level of expression in this subgroup, consistent with the upregulation of the canonical WNT signaling. Activating mutation in the *CTNNB1* gene encoding beta-catenin occurs in almost 86% WNT subgroup medulloblastomas. The tumors with wild type *CTNNB1* often harbor inactivating mutations in the *APC* gene. Monosomy 6 is found in 83% of the cases and it is the most frequent chromosomal alteration found in the WNT subgroup medulloblastomas [46]. Although Schwalbe *et al*. and Northcott *et al*. did not classify WNT subgroup into further subtypes, Cavalli et al classified WNT medulloblastomas into two subtypes WNTα and WNTβ based on their age of incidence. WNTα accounts for 70% of the total WNT subgroup tumors, characterized by monosomy chromosome 6 and occurs in young children, whereas WNTβ accounting for 30% of WNT subgroup tumors occurs primarily in adults and often does not carry chromosome 6 monosomy [45]. These two subtypes do not have a difference in their prognosis. The Lower Rhombic Lip Progenitor (LRLP) cells have been postulated to be the cell of origin of WNT medulloblastoma giving rise to the tumors closer to the brainstem than in the cerebellar hemisphere in a mouse model of the WNT subgroup [8, 12]. Next Generation sequencing studies have identified mutations in the multifunctional RNA binding protein DDX3X in almost 50% of the WNT tumors [47]. Additional mutations have been reported

in the SWI/SNF complex genes like *SMARCA4,* DNA methyl transferase gene *MLL3* and the tumor suppressor gene *p53* in a subset of the WNT subgroup medulloblastomas [47, 48]. Mutations in the epigenetic modifiers may result in the disruption of chromatin remodeling of the WNT responsive genes that would contribute to the pathogenesis of the tumors. [49]. The good prognosis of this subgroup led to clinical trials to reduce the aggressiveness of the current therapy for treating WNT subgroup medulloblastoma.

2.7.2 SHH subgroup medulloblastoma

SHH comprises of 30% of all medulloblastoma tumors. Desmoplastic histology is observed in almost 30% to 35% SHH subgroup medulloblastomas and classic histology in 40% to 45% SHH tumors [50]. The male: female ratio in the SHH subgroup medulloblastoma is also 1: 1. The age-related incidence is bimodal in nature and peaks at the infant stage (0 - 3 years) and again in the adults (> 16 years). The 5-year overall survival of the SHH subgroup is ~75% and 15% -20% of the cases show metastasis at the time of diagnosis [8, 12]. The upregulation of the SHH signaling pathway is evident in SHH subgroup tumors as the tumors show high expression of the SHH pathway genes like *HHIP, EYA1, PDLIM3,* and *MYCN* [51]. Mutations in the *PTCH1, SMO* or *SUFU* occur in the SHH subgroup in a mutually exclusive manner resulting in constitutive activation of the SHH signaling pathway. Loss of chromosome 9q (harboring the *PTCH1* gene) and 10q are the common cytogenetic alterations in SHH subgroup tumors. Focal amplification of *GLI2 (5.2 %), MYCN (8.2%),* and focal deletion of the *PTCH1*(24%) gene are also observed in SHH tumors [43]. SHH subgroup was further classified into various subtypes by Schwalbe *et. al* who classified the SHH tumors of the UK cohort into two subgroups- infants and childhood

based on their age group. Age in the case of the SHH subgroup was normally distributed and intersected at 4.3 years. So, patients below 4.3 years of age were classified as infant, whereas those above 4.3 years as children. Infant tumors had enrichment of the desmoplastic histology, whereas *MYCN* amplification and mutations in the *TP53* gene were associated with the SHH tumors in children. Mutations in the *TP53* gene, along with MYCN amplification and the LCA histology were associated with a very high-risk group of patients [44]. Cavalli *et. al* classified the SHH subgroup into four different subtypes namely- SHHα (29%), SHHβ (16%), SHHγ (21%) and SHHδ (34%). [45]. SHHα subgroup is the worst prognosis subgroup, occurring in children 3-16 years of age. It is associated with *TP53* mutations along with *MYCN* and *GLI2* amplification. SHHβ is the subgroup that occurs in infants and is frequently metastatic. Common genetic features of this subgroup are *PTEN* deletions and multiple focal amplifications. SHHγ subgroup has better outcome of 80% 5-years overall survival. It occurs in infants, and the tumors having MBEN (medulloblastoma with extensive nodularity) histology belonged to this subtype. It is characterized by low copy number variations. SHHδ occurs mostly in adults and has a favorable prognosis, and most of the *TERT* gene mutations occur in this subtype. This subtype is also enriched in mutations in the gene encoding U1 snRNA resulting in aberrant splicing, which bring about inactivation of the *PTCH1* gene or activation of the *GL12*/ *CCND2* gene [52]. This subtype classification of the SHH medulloblastomas has led to an improved risk stratification within the subgroup. SHH subgroup is also the most well-studied medulloblastoma subgroup. The initial characterization of the tumor was based on the germline mutation of the *PTCH1* gene in Gorlin syndrome. The availability of the transgenic mouse models also helped in deciphering the mechanism underlying the

pathogenesis of these tumors. Two mouse models of the SHH subgroup medulloblastoma were the first mouse models of medulloblastoma to be established. The *Ptch1*$^{+/-}$ mouse model showed a tumor incidence of 15% - 20% by six months of age, and the *Smo*$^{+/+}$ mice carrying activating mutation in the *Smo* gene have a tumor incidence of 90% by 2-3 months of age are the popular mouse models resulting from the activation of the Shh signaling pathway [53, 54]. The cerebellar granule neuron progenitors (CGNPs) are believed to be the cell of origin for the SHH subgroup tumors [55, 56]. These cells proliferate in response to the SHH signaling during the normal cerebellar development and lead to tumor development upon deregulated signaling. Recently mutations in *DDX3X* and *MLL2* genes were also reported in SHH medulloblastomas, although the functional role of this mutations is not understood [48]. The *TP53* mutations occurring in SHH subgroup medulloblastomas can be germline (Li Fraumeni) or somatic in nature, and these tumors are enriched in somatic copy number variations (SNVs) and complex chromosomal rearrangements as compared to the rest of the SHH tumors. Small molecule inhibitors of SMO activity have been tested in phase 1 clinical trials, but they were not successful as the patients acquired additional mutations leading to rapid disease progression [57]. A combination of chemotherapy with SMO inhibitors and PI3K inhibitors was shown to be promising in pre-clinical studies of medulloblastoma [58].

2.7.3 Group 3 medulloblastoma

Group 3 medulloblastoma comprises almost 25% of the medulloblastomas, and it is the most aggressive, worst prognosis subgroup. It occurs mostly in infants and in young children (0-16 years). Large cell anaplastic histology, focal amplifications of *MYC*

oncogene and metastatic dissemination indicates poor outcome for the Group 3 medulloblastoma patients. The incidence of metastasis at diagnosis is highest (46.5%) in this subgroup tumor, and it has a 5-year overall survival of less than 50%. Unlike WNT and SHH, the ratio of gender incidence in Group 3 medulloblastoma is 2:1; it occurs twice more in males than in females [8, 11]. No specific developmental pathway has been found to be associated with Group 3 tumors. There is an overlap in the gene expression profile with that of the Group 4 tumors that includes overexpression of transcription factors involved in brain development such as *OTX2, EOMES, FOXG1B,* testes specific gene *LEMD1*, *UNC5D,* and *EPHA8* [12, 13]. Group 3 tumors are characterized by the expression of proliferation-related genes like *MYC, CCND2, TGFβ1,* and retina-specific or photoreceptor genes such as *NRL, CRX, IMPG2* [12, 13]. Recent reports suggest that the the photoreceptor-specific transcription factors like *NRL* and *CRX,* which are the master gene regulators of retinal differentiation, are required for the tumor maintenance in this subgroup [59]. This subgroup also shows an amplification of the genes involved in the TGFβ signaling pathway like *ACVR2A, ACVR2B,* and *TGFBR1.* Recurrent deletions of the TGFβ pathway inhibitory genes like *CD109, FKBP1A* accounts for about 20% of the Group 3 tumors t indicating the involvement of deregulation of the TGFβ pathway in these tumors, which also makes it a potential therapeutic target. Cytogenetically, Group 3 has the largest number of both broad and focal copy number alterations like loss of chromosome 8p and 16q (50%) and gain of chromosome 1q (35%), 12q (17%), and 7 (55%). The most common aberration in Group 3 tumors is i17q, which is observed in almost 26% of the Group 3 tumors [8, 11]. In general, Group 3 tumors have an unstable genome. In the absence of mutations in the *TP53* gene, there is a widespread

chromothripsis that takes place in the Group 3 tumors. Chromothripsis results in potentially functionally significant fusions like *MYC-PVT1*. It can also lead to the phenomenon of enhancer hijacking, or the repositioning of active enhancer regions close to known oncogenes like *GFI1* or *GFI1B,* thereby leading to their activation that highlights the unstable nature of the genome [10, 60]. The region of *PVT1* gene that undergoes amplification, carries a microRNA cluster that could potentiate oncogenic *MYC* activation [10]. Group 3 tumors that do not possess these aberrations have recurrent somatic copy number variations (SCNVs) in chromatin modifier genes like *SMARCA4*, *MLL2*, *KMT2D*, and *CHD7*. Deep sequencing has also uncovered mutations in the lysine specific demethylase (KDM) gene family like *KDM6A, KDM3A, KDM4C, KDM5B,* and *KDM7A* in Group 3 tumors [61, 62]. Currently, the patients belonging to Group 3 medulloblastomas are treated with high-risk management protocols.

Subtypes of Group 3 medulloblastoma:

Group 3 medulloblastomas, having the worst prognosis, were further classified into subtypes that would aid in better risk stratification of the tumors. Schwalbe *et. al* combined the survival patterns of the subgroups (defined by transcriptome profiling and DNA methylation patterns) with the clinicopathological and molecular features, and then the risk factors were decided. Group 3 was divided into 'High risk' and 'Low risk' subtypes. The 5-year overall survival for the high-risk patients was 37%, and for the low-risk patients, it was 69%. Group 3 high-risk subtype was characterized by the P13K signaling activation, and overexpression of genes involved in ribosomal biogenesis. 64% of the tumors showed *MYC* amplification. Large cell anaplastic (LCA) histology was seen in 35% patients, and GFI1 mutation was seen in 29% of the patients. Most of the 'high risk' subgroup were

characterized by hypomethylation, as compared to the normal cerebellum whereas 'low-risk' patients showed hypermethylation of the genome as observed by the methylation pattern of the top 20 differentially methylated probes in the combined Group 3, Group 4 tumors [44]. Cavali *et al.* classified the Group 3 tumors into Group 3α (47%), Group 3β (26%), and Group 3γ (28%) subtypes. Group 3γ had the worst prognosis, whereas 3α and 3β did not show any difference in their overall survival. Group 3α tumors were enriched for the photoreceptor genes. They mostly occurred in the infants and had a high incidence of metastasis. The loss of chromosome 8q was frequent in this subtype (*MYC* is present at 8q24). This subtype had a better outcome than Group 3γ. Pathways involved in protein translation were enriched in the β and γ subtypes. Group 3β occurred mostly in slightly older patients and were less metastatic. They were characterized by *GFI1* activation and also *OTX2* amplification. Group 3γ having the worst prognosis were enriched in *MYC* amplification and telomere maintenance [45]. Northcott *et al.* performed the pathway analysis of recurrent genetic events and revealed the enrichment of NOTCH and TGFβ pathways in Group 3. They have classified Group 3, Group 4 tumors into 8 different subtypes, which will be discussed later [46].

2.7.4 Group 4 medulloblastoma

Group 4 medulloblastoma comprises 35% of all medulloblastomas. It is an intermediate prognosis subgroup that has a 5-year overall survival of 75%. It predominantly belongs to the classic histology and affects children and adults, rarely occurs in the infants. The highlighted feature of this subgroup is the gender skewness with the male: female ratio of 3:1. In the Indian cohort, the ratio observed is as high as 9:1 [8, 12]. Group 4 is the least

understood molecular subgroup of medulloblastoma. It demonstrates an overlap in the gene expression profile with that of Group 3 tumors. However, Group 4 is distinguished from Group 3 based on its neuronal differentiation and glutamate / GABA signaling related gene signature. Several genes that code for synaptic proteins like *MYRIP* and *SYN2*, for transmission of nerve impulse like *GRM8* and *GABR2*, axonal guidance proteins like *EPHA6* and *EPHB2* are overexpressed in Group 4 medulloblastomas [11, 13]. Isochromosome 17q is present in almost 66% - 80% of the tumors, which also occurs in Group 3. Group 4 medulloblastomas also have unstable genome like Group 3. Chromosomal level aberrations like gain of chromosome 7 (47%), 12q (20%), 18 (16%) and deletion of chromosome 8p (41%) and 10q (15%) were frequently identified in these tumors. Unlike Group 3, Group 4 tumors have amplification in *MYCN* rather than *MYC* gene [48, 61, 62]. The most frequent gene mutated in Group 4 medulloblastomas is *KDM6A* gene (13%), which codes for a demethylase that specifically demethylates lysine 27 residue of Histone H3. Focal amplification of *CDK6* gene is also known to occur in these tumors. Tandem duplications or single copy gain on 5q23.3 on the *SNCAIP* gene (10%), associated with Parkinson's disease and neurodegeneration, was also observed in Group 4 tumors [10]. *SNCAIP* gene is one of the most highly expressed genes in Group 4 medulloblastoma, and its expression and amplification is a distinguishing feature of the Group 4 tumors. Although the functional significance of this alteration is not known, mutual exclusivity of the *SNCAIP* duplication to the other most common alterations in Group 4 tumors like *MYCN* and *CDK6* amplification and its occurrence along with i17q indicates its role as one of the possible driver alteration of these tumors [10, 43].

Subtypes of Group 4 medulloblastoma

In a recent study by Schwalbe *et. al*, Group 4 tumors were also classified into 'High risk' and 'Low risk' subtypes similar to the Group 3 tumors. The high-risk subtype showed a five-year overall survival rate of 69%, frequent 7q gain, presence of metastasis at diagnosis, and prevalence in the male sex, whereas the low-risk subtype showed a survival of 80%. *MYCN* amplification, presence of residual disease, and LCA pathology did not seem to correlate with poor prognosis in this subgroup [46]. Cavalli *et. al* classified the Group 4 tumors in Group 4α (30%), Group 4β (33%), and Group 4γ (37%). Group 4α had the enrichment of the cell migration pathways. Group 4β was driven mostly by MAPK signaling pathway and overexpression of *FGFR1* gene. Group 4γ had an overexpression of *ERBB4* gene and activation of PI3K-Akt pathway. Both Group 4α and Group 4γ were enriched for MYCN amplification, loss of chromosome 8p, and gain of chromosome 7q. However, although the subtypes differed in copy numbers changes and associated signaling pathways there was no difference in their overall survival or the rate of metastatic dissemination [45]. Thus, it is clear that despite the integrated genomic approaches to classify Group 4 into its different subtypes, there is a paucity of good prognostication markers within the subgroup. Thus, there is an urgent need for a reliable and cost-effective prognostication marker in both Group 3 and Group 4 medulloblastomas.

2.8 Challenges in identifying and understanding the biology of Group 3, Group 4 medulloblastomas

We have already discussed the overlapping gene expression profile of the Group 3, Group 4 medulloblastomas that involves the expression of transcription factors involved in brain development. Besides, whole genome sequencing identified several genes, which are either mutated or harbor a copy number alteration to overlap between Group 3 and Group 4

tumors. For example, chromosomal aberrations like the gain of chromosome 7, 17q,18; loss of 8p, 11p; isochromosome 17q also take place in both the subgroups. The mutations affecting KDM family members like *KMT2D, KMT2C,* amplification of *OTX2*, deletion of *DDX31* gene, mutations in *CDH7* are also common to both Group 3, Group 4 tumors. Somatic structural variation at 9q34.13 region occurs in almost 7% of both the subgroups making it extremely difficult to distinguish between these two tumor types, which otherwise differ in their clinical outcome based on the structural alterations [9, 11, 41]. The unstable nature of the genome in these tumors, which further gives rise to phenomenon like 'enhancer hijacking' leading to the oncogenic activation of *GFI1* and *GFI1B* occurs in both the tumors [60]. In order to address the inter and intratumoral heterogeneity within Group 3, Group 4 medulloblastomas, Northcott *et. al* studied 1256 medulloblastomas profiled by Illumina 450k methylation array. They carried out analysis of pairwise sample similarities using t-distributed stochastic neighbor embedding (t-sne) that uncovered notable heterogeneity within the Group 3/ Group 4 tumors (n = 740). This analysis separated the parental subgroups into eight subtypes I-VIII [46]. Out of these 8 subtypes, subtypes II, III, and IV solely belonged to Group 3 tumors, whereas subtype VI and VIII exclusively belonged to Group 4. On the other hand, subtypes I, V and VII had a mixed gene signature of the Group 3/ Group 4 subgroups, thereby suggesting the existence of a subset of tumors that share the gene expression profile of both the subgroups [46]. Integration of the methylation subtypes with sample matched genomic and transcriptomic data suggested the enrichment of driver events in specific subtypes. The somatic events targeting *GFI1B* were found to be restricted to subtype I having mixed Group 3/ Group 4 expression profile. *MYC* amplification was mostly observed in subtype II (Group 3), whereas mutations in the

chromatin modifier genes like *KDM6A, ZMYM3* was mostly observed in subtype VIII (Group 4). In a recent study, a consensus was reached among the investigators who described subtypes within Group 3 and Group 4 based on the analysis of a combined cohort of 1501 medulloblastomas having DNA methylation profiling data, including 852 samples with matched transcriptome data. The final consensus of 8 subtypes present in the Group 3/ Group 4 tumors with the help of multiple complementary bioinformatic approaches confirmed the existence of a mixed Group 3/ Group 4 subtypes [63]. They further studied the clinical characteristics of these subtypes, and observed that the combined subtypes I, V and VII had a much better prognosis than the subtypes II and III, which exclusively belonged to Group 3 tumors. In another study carried out by Lastowska *et. al* also identified a subset of tumors in the non-WNT, non-SHH subgroups that share a common Group 3, Group 4 gene signature, with the help of Nanostring nCounter technology [64]. They also observed that this Group 3 /Group 4 intermediate subgroup showed the best survival rate (100%), as compared to the clinical outcome of Group 3 that showed poor prognosis with a survival rate of less than 40%. Thus, the challenges involved in identifying these subtypes need to be addressed, and accurate risk-stratification of the tumors with the help of molecular markers is extremely important to design the appropriate treatment strategy for these non-WNT, non-SHH subgroup tumors.

Not only does the identification of these tumors pose a challenge for researchers, there is a great deal of difficulty involved in understanding the biology of these tumors as well. Unlike WNT and SHH pathways, there is no signaling pathway that is found to be deregulated in the Group3 / Group 4 medulloblastomas that could be attributed to be the potential driver of tumorigenicty in these tumors. Group 3 tumors show tetraploidy (54%),

and it is characterized by an unstable genome showing multiple focal and broad somatic copy number alterations [10, 48]. However, the biological relevance and clinical importance of these aberrations is not yet understood. Amplification of *MYC* (12-16%) and *OTX2* (7%) are mutually exclusive in Group 3 tumors, thus indicating that they might be crucial event in the pathogenesis of the disease, but only about 8% group 3 tumors show amplification of these genes. In a mouse model of Group 3 tumors, concomitant knock out of *TP53* gene and overexpression of *MYC* in the cerebellar neural progenitor cells led to the development of tumor mimicking the gene expression profile of the Group 3 tumors [65]. But human Group 3 tumors rarely show *TP53* mutation. Genome sequencing also showed a consistent structural variation at chromosome 9q34.13 in approximately 6.6% of Group 3/ Group 4 tumors. Tumors carrying this somatic variation also show the oncogenic activation of *GFI1* and *GFI1B* as a result of its relocation in proximity of the enhancer regions. It was also seen that transduction of the neural stem cells with MYC and GFI1/ GFI1B resulted in the formation of tumors when xenografted into the cerebella of nude mice. Thus, *GFI1* and *GFI1B* may cooperate with MYC in a small subset of tumors to drive tumorigenicity [60, 66]. In a recent study by Northcott *et. al*, along with *GFI1B, PRDM6* gene (5q23) was one of the top ranking gene that was suspected to undergo enhancer hijacking as observed by the CESAM (cis expression structural alteration mapping) method [46]. P*RDM6* codes for a SET domain containing protein and is presumed to be a histone methyl transferase [67]. Interestingly, P*RDM6* gene is located just 600 kb downstream of the *SNCAIP* gene. Group 4 patients who harbored *SNCAIP* associated structural variants had *PRDM6* highly upregulated in them. This finding suggests that the structural variants targeting S*NCAIP* locus disrupt the local chromatin

environment to promote interchange between the *SNCAIP* super-enhancer region and gene promoters in the neighboring topologically associated domains (TAD) leading to aberrant gene induction of *PRDM6*. Although the physiological and cellular functions of SNCAIP or PRDM6 is not known, this phenomenon gives us an insight into how somatic alterations can contribute to medulloblastoma pathogenesis.

In the case of the Group 4 tumors, amplification of *CDK6, SNCAIP*, and *MYCN* could be observed only in a small subset of tumors. Group 4 carries fewer somatic copy number alterations as compared to the Group 3 tumors. *MYCN* expression is deregulated in both Group 4 and SHH tumors. Overexpression of *MYCN* under *GLT1* promoter gives rise to tumors, which can be both SHH dependent or independent in nature in a mouse model [66]. However, it is not clear whether these MYCN overexpressing, SHH-independent tumors recapitulate the genetic profile of the Group 4 tumors or not [68]. Deep sequencing has identified mutations in genes involved in epigenetic regulation in the Group 4 tumors. Mutations in *KDM6A* (13%), which is a histone demethylase is postulated to maintain the trimethylation mark on H3K27, retaining the stem cell like properties of the cells [62]. However, the number of tumors that actually harbor alterations in the epigenetic modifiers are few in number, and hence they seem unlikely to be the driver of tumorigenesis in these tumors. Thus, the molecular mechanism underlying pathogenesis of Group 3, Group 4 tumors in not understood despite extensive integrated genomic analysis of a large cohort of medulloblastomas.

A phosphoproteomic study shows a lack of correlation between the mRNA and protein levels in group 3 and group 4 medulloblastomas: Impact of post- transcriptional regulation

Despite the fact that the four core subgroups of medulloblastoma have been extensively characterized on the basis of their epigenetic and transcriptional regulation, driver oncogenic pathways or therapeutic targets in the non-WNT, non-SHH pathways have not yet been identified. A recent study based on quantitative phosphoproteomic of the primary medulloblastoma tumors has identified ERBB4-SRC to be a novel oncogenic driver pathway that is aberrantly activated in the Group 4 tumors. The phosphoproteomic analysis showed a significant enrichment of MAPK signaling its downstream effectors, AKT, and mTOR signaling pathways in Group 4 tumors [69]. The correlation between the transcript and protein level showed that the post-transcriptional regulation differed significantly in Group 3, Group 4 tumors. In group 3 tumors, the ratio of mRNA: protein had a global shift towards mRNA expression, while in group 4 tumors, there was a global increase in protein expression. The gene set enrichment analysis showed an increased expression of genes involved in translation and mRNA processing related function in Group 3 tumors, which is consistent with its highly proliferative nature (as discussed previously). In contrast, group 4 showed higher expression of genes involved in post-translational functions regulating ubiquitin proteasomal system. The study highlighted a complex regulation between the mRNA: protein balance in group 3, group 4 tumors, and indicated the pivotal role of post-transcriptional and post-translational mechanisms in its pathogenesis.

2.9 MicroRNAs: Post transcriptional regulators of gene expression

As discussed above, post-transcriptional and post-translational mechanisms could play a crucial role in pathogenesis of non-WNT, non-SHH medulloblastomas. Non-coding RNAs are known post-transcriptional regulators of gene expression. The importance of studying the role of non-coding RNAs in cell growth and disease has gained enough impetus in the last two decades. MicroRNAs are a class of endogenous, small, non-coding, single-stranded molecules, which are 22 – 25 nucleotides in length. They function by complementary base pairing to the 3' UTR region of the target mRNAs, which leads to translation repression or mRNA degradation. Since their discovery by Victor Ambros and colleagues in *C. elegans* in the year 1993 [70], discovery of several microRNAs and their functioning in several normal cellular processes like proliferation, differentiation, apoptosis, neuronal development, and cancer has been the focus of a large number of studies. [14]

2.9.1 MicroRNA Biogenesis and mode of action

The miRNA coding genes are located either within the introns of protein-coding genes or in the intergenic regions. The transcription of these genes by the RNA-polymerase II enzyme generates a primary transcript (pri-miRNA), as shown in Figure 2.2. In the pri-miRNA the region encoding the miRNA forms an imperfect stem-loop hairpin structure. The pri-miRNA is converted to a pre-miRNA. This process is mediated by a complex of Drosha type II RNase, the double-stranded RNA binding protein DGCR8, and other proteins, which cleave the hairpin-loop to generate the pre-miRNA. This pre-miRNA is

then exported to the cytoplasm by exportin 5. In the cytoplasm, the pre-miRNA is processed into the mature miRNA by the Dicer type III RNase. Only a single strand of the pre-miRNA is retained as the mature miRNA while the other stand often gets degraded [14].

The region of the miRNA that binds to its target is called as the seed region (generally from the 2^{nd} nucleotide to the 8^{th} nucleotide). This is important for pairing of the miRNA with the target mRNA although unlike siRNAs they form imperfect complementary stem-loop structures and pair imperfectly with sites in the 3' UTR region of their target mRNAs. The miRNA brings about downregulation of its targets by associating in microRNA induced silencing complex (miRISC) which contains an Argonaute family protein. [14]. The miRNA may act by decreasing the level of target mRNAs due to their degradation or by interfering with the process of translation resulting in decrease in the level of protein.

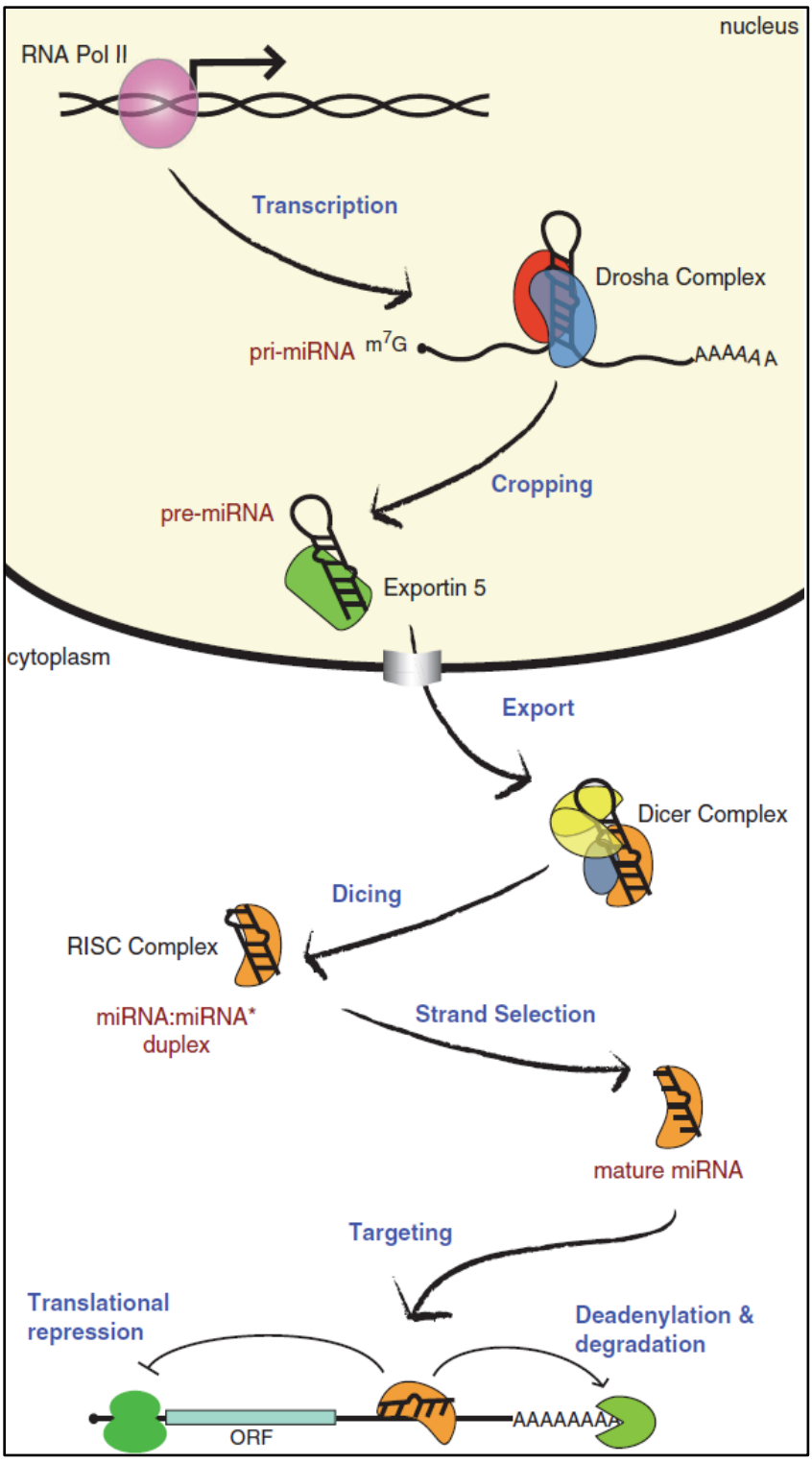

Figure 2.2 MicroRNA Biogenesis: Schematic diagram showing the miRNA biogenesis, its maturation and mechanism of action. Adapted from [14].

2.9.2 Role of microRNAs in cancer

One single microRNA can target 100 different genes, and 60% of protein-coding genes in human are known to contain micro-RNA binding sites. The first report of involvement of a microRNA in cancer was that of miR-15 and miR-16 located in chromosome 13q14, a region that is frequently deleted in more than 60% of Chronic lymphocytic leukemia (CLL) cases [71]. Most of the microRNAs reported be deregulated in cancer were found to be located inside or close to the fragile sites of the genome, in the minimal region of loss of heterozygosity or amplification or in the common breakpoint regions associated with cancer [72]. MiR-15 and miR-16-1 act as a tumor suppressor microRNAs and target anti-apoptotic *BCL2* gene expression [73]. Let-7 is another known tumor suppressor microRNA downregulated in lung cancer, that targets the *RAS* oncogene [74]. MiR-34 is another tumor-suppressive miRNA that is downregulated in gastric cancer, ovarian cancer, lung cancer, colon cancer, and is known to induce apoptosis by targeting genes like *BCL2* and *NOTCH* [75]. In contrast, there are microRNAs that are reported to be oncogenic in nature. MiR-155, one of the first oncogenic miRNAs described, is overexpressed in several malignancies like breast cancer, colon cancer, lung cancer, chronic lymphocytic leukemia (LL), and acute myeloid leukemia (AML). MiR-21 was the first miRNA to be coined an oncomiR due to its universal overexpression in several cancers including Acute Myeloid Leukemia, CLL, breast cancer, glioblastoma, and medulloblastoma, with PTEN and PDCD4 identified as its targets [76]. Like miR-21, the polycistronic miR-17 / 92 cluster, also known as oncomiR-1 has also been found to play an oncogenic role in several tumor types including medulloblastoma [77, 78]. The tumor-suppressors PTEN and p21 and the

anti-apoptotic protein BIM have been shown as their targets [76]. Along with microRNAs, several long non-coding RNAs as well as small nucleolar RNAs (snRNAs) are increasingly gaining importance in studying cancer biology. In a recent breakthrough study, it is revealed that there are recurrent hotspot mutations of U1 spliceosomal small nucleolar RNA (U1snRNA) in 50% SHH medulloblastomas. Almost 97% adult SHH and 25% adolescent tumors possess these mutations and it is not present in infants, other medulloblastoma subgroups or any other cancers that have been studied, thus pointing out to the specificity of such mutations. This kind of mutation occurs in the 5' splice site binding region of the U1 snRNA which significantly disrupt RNA splicing, giving rise to excess of 5' cryptic splicing events. Alternative splicing inactivates the tumor suppressor genes like *PTCH1* and activates oncogenes like *GLI2* and *CCND2* and thereby serves as a therapeutic target. These U1 snRNA mutations provide an example of highly recurrent and tissue-specific mutations of a non-protein-coding gene in cancer [52].

2.9.3 MicroRNAs in medulloblastoma

The extensively studied involvement of miRNAs in brain development and neuronal differentiation suggested that the deregulation of miRNA expression will also be prevalent in brain tumors. About 60% of the microRNAs deregulated in medulloblastoma are detected in the adult brain and they may change their level of expression over brain development [79]. In medulloblastoma, the first report of microRNA deregulation came from a study by Ferretti et al., who reported consistent downregulation of several microRNAs in medulloblastoma as compared to the normal cerebellum [80]. Functional studies with two of the downregulated miRNAs miR-9 and miR-125a showed inhibition

of tumorigenic behavior of the medulloblastoma cells upon restoration of their expression. However, in this study molecular subgrouping of medulloblastoma was not done. Hence subgroup-specific microRNAs were not studied. Cho et al. reported upregulation of miR-21 and miR-17-92 cluster in all medulloblastoma subgroups and that their expression correlated with significantly poorer overall and event-free survival [41]. These microRNAs were also proved to be oncogenic in the case of medulloblastomas.

For better understanding of the biology of medulloblastoma, our lab carried out microRNA profiling on a set of normal cerebellar tissues and medulloblastoma samples. Out of the 365 miRNAs that were studied, 216 were found to be expressed in medulloblastoma. The expressed miRNAs could successfully differentiate the normal cerebellum from the tumor tissues. Interestingly, the miRNA profiling could independently classify the medulloblastomas into its four subgroups (Figure 2.3) [13]. The WNT subgroup medulloblastoma had a distinct microRNA profile where a set of microRNAs like miR-148a, miR-193a, miR-204, miR-224, miR-365 were overexpressed etc. SHH subgroup showed downregulation of miR-135b and miR-204. MiR-135b was upregulated in the non-WNT, non-SHH subgroups. This differential expression of microRNAs was also validated in a large cohort of 101 medulloblastoma tissues. A real-time RT-PCR assay based on the expression level of a set of 12 protein-coding genes and 9 microRNAs was designed in the lab, which was validated in a western cohort. The assay has 97% accuracy and is now used at Tata Memorial Hospital for molecular classification of medulloblastomas in routine clinical practice for risk stratification [17].

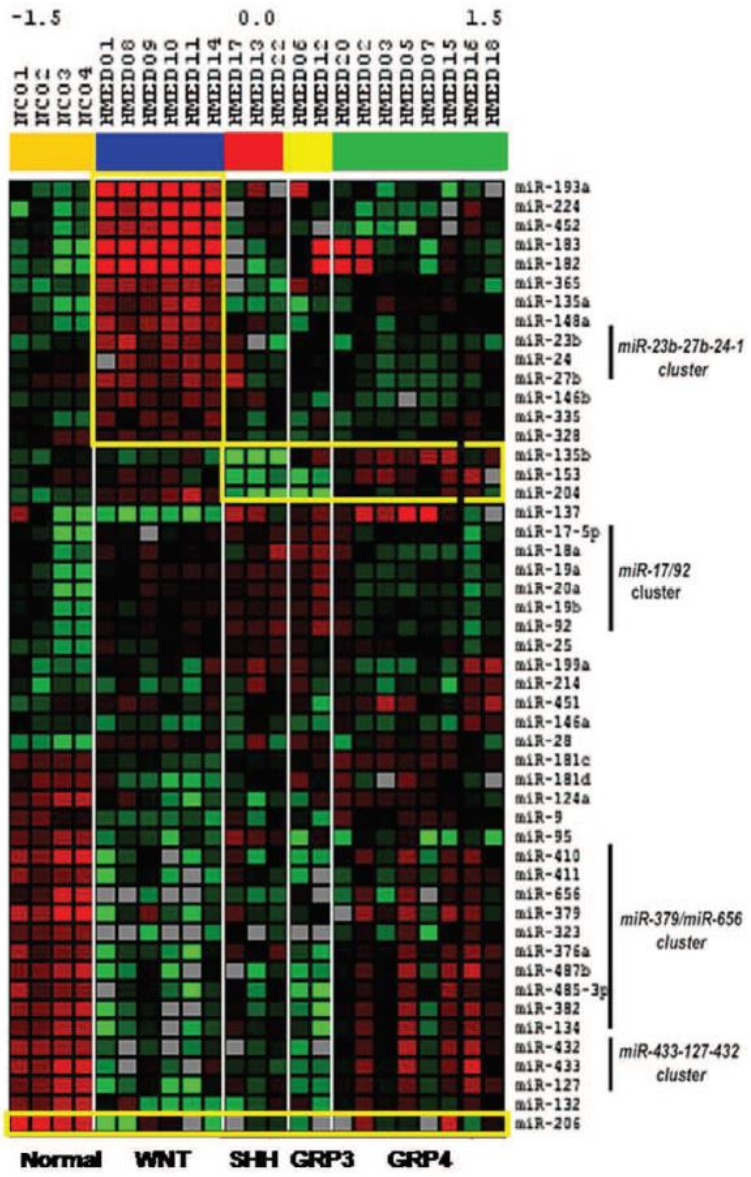

Figure 2.3 Differential expression of miRNAs in medulloblastoma: Heat map showing the differentially expressed miRNAs across normal cerebellar tissues and medulloblastomas [13].

The miRNAs that were drastically over expressed in the WNT subgroup medulloblastomas including miR-193a, miR-224 and miR-148a were studied for their functional role in the disease pathogenesis. Upon expression of miR-193a and miR-224 to levels similar to those in the WNT subgroup, there was proliferation inhibition, increased radiation sensitivity,

inhibition of anchorage independent growth of the medulloblastoma cells [13]. MiR-224 expression also led to increased radiation sensitivity by targeting *API5* gene in glioblastoma cells [13, 18, 81]. The expression of miR-148a in the medulloblastoma cells to levels similar to that in the WNT subgroup medulloblastoma, the proliferation, clonogenic, invasion and tumorigenic potential of the cells were significantly inhibited. *NRP1* was identified as a novel target of miR-148a, restoration of whose levels rescued the reduction of the malignant properties of the cells brought about by miR-148a expression [18]. These studies indicated that the upregulation of these miRNAs in the WNT subgroup medulloblastomas may contribute to the excellent survival of this subgroup by post transcriptionally regulating the expression level of various target genes. The present study focuses on studying the miRNAs differentially expressed in the non-WNT, non-SHH subgroups and explores their functional role in medulloblastoma cell growth and behaviour.

2.10 Aim and rationale of the present study

Despite extensive molecular profiling and integrated genomics performed in medulloblastoma tumors, the driver oncogenic signaling or potential therapeutic targets of the non-WNT, non-SHH tumors have not been clearly identified. Besides, the molecular basis for difference in the overall survival rates of Group 3, Group 4 medulloblastoma that have an overlap in the gene expression profiles and genetic alterations is also not understood. A proteomic analysis has shown the mRNA: protein ratios to be skewed in Group 3, Group 4 medulloblastomas indicating the role of post-transcriptional regulation

of gene expression in their pathogenesis. Earlier studies from the lab have shown microRNAs, which regulate gene expression at post-transcriptional level, to be differentially expressed in the four molecular subgroups of medulloblastomas. The present study investigated the functional role of two microRNAs miR-592 and miR-204, which are differentially expressed in Group 3, Group 4 medulloblastomas. in biology of medulloblastoma cells. The expression of these two microRNAs was also studied in a large cohort of medulloblastomas and correlated with clinical parameters.

MiR-592 is a microRNA that is almost exclusively expressed in group 4 medulloblastomas along with its host gene *GRM8* that encodes for a metabotropic glutamate receptor. MiR-592 has not been extensively studied. It has been reported both as an oncogenic and as a tumor suppressor miRNA in some cancers. It plays an oncogenic role in colon cancers [82] and prostate cancers [83] and has a tumor suppressive role in hepatocellular cancers [19] glioma [84, 85] and breast cancers [86]. MiR-204, on the other hand, is extensively studied miRNA. It is a cerebellum enriched microRNA that is highly expressed in the WNT subgroup medulloblastoma, not at all expressed in the SHH medulloblastomas and differentially expressed in the Group 3, Group 4 medulloblastomas. The tumor suppressive role of miR-204 has been investigated in various cancers like glioma, colorectal cancers, and endometrial cancers [87, 88]. Moreover, MiR-204 is reported to be one of the topmost deleted miRNA family in a large-scale study comprising of 51 different tumor types [21]. Thus, it is intriguing to study the potential role of mir-204 in medulloblastoma pathogenesis and explore its role as a potential prognostication marker.

The main objectives of the study thus can be stated as:

i. To study the expression of miR-592 in a large cohort of molecularly classified medulloblastoma and correlate the expression with clinical parameters. To study the role of miR-592 expression in medulloblastoma cell growth and behavior and identify the novel targets of miR-592, thereby elucidating the molecular mechanism.

ii. To study the role of miR-204 expression in medulloblastoma pathogenesis and understanding the molecular mechanism by which miR-204 exerts its effects and correlate its expression in Group 3. Group 4 medulloblastoma with clinical parameters like metastasis and survival.

Chapter – 3: MATERIALS AND METHODS

Materials:

The following chemicals were obtained from Applied Biosystems, Life technologies, Carlsbad, CA, USA:

2X TaqMan Universal PCR Master Mix (Part No. 4304437); 2X Power SYBR Green PCR Master Mix (Part No. 4367659), 2X TaqMan PreAmp Master Mix (Part No.4384266), TaqMan MicroRNA Assays (Part No. 4427975) - Assay IDs for the miRNA assays are: hsamiR- 204 (000508), hsa-miR-592 (001546) and RNU48 (001006); MicroAmp optical 384-well Reaction Plate with Barcode (Part No. 4309849) and MicroAmp Optical Adhesive Film Kit (Part No.4313663).

The following chemicals were obtained from Invitrogen, Life technologies, Carlsbad, CA, USA:

MMLV-RT 200 U/ul (Cat No. 28025-013), Dulbecco‟s modified Eagle medium (Cat. No.12800-058), DNAse I, amplification grade (Cat No. 18068-015), Fetal bovine serum (CatNo. 16140-071), LMP (low melting point) agarose, Trypsin, L-Glutamine

The following chemicals were obtained from Sigma-Aldrich, St Louis, MO, USA:

Agarose, Proteinase K, Guanidium Isothiocyanate (GITC), Diethyl pyrocarbonate (DEPC), DMSO, EDTA, Ethidium bromide, BES (B4554-25G), Puromycin (Cat No. P8833-25MG), Ammonium persulphate.

The following chemicals were obtained from Amersham Lifesciences, GE Healthcare Life Sciences, Pittsburgh, PA, USA:

dATP, dGTP, dTTP, dCTP (100 mM each) (Cat. No.27-2035-01), Random hexamers pd(N)6 Sodium salt.

The following chemicals were obtained from Thermo Scientific, Life technologies, Carlsbad, CA, USA:

10X PCR Buffer, Exonuclease I, Gene Ruler 1 Kb DNA ladder, Shrimp Alkaline Phosphatase (SAP) (Cat. No. EF0511), 25 mM MgCl2, Taq DNA polymerase (1U/ µl) (Cat. No. EP0404). T4-DNA ligase (Cat No. E0011), DpnI (Cat No- ER1701), SuperSignal® West Pico chemiluminescent substrate (Pierce-Thermo scientific, Cat. No.34077)

The following chemicals were obtained from Merck millipore, Darmstadt, Germany;

Qualigens, Thermo Fischer Scientific India Pvt Ltd, Mumbai, India or s d fine-chem limited,

Mumbai, India:

Xylene, Methanol, Glacial Acetic Acid, Potassium Acetate, Sodium Acetate, Nlaurylsarcosine. Sulfuric Acid (LR), Potassium dichromate (LR), Tri-Sodium citrate (LR), Citric Acid (LR), Hydrogen peroxide, Methanol.

The following reagents were obtained from New England Biosciences (NEB), Ipswich, MA, USA: Standard Taq (Cat No.M0273L), T4PNK (M0201)

The following reagents were obtained from s d fine-chem limited, Mumbai, India:

NaCl (Cat No.20241 AR), Na2HPO4.2H2O (Product no. 20383 AR), CaCl2.2H2O (Sigma C-3306)

The following kits were obtained from the companies specified in brackets:

Recover All RNA extraction kit (Ambion, Life Technologies, carlsabd, CA, USA; Cat No.AM1975), QiaAmp DNA mini kit (Qiagen, Limburg, Netherlands; Cat No.51304), Qiagen Plasmid Midi kit (Qiagen, Limburg, Netherlands; Cat No.12143) QIAquick Gel Extraction Kit (Qiagen, Limburg, Netherlands; Cat No.28704)

The water used for the preparation of all solutions and reagents was Ultrapure water (Resistivity = 18 MΩ cm) obtained from a Milli-Q water plant (Millipore, Billerica, MA, USA). Disposable plastic ware (certified DNase, RNase, and protease-free) was obtained from Axygen, California, USA.

Disposable sterile plastic ware for tissue culture was obtained from Nunc, Rochester, NY, USA.

Primers:

All PCR primers were synthesized and obtained from Merck (Sigma Aldrich) in the lyophilized form.

Methodology

3.1 Collection of sporadic medulloblastoma tumour tissues and normal cerebellar tissues:

The project was approved by the Institutional Review Board and Ethics Committee of Tata Memorial Hospital, Mumbai. 260 tumour tissue samples including Fresh tissues and Formalin Fixed Paraffin embedded (FFPE) tissues samples of sporadic medulloblastoma were obtained from patients who underwent surgery at the Tata Memorial Hospital after obtaining written informed consent from them or their parents (in case of patients below 16 years of age). In addition to the parent's consent, assent was also obtained from the minor patients aged between 7 to 16 years. These assents were also approved by Institutional Ethics Committee. In case of the fresh tissues, immediately following surgery, the tumour tissues were snap frozen in liquid nitrogen and stored at -80°C till further use. All the patients included in the study followed the standard treatment regimen of surgery along with radiation (except for infants) and adjuvant chemotherapy. The follow-up details of the patients were thoroughly updated in the Electronic Medical Records (EMR) maintained by TMH.

The normal cerebellar tissues were obtained from Brain tissue Repository, NIMHANS, Bangalore that include two normal developing cerebellar tissues from children less than 1 year of age and 6 normal adult cerebellar tissues.

3.2 Extraction of Nucleic acids:

Prior to nucleic acid extraction, cryosections of Fresh, frozen tumours and 5µm sections of FFPE tumour tissues were stained with haematoxylin and eosin and examined by light microscopy to ensure at least 80% tumour content.

3.2.1 Total RNA extraction:

a) RNA was extracted from the fresh frozen tumour tissues and tissue cultured cells by the Acid guanidium thiocyanate- phenol chloroform extraction method [89].

Materials:

Preparation of DEPC treated Milli-Q water: Water was collected from the Milli-Q plant directly in sterile 50ml NUNC tubes. 50 µl DEPC was added to 50ml Milli-Q water mixed vigorously and left overnight at 37**°**C with the tubes loosely capped. The tubes are autoclaved the following day and the water is used for preparing rest of the reagents that are to be used for RNA extraction.

1. *1M Sodium citrate, pH 7.0:* 14.7 gm sodium citrate was dissolved in 35ml Milli Q water. pH is adjusted to 7.0 with 1 M citric acid. The volume is made up till 50 ml. (1 M Citric acid was prepared by dissolving 10.5 g powder in 50 ml DEPC-treated water.) 50 µl of DEPC was added to both 1 M citrate and citric acid solution, tubes were mixed vigorously and left at 37 °C overnight. The solutions were autoclaved on the next day, and stored at room temperature.

2. 10 % N-lauryl-sarcosine: 5 g N-lauryl-sarcosine was dissolved in DEPC-treated water and the final volume was made up to 50 ml. The resulting solution was

neither treated with DEPC, nor autoclaved. It was kept at 65 °C for 1 h, and stored at room temperature.

3. 4 M Guanidinium Isothiocyanate (GITC): (Prepared in 25 mM Sodium citrate pH 7.0, 0.5 % Sarcosyl). 23.6 g of guanidine isothiocyanate was dissolved in 40 ml DEPC-treated water. 1.25 ml of 1 M sodium citrate and 2.5 ml of 10 % sarcosine were added and the final volume was made up to 50 ml with DEPC-treated water. The final solution was neither treated with DEPC nor autoclaved. Solution D was prepared from GITC by adding β-mercaptoethanol at a final concentration of 0.1 M (7.2 µl for 1 ml of 4M GITC solution). This solution is stable at room temperature for one month.

4. Phenol (Saturated with DEPC-treated water): 25 ml DEPC-treated water was added to 25 ml distilled phenol at room temperature in a sterile NUNC tube. The tube was mixed vigorously by inverting several times. The tube was kept at 4 °C until the two phases separated (30-60 min). The upper phase of water was replaced with fresh DEPC-treated water, mixed once again and stored at 4 °C.

5. 2 M Sodium acetate, pH 4.0: 13.6 g sodium acetate was dissolved in about 25 ml of Milli-Q water and pH was adjusted to 4.0 with glacial acetic acid. Final volume was made up to 50 ml with Milli-Q water. 50 µl DEPC was added to the solution, mixed vigorously and left at 37°C overnight. The solution was autoclaved the following day and stored at room temperature.

6. Chloroform

7. Absolute alcohol

8. 70% alcohol

Only RNAse free sterile plastic wares were used.

3.2.2. Methodology for RNA extraction

1a. Approximately 30-50 mg of frozen tumour tissue was collected in a chilled homogenization collection tube. This was homogenized with approximately 2-3 ml of Solution D. The tissue lysate was collected in a microcentrifuge tube and immediately passed through a 26-gauge needle at least ten times. The lysate was triturated until it loses its viscosity, resulting in complete shearing of genomic DNA.

1b. For tissue culture cells, medium was poured off, cells were washed with 1 X PBS twice and 0.5 ml of Solution D was added per well of 24 well plate (1ml for approximately 1 X 10^7 cells). The cell lysate was collected by tilting the plate and passed immediately through a sterile syringe fitted with a 26-gauge needle. This was done at least ten times until the lysate lost its viscosity, resulting in complete shearing of the genomic DNA. At this stage the lysate was either stored at -20°C or processed further immediately.

2. 50 µl of 2 M Sodium acetate pH 4.0 was added per 0.5 ml lysate and mixed by inverting the tubes.

3. Next, 0.5 ml DEPC-water-saturated phenol and 0.25 ml chloroform was added successively to the tube and the contents of the tube were mixed thoroughly by vortexing for 1 min. The cap of the tube was loosened to release the pressure and then vortexed again for 30 sec.

4. The tube was kept on ice for 15 min and then centrifuged for 15 min at 4°C at 10,000 rpm in a table-top centrifuge. The upper aqueous layer obtained was transferred to a fresh microcentrifuge tube and centrifuged once again to settle any traces of phenol.

5. The aqueous phase was then transferred to a fresh tube and an equal volume of isopropanol (0.5 ml per tube) was added. This was mixed by brief vortexing and kept at -20°C overnight for precipitation of RNA.

6. Next day, the tube was centrifuged at 12,000 rpm at 4°C for 20 min to pellet down the precipitated RNA. The supernatant was decanted carefully without disturbing the RNA pellet.

7. The RNA pellet was washed with 0.5 ml of 70 % ethanol, kept at room temperature for 2 min, and re-centrifuged at 12,000 rpm at 4°C for 10 min. The supernatant was decanted, and the left-over alcohol was allowed to dry by keeping the tube open with a clean tissue paper to cover it. The RNA pellet was air-dried, and dissolved in a minimum of 10 µl DEPC-treated water.

8. For dissolving the RNA, it was first kept on ice for about 60 min with intermittent vortexing and spinning, followed by heating at 65°C for 10 min. This would denature the secondary structure of the RNA. It would then be subjected to quick chilling on ice. The dissolved RNA was subsequently stored at -80°C for long term storage. Repeated freeze thawing of the samples was avoided to prevent degradation of RNA. When required, the frozen RNA was strictly allowed to thaw completely on ice before use. RNA was quantified spectrophotometrically (O.D. at 260/280 nm) using the NanoDrop UV-Vis spectrophotometer. The integrity of RNA was ascertained by 1.8 % denaturing agarose gel electrophoresis. The ratio of 28s rRNA to 18s rRNA is approximately 2:1 in a good quality RNA.

9. For ensuring the isolated RNA samples are free from gDNA, the RNA was treated with RNase free Dnase1 in a DNase1 reaction buffer. 1U of DNase1 per ug of RNA was used. The DNase1 treatment was carried out at 37^{o}C for 10 min.

10. The activity of DNase1 in the reaction was attenuated by addition of 0.5 M EDTA, pH 8.0, upto the concentration of 5 mM and the enzyme was heat inactivated for 10 min at 70^{o}C. The DNA free RNA was further used for complementary DNA (cDNA) synthesis.

RNA extraction from FFPE tumour tissues by using RecoverAll^{TM} Total Nucleic Acid Isolation Kit:

5 to 10, 10 μm sections were taken as starting material to extract RNA. RNA was extracted from these FFPE tissues using Recover All RNA extraction kit. As FFPE RNA is known to be considerably degraded, denaturing gels for quality assessment do not yield significant results. Therefore, RNA quality and quantity were ascertained spectrophotometrically (O.D.260/280 ratio) using the NanoDrop UV-Vis spectrophotometer.

3.3 Gene expression analysis by real time Reverse Transciptase PCR (Real time RT-PCR):

The 18-24 base pair primer sequences for Real Time RT-PCR were designed in a way that they correspond to two adjacent exons of a target gene. In order to prevent amplification of the genomic DNA, they are mostly located at the exon boundaries. Oligo explorer software version 1.4 http://www.genelink.com/tools/gl-oe.asp was generally used to design the primers. The amplicon that is to be analysed by Real Time RT-PCR is generally less than 200 bp sequences of the target gene. The melting temperature for both the forward and reverse primers are generally kept at 54 to 60 ^{o}C and the GC content is kept between 40 to 60%. Primer specificity has been ensured by the e-PCR feature of BiSearch software.

The primers were obtained in the form of lyophilized powder and it was reconstituted to the stock of 100µM using nuclease free 1X TE buffer, pH 8.0. the working stock of the primers are generally at 10pmole/µl which was prepared by diluting the stock solution by 1:10 using 1X TE Buffer, pH 8.0 and stored at -20 ^{o}C.

The primer pairs used in the study are as follows:

Name of sequence	Forward	Reverse
Primers used for amplification of genomic region encoding hsa-miR-592	AGTCTCGAGCCATGAAATCTATCCCCGT	TTTGAATTCGCACCAGCTCATATCCC

Primers used for Real Time PCR		
Name of sequence	**Forward**	**Reverse**
EML1	AAGGACCTACCAAAGCAAGA	TTCTTTGGTAACACAGTGCC
DEPTOR	GTGTGTGATGAGCATAAGG	GGTGCCGTCATCCTTTCTAA

Table 3.1 List of different primers used in the study

i) **Reverse Transcriptase reaction for cDNA synthesis:**

Materials:

1) *5X First Strand Buffer*
2) *100 mM dNTP mix*
3) *0.1M Dithiothritol (DTT) solution*
4) *pdN(6) Random hexamer peimers (100 ng/µl) or OligodT primers*
5) *RNase inhibitor (20 U/µl)*
6) *M-MLV RT (200 U/µl)*

7) *DEPC treated ultrapure water*

Method:

For gene expression analysis by real-time RT-PCR analysis, 500 ng of total RNA was reverse transcribed in a 10 µl reaction as follows.

The reaction volume was scaled up depending upon the number of samples.

1. The RNA samples were thawed on ice and diluted to a concentration of 250 ng/µl with DEPC treated ultrapure water.
2. The following components were mixed in 0.5 ml centrifuge tube as follows:

Component	**Volume**	**Final concentration**
Total RNA (250 ng/µl)	2 µl	500 ng
10 mM dNTP mix	0.5 µl	0.2 mM
pdN6 Random hexamer primers (100 ng/µl)	0.5 µl	5 ng
DEPC treated ultrapure water	3 µl	
Total volume	6 µl	

3. The contents were mixed, the tube was pulse spun. The sample was then heated at 65^{o}C for 5 min to denature the secondary structures in RNA and quickly chilled on ice for 2 min.
4. The following reaction mix was prepared

Component	**Volume**	**Final concentration**
5X First Strand Buffer	2 µl	1X

0.1 M DTT	1 µl	10 mM
RNase inhibitor (20 U/µl)	0.25 µl	5 units
DEPC treated ultrapure water	0.25 µl	
Total volume	3.5 µl	

5. 3.5 µl of the above reaction mix was added to the denatured RNA, the contents were mixed and the tube was incubated at 37oC for 5 min to allow annealing of the random hexamer primers.
6. 0.5 µl of M-MLV RT was added to the reaction, the contents were mixed properly and the tube was further transferred to the thermal cycler set at below mentioned parameters.

Temperature	**Time**
25^{o}C	10 min
37^{o}C	60 min
70^{o}C	10 min
4^{o}C	∞

7. The synthesized cDNA was either immediately used for gene expression analysis or stored at -20^{o}C until further used.

ii. **Real time PCR for gene expression analysis**

Materials:

1) *2X PowerUP SYBR Green master mix*
2) *Gene specific forward primer*
3) *Gene specific reverse primer*

4) DEPC treated ultrapure water

Method:

1. The primers were thawed on ice and tap mixed. The cDNA was diluted to 5 ng/µl (1:10) with DEPC treated ultrapure water and the reaction was set using 10 ng of cDNA per reaction.
2. The master mix for 5 µl real-time RT-PCR reaction was set up as mentioned below:

Component	**Volume**	**Final concentration**
2X Power Up SYBR Green master mix	2.5 µl	1X
Forward primer (10 pmol/µl)	0.25 µl	0.5 pmol
Reverse primer (10 pmol/µl)	0.25 µl	0.5 pmol
Total volume	3 µl	

   Each real-time reaction was set up at least in duplicate. Master mix for each gene to be detected was prepared by scaling up the volumes depending upon the number of reactions to set. No template control (NTC) reaction was set up for each master mix prepared and DEPC treated ultrapure water was added instead of cDNA to rule out the chances of erroneous measurement of gene expression due to accidental cross contamination of the reagents.
3. 3 µl master mix was aliquot in separate tubes and the final reaction was prepared by addition of 2 µl of diluted cDNA to the tubes. The contents were mixed and pulse spun.
4. The prepared reactions were loaded in 384 well plate and the position of each sample in the plate was documented.

5. The wells were sealed with optical adhesive sheet with the help of plastic applicator. The sealing of the wells was ensured by evenly moving the applicator through horizontal and vertical groves between the wells.
6. The bubbles in the wells were removed by gentle tapping and the plate was spun in a moving angle rotor at 2000 rpm for 2 min at RT to gather the contents of the wells to the bottom.
7. Appropriate program for SYBR Green method was selected and parameters were set in the QuntStudio 12K Flex/QuantStudio 5 real-time RT-PCR thermal cycler instruments, Applied Biosystems, Waltham, MA, USA using the QuantStudio software. The 384 well plate was kept in the heating block and the program was run. The PCR cycling parameters were as mentioned below:

Stage	**Temperature**	**Time**	**Condition**	**No. of cycles**
Hold	50^{o}C	2 min		1
	95^{o}C	10 min		1
PCR	95^{o}C	15 sec		40
	60^{o}C	1 min	Fluorescence data acquisition	
Melt curve	95^{o}C	15 sec		1
	60^{o}C	1 min	Fluorescence data acquisition	
	95^{o}C	15 sec		

8. The data was analysed using QuantStudio software by comparative Delta Delta Ct method and the expression of target genes relative to the expression of GAPDH was expressed in terms of Relative quantity using the formula $RQ=2^{\wedge(Ct\ Gene - Ct\ GAPDH)}*100$ where GAPDH is an endogenous control gene that is abundantly expressed.

9. The data was exported in Microsoft Excel format. Both raw data file and the analyzed data file were preserved for record.

3.4 Quantification of microRNA expression by Real Time PCR [91]

MicroRNAs are 22 to 24 nucleotides in length and their quantification involve 2 steps- a stem-loop reverse transcription that is followed by Real time PCR. The stem loop RT primers hybridize to mature miRNA molecule at the 3' end and then gets reverse transcribed with the help of reverse transcriptase enzyme. The RT product is then quantified by conventional TaqMan PCR with miRNA specific forward primer, reverse primer corresponding to the stem and loop RT primer (excluding the loop region) and the Taqman probe.

For microRNA detection in total RNA extracted from medulloblastoma cell lines, 50 ng of total RNA was reverse transcribed using Moloney-Murine Leukemia Virus Reverse Transcriptase (M-MLV RT) following the manufacturer's instructions. A pool of stem-loop primers for the target microRNAs and RNU48, a small endogenous non-coding RNA was used for Reverse transcription for Taqman based detection.

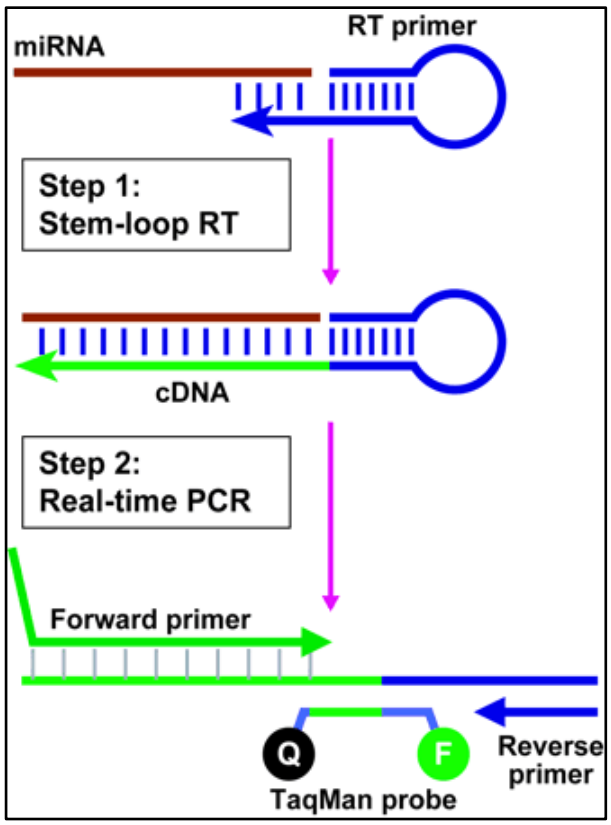

Figure 3.1 Stem-loop RT-PCR of miRNA: Schematic diagram of stem-loop RT-PCR for miRNA quantification using Taqman miRNA assays. Adapted from [91]

(a) Stem-loop Reverse transcription of microRNAs:

Materials:

1) *5X First Strand Buffer*
2) *100 mM dNTP mix*
3) *0.1M Dithiothritol (DTT) solution*
4) *RNase inhibitor (20 U/µl)*
5) *M-MLV RT (200 U/µl)*
6) *DEPC treated ultrapure water*

7) Multiplex RT primer pool containing 5X RT primers for miR-592/miR-204 and RNU48 in 1X TE buffer, pH 8.0) for Taqman RT

Name of assay	Catalogue no.	Assay id
hsa-miR-592	4427975	001546
hsa-miR-204-5p		000508
RNU48		001006

Table 3.2 Assay ID for Taqman probes used in the study

Method:

1. The RNA samples were thawed on ice and diluted to 50 ng/µl concentration using DEPC treated ultrapure water.
2. All the reagents were thawed on ice, tap mixed, and the tubes were spun to gather the content of the tubes to the bottom.
3. A 5 µl reverse transcription reaction was assembled as follows:

RT reaction for Taqman based detection

Component	Volume	Final concentration
5X First Strand Buffer	1 µl	1X
0.1 M DTT solution	0.5 µl	10 mM
100 mM dNTP mix	0.1 µl	0.5 mM
Multiplex RT primer pool	2 µl	1X
RNase inhibitor (20 U/µl)	0.1 µl	2 units
M-MLV RT (200 U/µl)	0.25 µl	50 units
RNA (50 ng/µl)	1 µl	50 ng

DEPC treated ultrapure water	0.05 µl	To make up total volume to 5 µl

4. The reaction was scaled up depending upon the number of samples and master mix was prepared except the addition of RNA. 4 µl of master mix was aliquot in 0.2 ml thin-walled PCR tube and 1 µl of RNA was added separately. The content of the tubes was tap mixed, and the tubes were pulse spun and placed in a master cycler previously set at 16^{o}C to prevent the denaturation of the stem and loop RT primers.

   The below mentioned program was set in the thermal cycler:

Temperature	**Time**
16^{o}C	30 min
42^{o}C	30 min
85^{o}C	5 min
4^{o}C	∞

5. The RT reactions were either used for setting real-time RT-PCR assay or stored at -20^{o}C until further used. The RTs were used within 2 weeks.

(b) Real-time PCR for microRNA expression analysis

Materials for Taqman based detection

1) *2X Universal Taqman PCR master mix*
2) *20X microRNA primer-probe*
3) *DEPC treated ultrapure water*

Method:

1) The 20X microRNA primer-probes were removed for the storage and strictly thawed on ice.
2) The RT reactions were diluted in equal ratio with DEPC treated ultrapure water.
3) The master mix for 5 µl real-time RT-PCR reaction was set up as mentioned below:

Reaction for Taqman based detection		
Component	**Volume**	**Final concentration**
2X Universal Taqman master mix	2.5 µl	1X
20X microRNA primer probe	0.25 µl	1X
DEPC treated ultrapure water	0.25 µl	To make up total volume to 3 µl
Diluted RT reaction (5ng/µl)	2 µl	10 ng

Each real-time reaction was at least set up in duplicate. Master mix for each microRNA to be detected was prepared by scaling up the volumes depending upon the number of reactions to set. No template control (NTC) reaction was set up for each master mix prepared and DEPC treated ultrapure water was added instead of cDNA to rule out the chances of erroneous measurement of gene expression due to accidental cross contamination.

4) 3 µl master mix was aliquoted in separate tubes and the final reaction was prepared by addition of 2 µl of diluted cDNA to the tubes. The contents were mixed and pulse spun.
5) The prepared reactions were loaded in 384 well plate and the position of each sample in the plate was documented.

6) The wells were sealed with optical adhesive sheet with the help of plastic applicator. The sealing of the wells was ensured by evenly moving the applicator through horizontal and vertical groves between the wells.

7) The bubbles in the wells were removed by gentle tapping and the plate was spun in a moving angle rotor at 2000 rpm for 2 min at RT to gather the contents of the wells to the bottom.

8) Appropriate program for Taqman or SYBR Green method was selected and parameters were set in the QuantStudio 12K Flex/QuantStudio 5 real-time RT-PCR thermal cycler instruments, Applied Biosystems, Waltham, MA, USA using the QuantStudio software. The 384 well plate was kept in the heating block and the program was run.

   The PCR cycling condition were set as follows:

Stage	**Temperature**	**Time**	**Condition**	**No. of cycles**
Hold	50^{o}C	2 min		1
	95^{o}C	10 min		1
PCR	95^{o}C	15 sec		40
	60^{o}C	1 min	Fluorescence data acquisition	

9) The data was analysed using QuantStudio software by comparative Delta Ct method and the expression of miR-592 and miR-204 relative to the expression of endogenous small RNA control (RNU48) was expressed in terms of Relative quantity.

   $RQ=2^{\wedge(Ct\ miRNA - Ct\ RNU48)}*100$

10) The data was exported in Microsoft Excel format. Both raw data file and the analyzed data file were preserved for record.

a. Molecular subgrouping of medulloblastoma tumor tissues:

Molecular subgrouping of medulloblastoma tumor tissues was done by a Real-Time PCR based assay that studied the differential level of expression of 12 genes and 9 miRNAs [17]. The assay was developed in the lab and is now being routinely used in the clinical practice to identify the molecular subgroup of a medulloblastoma patient. In addition to the published protocol, a pre amplification step was also introduced post the stem and loop RT-PCR for miRNAs that gives an advantage while working with limiting amount of RNA like that obtained from the FFPE tumor tissues (Thesis, Pooja Panwalkar). Basically, for the pre amplification reaction, a multiplexed RT reaction for the pool of 9 Taqman miRNAs and the endogenous control RNU48 were used.

3.5 Cloning of PCR products in target vectors

The following section describes the general procedure for molecular cloning. It was used to for cloning the genomic region of miR-592 into the lentiviral pTRIPZ vector and the mammalian expression vector pcDNA3. It was also used for cloning the 3' UTR region of putative miR-592 targets into the pcDNA3.0 Luciferase reporter vector. The genomic region encoding miR-204 was cloned into the lentiviral vector pTRIPZ by the restriction digestion cloning method earlier in the lab (Thesis- Pratibha Boga).

3.5.1 Construction of miR-592 expressing pTRIPZ vector

MiR-592 is encoded from the intronic region of its host gene *GRM8* (negative strand) present in chromosome 7q31.33. A 642 base pair genomic region encompassing the region encoding for miR-592 was cloned into the lentiviral vector pTRIPZ by restriction digestion of both the vector and the insert with EcoR1 and Xho1 sites and thereafter cohesive end ligation. The genomic region encoding miR-592 was PCR amplified by using Taq polymerase enzyme. The forward and reverse primers were designed in such a manner that the restriction enzyme sites were incorporated at the ends. The insert as well as the vector was double digested with the respective enzymes. After digestion and checking them on agarose gel electrophoresis, they were further being ligated by using T4 DNA Ligase enzyme.

a) **PCR amplification and phenol chloroform method of DNA purification:**

Materials:

1. 10X Taq Polymerase buffer
2. 10mM dNTP mix
3. Forward and Reverse primers (10pmole/µl)
4. Human genomic DNA (25ng/ µl)
5. Taq DNA polymerase enzyme (diluted to 1U/ µl with Diluent F)
6. Mgcl2
7. Autoclaved MilliQ

8. Tris saturated phenol

A) **Genomic region encoding hsa-miR-592**

```
Chromosome 7 (len: 642)
126697835                  TTAAATTTA GCACCAGCTC ATATCCCACA AAAAAAAAAA
          CCTAATATAG GGAAAACTTG TGATAGAAAC AGTCTATTAA ATGAAATTAT
          ATTTTGATTT CTAAAGCTGC CTTGCAAGAA CAGAGGTTAC AATTTCTAGA
          AGGAGCCATA TACAAATTTA AAAAGAGCCA TAATTCATGC AAAGAAACAT
          TTTCTAACCT GTAATTTATA GTTCAGCTGC CTTTCTAAAA TCTCAAGCTT
          TTAGTTAAAT AATTGT AGAT TTGTTGCTCA GTTTAAAAAC CCTTCTGGAA
          TCACGTCTTT AACTGGCGTT GTGACGTCTT ACGTCATGAT GTTGCGTCAC
          CACGTGATGA CGCTGTGCCA TCACAACACA TCATCGCATA TTGACACAAT
          GTCATGGCAT AATATCATCA AATTAAATTC ATCAGCACTC CCCACAGCCT
          GGCCCCAGGA AGGGCAAGAG AGCTTTAAAG TTTCTCTTTG TTCTTGTCAA
          CACACTCCTG GTTGGTAGGC GAGAACAGCA ACTGGACAAA TCATTTCCTG
          GTCTATTAAA ACTTCCTAGA TCTCAAATTA GGAGAATTTG AAAGTTACAG
          CTTAGAGTTG GAGGAAATAG TTTTCACGGG GATAGATTTC ATGGCTTGTT
          ACT                                                  126698477
```

B)

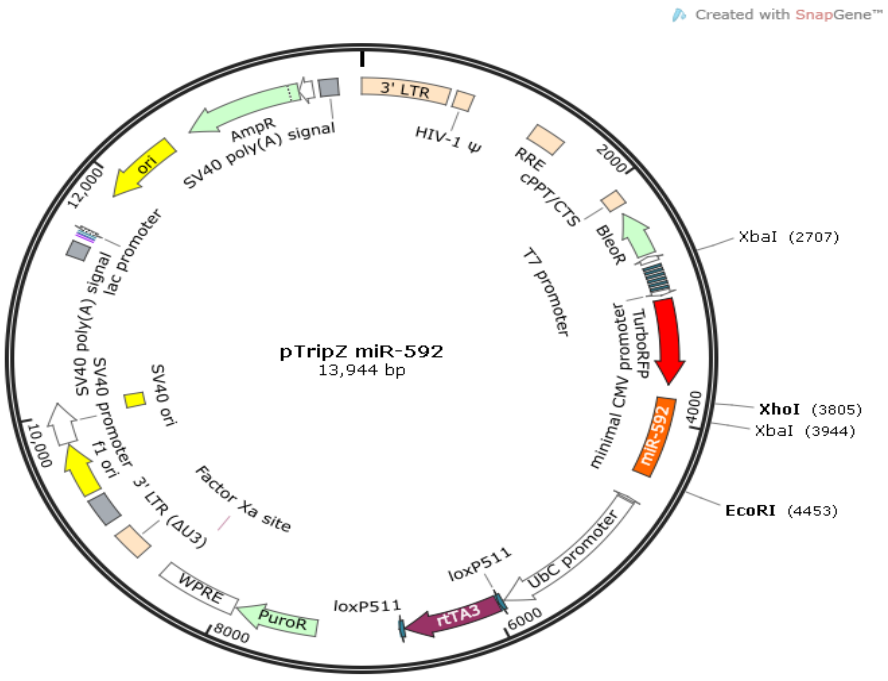

Figure 3.2: Construction of the miR-592 expressing lentiviral pTripz vector: A) Genomic sequence encoding miR-592 (mature miRNA sequence in red) that was used for expressing miR-592 in the lentiviral pTripz vector. B) Vector map of the pTripz, a doxycycline inducible lentiviral vector consisting of the tetracycline response element

(TRE) fused to minimal CMV promoter which drives turboRFP and miR-592 expression upon binding of its reverse tetracycline transactivator 3 (rtTA3) in the presence of doxycycline. The expression of TurboRFP enables the user to easily observe expression from the TRE promoter, allowing quick assessment of factors such as expression, viral titre, and transduction efficiency. Constitutively active Ubiquitin C promoter (UBC) drives expression of rtTA3 and puromycin resistance (PuroR).

Tris Saturated Phenol: Distilled phenol kept at –20 0C was carefully thawed to RT by keeping it at 60 0C preferably in water bath. The cap of the bottle was loosened to release any pressure built on thawing the phenol. As phenol is acidic, it needs to be neutralised to avoid degradation of DNA. 25 ml of phenol was taken and equal volume of autoclaved Milli-Q in sterile Nunc tube. It was mixed thoroughly by shaking the tube and allowed to rest until two phases separate. Upper phase was removed. This was repeated once to saturate phenol with water. To the water saturated phenol, equal volume of 1 M Tris, pH 8.0 is added and mixed thoroughly by shaking the tube and allowed two phases to separate. Upper phase was removed and same set of steps were repeated with 0.1 M Tris, pH 8.0. pH of the phenol phase was subsequently achieved to be 7.0 or above. 10-15 ml of 10 mM Tris, pH 8.0 was added on top of the phenol phase for long-term storage in refrigerator and exposure to light was avoided by covering tube with Aluminium foil.

Primers used for the amplification of miR-592 from the genomic DNA obtained from normal human lymphocytes are as follows:

Forward Primer: AGTCTCGAGCCATGAAATCTATCCCCGT

Reverse Primer: TTTGAATTCGCACCAGCTCATATCCC

Methodology:

1. All reagents required for the reaction except for the enzyme were thawed and kept on ice.
2. For each PCR reaction 25 ng of human lymphocytic genomic DNA was added in the end to the 0.2 ml tube containing the PCR components.
3. The PCR Reaction mix was prepared as follows for Taq DNA polymerase:

Components	Volume	Final Concentration
10X Taq Polymerase buffer	1 µl	1X
10mM dNTP	0.2 µl	0.2mM
Forward primer	0.2 µl	2 pmol
Reverse primer	0.2 µl	2 pmol
Human genomic DNA (25ng/µl)	1 µl	25ng
Taq DNA Polymerase (1U/ µl)	0.25 µl	0.25 U
Autoclaved Milli Q water	Make up volume till 10 µl	

4. Reactions were carried out in Eppendorf Master Cycler 5333 (Eppendorf, Germany). All precautions were taken to avoid PCR related contamination. All reagents and PCR products were handled using filter tips.
5. The PCR cycling parameters were as follows:

Temperature	Time	Cycles
95°C	3 mins	1
95°C	1 min	
Annealing temperature	45 secs	

68°C	45 secs	35
68°C	10 mins	1

6. 5 µl of the PCR product was run on 1% agarose gel and visualized using UV transilluminator. The PCR product was further purified using phenol: chloroform, before using it for cloning.

7. Equal volume of Tris Saturated phenol was added to the PCR, mixed and centrifuged at 12,000 rpm, for 15 min, at 20°C.

8. To the supernatant equal volume of phenol: chloroform (1:1) was added, mixed and centrifuged at 12,000 rpm, for 15 min, at 20°C.

9. To the supernatant equal volume of chloroform was added, mixed and centrifuged at 12,000 rpm, for 15 min, at 20°C.

10. Upper layer was separated and $1/10^{th}$ volume of 3M sodium acetate pH 5.2 was added and mixed.

11. Then 2.5X volume chilled absolute alcohol (kept at -20°C to chill) was added, mixed well and kept for precipitation overnight at -20°C.

12. Next day, the mixture was centrifuged at high speed (16,000 rpm) for 20 min at 4°C and the pellet was washed with 500 µl of 70% alcohol and centrifuged at 12000 rpm for 10min at 4°C; twice.

13. The pellet was air-dried and dissolved in minimum of 10 µl T.E buffer.

a) Agarose Gel Electrophoresis

Reagents:

1) 50 X Tris-acetate-EDTA (TAE) buffer: 121 g Tris and 18.6 g EDTA was dissolved in 300 ml of Milli-Q water followed by addition of 28.55 ml glacial acetic acid. Volume was made up to 500 ml and was autoclaved.

2) Ethidium Bromide stock (10 mg/ml): Dissolve 10mg Ethidium Bromide in 1 ml of autoclaved Milli-Q water.

3) 6X DNA loading dye: Dissolve 0.25% bromophenol blue, 40% (w/v) sucrose in Milli-Q water.

Method

1. The appropriate amount of agarose was weighed into a measured volume of 1X TAE buffer to make a 1% gel. The slurry was heated in a microwave oven until the agarose was dissolved completely and ethidium bromide to a final concentration of 0.5 µg/ml (from a 10 mg/ml stock) was added when the gel solution had cooled to about 40°C.
2. A gel tray was cleaned; the gel was poured into the gel tray and a clean comb was inserted in the slot provided in the tray. The gel was allowed to set at room temperature for 30-45 minutes.
3. After the gel had completely set, the gel was placed in the electrophoresis tank filled with 1X TAE buffer. The buffer should be just enough to cover the gel to a depth of about 3 mm and the comb was carefully removed.
4. The DNA samples were mixed with 6X loading buffer at 1X final concentration and loaded into the wells of the gel. The gel was run in electrophoresis chamber at 40mA constant current, till the dye had migrated about three-fourths of the gel.
5. The DNA was visualized by observing the gel on a UV transilluminator.

b) Restriction Digestion

Reagents: 10X buffer, Restriction Enzyme

Method:

1. All reagents required for the reaction except for the enzyme were thawed and kept on ice.

2. For a typical restriction enzyme reaction, 2-3 U of enzyme was used to digest ~1µg DNA in a reaction volume of 20µl; at the recommended temperature for at least 4 hr. (If more than one reaction was performed a master mix was prepared containing the buffer, enzyme and Milli-Q water).

3. The reaction was heat inactivated at the recommended temperature for 15-20 min (most enzymes are inactivated at 65°C for 15 min).

4. For cloning the digested product, the volume of the reaction was made to 200 – 300 µl with TE. The mixture was purified by phenol-chloroform method and precipitated with ethanol as described for PCR products (Refer to section 3.6.1a).

c) Dephosphorylation of vector using Shrimp Alkaline phosphatase (SAP)

Reagents: 10X RE digestion buffer, Shrimp Alkaline Phosphatase (1 U/ µl).

Method:

1. All reagents required for the reaction except for the enzyme were thawed and kept on ice.

2. The reaction was set up as follows and incubated at 37°C for 60 min.

Components	Volume
10X RE Digestion Buffer	3 µl
Shrimp alkaline phosphatase (1U/ µl)	1 µl
RE Digested DNA	10-20 µl (1-10 pmole termini)
Autoclaved Milli Q water	Make up volume till 30 µl

3. The reaction was terminated by incubating at 65**°**C for 15 mins.

d) Ligation Reaction

Reagents: 10X Ligation Buffer, T4 DNA Ligase (5U/µl)

Method:

1. All reagents required for the reaction except for the enzyme were thawed and kept on ice. The reaction was setup as follows:

Components	Volume /amount
Linear vector DNA	30 fmole vector ends
Insert DNA (PCR product)	90 fmole insert ends
10X Ligation Buffer	2µl
T4 DNA Ligase (5U/µl)	0.4µl (2 U)
Autoclaved MilliQ water	Make up volume to 20 µl

2. The mixture was incubated for 16 hours at 22°C (cold bath) and inactivated by incubating at

65°C for 10 min.

e) Preparation of competent cells

Reagents:

Transformation buffer (TB): 0.3 g PIPES, 0.22 g of CaCl2-2H20, 1.86 g of KCl were dissolved in 95 ml Milli-Q and pH was adjusted to 6.7-6.8 with 5 M KOH. The initial white precipitate may form at low pH, however once the right pH is adjusted, solution should become clear. 1.09 g of MnCl2 was added in this solution and final volume was made up to 100 ml and filter-sterilised using 0.22 μm filter.

Super Optimal Broth (SOB): 20 g of tryptone, 5 g of yeast extract was dissolved in 995 ml of Milli-Q water. 2 ml of 5 M NaCl and 1.25 ml of 2 M KCl was added to achieve final concentrations of 10 mM and 2.5 mM respectively. Solution was autoclaved and 5 ml of 2M MgCl2 solution prepared and sterilised separately was added just before use.

Luria Broth (LB): 1 g of tryptone, 0.5 g of yeast extract and 0.5 g of NaCl was dissolved in 100 ml of milli-Q water and autoclaved SOB agar plates: 1.5-2 g Agar agar was dissolved in 100 ml of SOB (or LB), autoclaved and poured in pre-sterilised plastic plates.

Method:

1. Escherichia coli strains DH5α or stbl3 cells were freshly streaked from the glycerol stocks on the SOB agar plates one day prior to inoculation into SOB for competent cells preparation.
2. 200 ml of SOB medium (10% of flask volume) was prepared and autoclaved in wider neck 2L flask. All the steps here onwards are performed in aseptic conditions created by laminar hood.
3. A single colony from freshly streaked SOB plate was inoculated into the 200 ml SOB and flask was incubated at 180C at 150-200 rpm till O.D at 600nm reaches to

0.4. O.D at 600 nm was checked at regular intervals by taking out 1ml of growing culture in aseptic conditions by using spectrophotometer.

4. Culture was centrifuged at 3000 rpm for 15 min at 40C when O.D reaches 0.4 or in when it is in between 0.4 to 0.7.

5. Supernatant was discarded and one third volume of ice-cold transformation buffer (134 ml for 200 ml culture) was added slowly onto the pellet so as to disturb the pellet gently.

6. Cell pellet was resuspended in TB with gentle pipetting for 5-10 min and was incubated on ice for additional 10 min. Care was taken to avoid any bubbling during re-suspension of cell pellet.

7. After incubation this was centrifuged at 3000 rpm for 15 min at 40C and cell pellet was resuspended in 16 ml of TB (1/12.5 volume of initial culture volume i.e. for 200 ml) as described in earlier step.

8. 1.12 ml of DMSO (final concentration of 7%) was added on walls of suspension tubes slowly and was mixed by shaking or by gentle pipetting once or twice.

9. This solution was then aliquoted in volumes of 100 µl in 1.75 ml prechilled sterilized eppenderoff tubes and snap-freezed in liquid nitrogen as quickly as possible.

10. The competent cell vials were stored at -80°C and were taken out on ice just before use.

f) Transformation of competent cells

Reagents: Stbl3 or DH5α ultra-competent cells, SOC broth, LB broth

Method:

1. Stbl3 or DH5α ultra-competent cells, stored at -80°C was thawed on ice by tap-mixing intermittently and kept on ice.

2. 2-10 µl of the ligation mixture DNA was added to the cells and incubated on ice for 30 min, followed by heat shock for 45 sec at 42°C.

3. Then the transformation mixture was subjected to cold shock by immediately transferring on ice for 5 min.

4. 900 µl of SOC broth was added and incubated on shaker incubator for 1 hr at 37°C.

5. The mixture was spread on LB agar plate containing ampicillin (100 µg/ml) and incubated at 37°C for 16-18 hr.

6. The colonies obtained were then inoculated in LB broth containing ampicillin (100 µg/ml) and plasmid DNA was extracted from the cultures using alkaline lysis method.

g) Plasmid extraction by alkaline lysis method

Reagents

Solution I: Glucose-Tris-EDTA solution:

Components	Volume /amount	Final Concentration
2M Glucose	1.25 ml	50mM
0.5M EDTA	1.0 ml	10mM
2M Tris, pH 8.0	0.625 ml	25mM
Autoclaved Milli Q water	Volume make up till 50ml	

Solution I stored in 4°C.

Solution II (Prepared just before use)

	For 5 ml	Final conc.
5 M NaOH	200µl	0.2 N
20 % SDS	250µl	1 %
Autoclaved Pyro MilliQ	4.55 ml	

Solution III (3M Potassium 5M acetate pH 4.8)

14.7 g of Potassium acetate was dissolved in 20 ml Milli Q water and volume was made upto 30 ml. To this, 5 M Potassium acetate, 5.5 ml of glacial acetic acid and 10 ml of Milli-Q water was added. pH was checked. If it is not approx 4.8 more acetic acid was added and finally volume was made to 50 ml with MilliQ water and solution was autoclaved.

Method:

1. 1-2 ml of bacterial cultures was centrifuged at 3000 rpm for 5 min at room temperature in 1.5 ml eppendorf tube. The cell pellet was resuspended in ice cold 100 µl solution I by vortexing and incubated for 5 min at room temperature.

2. 200 µl freshly made solution II was added and mixed by gentle inversion followed by incubation for 5 min on ice.

3. 150 µl solution III was added and immediately mixed by vortexing for 10 sec, followed by incubation for 5 min on ice.

4. The tube was centrifuged at 13000 rpm for 5 min and clear supernatant was removed in a fresh tube without disturbing the pellet.

5. To this supernatant, equal volume of phenol-chloroform (1:1) (for example, 250 µl of Tris saturated phenol and 250 µl of chloroform was added for 500 µl of supernatant.

6. The tube was vortexed and centrifuged at 12000 rpm for 5 min, aqueous layer was removed carefully to fresh tube.

7. Equal volume of chloroform was added to the aqueous layer and tube was vortexed to thoroughly mix the contents. Step 6 was repeated.

8. 1 ml (or 2X volume) of absolute ethanol was added to the supernatant, mixed by inversion and allowed to precipitate at room temperature for 5 min.

9. The tube was centrifuged at 13000 rpm at room temperature for 5 min, the supernatant decanted carefully; 1 ml of 70% ethanol was added to the DNA pellet and re-spun at 13000 rpm for 5 min. The ethanol was aspirated and the DNA pellet was air dried.

10. The plasmid pellet was dissolved in 10-25 µl TE containing RNase (1µg/ml) and further screened for insert and orientation by Restriction digestion analysis.

11. The positive constructs were further prepared on a large scale and purified using, Qiagen DNA Midi kit according to manufacturer's protocol.

3.5.2 Cloning of 3' UTR region of putative target genes of miR-592 and their target site mutated counterparts into the pcDNA3.0 Luciferase vector

The 3'-untranslated (3'-UTR) region of potential miR-592 target genes, *DEPTOR* and *EML1* were PCR amplified from normal human lymphocyte DNA, and cloned in a luciferase reporter vector downstream of the firefly luciferase cDNA. Following the general method of molecular cloning by restriction enzyme (Referred in section 3.6.1), both the insert (PCR product) and the vector was digested with HindIII and Xho1 enzymes (Fermentas) and then ligated. Another method used for preparing the 3' UTR region of *DEPTOR* was by the annealing of synthetic oligos and then ligating the oligos to the already digested pcDNA3.0 vector.

Primers used for cloning 3' UTR		
Name of sequence	**Forward**	**Reverse**
EML1	TCGGGATCCAAGGAAGACACAG ACTCGC	CACAAAAGACAGGAAAAGCAGC
DEPTOR	GATCGAATTCCTGGGCCTCCCA GCCCTCCAGTGGCCTGTGGGTG AGGGAAGCCAGAATGACACAA	TCGAATTTGCATGGCAATCTTGT CTTTGCATTGCTTTGTGTCATTCT GGCYYCCCTCACCCACAGGC

Table 3.3 Primers used for cloning 3' UTR sequences in the study

Method:

Component	Volume
100µM Forward oligos	1µl
100µM Reverse oligos	1µl
T4 DNA Ligase Buffer (Fermentas)	2.5µl

Poly Nucleotide Kinase	1 µl
Autoclaved Milli Q	Volume make up to 25 µl

The oligos were made to anneal at 37°C for an hour and then the temperature was raised to 90°C and gradually dropped to 25°C by a 5° interval at each step and keeping the reaction 1min each at every step.

The annealed oligos were diluted 1:100 in autoclaved MilliQ and then ligated with an already digested pcDNA3.0 Luciferase vector by following the normal protocol (Section 3.6.1 e). Next they were transformed into ultra-competent E.coli DH5 alpha cells. Plasmid DNA were extracted from the transformants, screened with restriction digestion and positive constructs were purified on a large scale by using the Qiagen DNA midi kit by following the manufacturers protocol.

b) Site directed mutagenesis of the seed sequence of miRNA binding site present in the 3' UTR region of putative target genes of miR-592

For further confirmation of the direct binding of miR-592 to the 3'-UTR region, the putative miR-592 binding site in the 3'-UTR constructs were altered by site directed mutagenesis. Briefly, two primers about 50 nucleotide length having complementary sequence overlapping the miR-592 binding site sequence with altered 3 to 4 nucleotides in the binding site were designed such that they create a unique restriction site. The miR-592 binding site altered sequence in the primers was flanked by at least 15 nucleotide sequence on both 5' and 3'-end. 50 ng - 100 ng of original 3'-UTR luciferase reporter construct was used as a template and amplified for 15 cycles -20 cycles using Q5 High Fidelity DNA polymerase (New England Biolabs, Ipswich, MA, USA).

Primers used for SDM of 3' UTR		
Name of sequence	**Forward**	**Reverse**
EML1	GTTGTACAATATATGATATCGTGCACATTGAATAC	GTATTCAATGTGCACGATATCATATATTGTACAAC
DEPTOR	GGGTGAGGGAAGCCAGAATGATATCAAGCAATGCAAAGACAAGA	TCTTGTCTTTGCATTGCTTGATATCATTCTGGCTTCCCTCACCC

Table 3.4 Primers used for Site directed mutagenesis within the 3' UTR region of the target genes

Method:

Component	Volume
5X Q5 Reaction Buffer	8.0µl
10mM dNTPs	0.8µl
Forward primer	0.8µl
Reverse primer	0.8µl
Template DNA (50ng/µl)	2µl
Q5 High Fidelity DNA Polymerase	0.5µl
Nuclease free Milli Q water	Volume make up till 40 µl

Programme for Site-Directed Mutagenesis

Temperature	Time	Cycles
98°C	3 mins	1
98°C	15 secs	
68°C	20 secs	

72°C	4.5 mins	25
72°C	5 mins	1

The PCR reactions were digested with the DAM methylation sensitive DpnI restriction enzyme for degradation of the template strand. The digested PCR reactions were then transformed into ultra-competent E.coli DH5 alpha cells. Plasmid DNA were extracted from the transformants, screened with restriction digestion and mutations were confirmed by Sanger sequencing.

3.6 Tissue culture medium and reagents

1) **Tissue culture media:** The Dulbecco's Modified Eagle Medium (DMEM)+ and DMEM:Nutrient Mixture F12 (DMEM/F12) media were used for the routine maintenance of the cell lines. The DMEM medium contains glucose, high levels of amino acids, vitamins and sodium pyruvate. The DMEM/F12 is 1:1 mixture of DMEM and Ham's F12 medium. The media were prepared as per the manufacturer's instructions.

Method:

1. The powder from 1 packet of the either medium was dissolved in around 800 ml of sterile ultrapure water in sterile glass volumetric flask (1 lit capacity). Required quantity of anhydrous sodium bicarbonate (3.7 g/lit for DMEM and 2.438 g/lit for DMEM/F12) was added and dissolved in the medium.
2. The pH of the medium was adjusted to 7.5 with 1N hydrochloric acid (HCl) and the final volume of the medium was adjusted to 1 lit with sterile ultrapure water.

3. The medium was further filtered through a 0.22 µ membrane filter using a vacuum-assisted filter assembly and stored in sterile glass bottles at 4^{o}C until further use.
4. Both media are supplied by the manufacturer devoid of the growth factors. Thus, for the maintenance of the cell lines, the media were supplemented with 10 % Fetal Bovine Serum (FBS). Penicillin (50-100 I.U./ml), streptomycin (50-100 µg/ml) and amphotericin-B (0.25 µg/ml) were added to the culture medium to reduce the chances of bacterial and fungal contamination in cell cultures (1 ml of 100X antibiotic antimycotic solution per 100 ml of complete medium).

2) 100X Antibiotic solution: 10,000 units penicillin G (Alembic Ltd, Vadodara, India) and 10,000 µg streptomycin sulphate, available as injection vials (Abbott Healthcare Pvt. Ltd, Ahmedabad, India) were dissolved per ml in Milli-Q water, filter sterilized and stored at 4°C.
3) 10X Trypsin solution: 2.5 g of Trypsin powder was dissolved in 90 ml of ultrapure water in sterile volumetric flask and the final volume was adjusted to 1 lit. The solution was filter sterilized by passing through a 0.22 µ membrane filter. The filtered solution was stored as 10 ml aliquots at -20°C. The working stock of trypsin solution was prepared by diluting 10 ml of 10x trypsin to 100 ml with 1X PBS. The working stock was stored at 4°C.
4) 10X phosphate buffered saline (PBS): 80.81 g NaCl, 2.01 g KCl, 17.8 g Na2HPO4. 2 H2O, 2 g KH2PO4, and 10 g glucose were dissolved in sterile ultrapure water in a volumetric flask. The pH of the solution was adjusted to 7.4 using conc. HCl and the final volume was adjusted to 1 lit using ultrapure water. The solution was filtered through a 0.22 µ membrane filter and stored in sterile glass bottle at 4°C. For working

stock, the 10 ml of 10X stock PBS solution was diluted to 100 ml with sterile ultrapure water.

3.7 Cell lines

The human medulloblastoma cell lines Daoy, D283, D425 and HD-MB03 and the Human Embryonal Kidney cell line HEK293FT were used in this study. The cell lines Daoy and D283 were procured from the American Type Culture Collection (ATCC), Manassas, VA, USA. The cell lines D341 Med and D425 were kind gift from Dr. Darell Bigner, Duke University Medical Centre, Durham, NC, USA. Dr. Till Milde, German Cancer Research Center (DKFZ), Heidelberg, Germany, gifted the recently established cell line HD-MB03. The Human Embryonal Kidney cell line HEK293FT was procured from the Thermo Fisher Scientific, Waltham, MA, United States. The cell lines were characterized for the subgroup-specific gene expression using a real-time RT-PCR assay as described earlier (Thesis, Pooja Panwalkar), and accordingly their subgroup has been assigned. The cell line Daoy has high expression of gene *HHIP* and low expression *OTX2*. Moreover, the tumor from which the cell line was established was found to have desmoplastic histology. All these characteristics are known to be associated with SHH subgroup medulloblastoma. Thus, the cell line Daoy belongs to the SHH subgroup medulloblastoma. The cell lines D283 overexpress MYC without amplification of MYC locus, whereas the cell line D425 and HD-MB03 have MYC overexpression due to *MYC* locus amplification. These cell lines harbor isochromosome 17q (*i17q*) chromosomal aberration which is known to be associated with Group 3 and Group 4 medulloblastomas. Also, the genes specific to Group 3 medulloblastomas, like IMPG2, CRX and NPR3 are expressed in these cell lines. Thus, the cell lines D425 and HD-MB03 belongs to the Group 3 medulloblastomas (Thesis- Pooja

Panwalkar). D283 however has been reported both as a group 3 [92] and group 4 [93] cell line and is likely to have intermediate characteristics. HD-MB03 is the relatively recently established cell line characterized as Group 3 cell line. All the cell lines that has been used in the study have been recently authenticated by Short Tandem repeats (STR) profiling (Thesis, Harish Bharambe).

3.8 Routine maintenance of cell lines

Cell culture have been strictly been performed by using sterile cell culture grade glassware and plastic ware. All the cell culture operations were performed inside the laminar flow cabinets in the designated area. All the working reagents were brought to room temperature prior to their use.

The cell lines Daoy and HEK293FT grow in adherent manner and were cultured in DMEM medium supplemented with 10 % FBS. The cell lines D283 and HD-MB03 grow in semi-adherent manner whereas the cell line D425 grow in suspension manner and form clumps. These cell lines were cultured in DMEM/F12 medium supplemented with 10 % FBS. The cells were maintained at 37^{o}C, in a humidified chamber with 5 % carbon dioxide (CO_2). For routine maintenance, the cells were passaged at 70-80 % confluence and were splitted and seeded as per the need of the experiments. The cells were passaged at least twice a week and all the experiments were carried out within 10-12 passages after revival of the cells from the frozen stocks.

3.8.1 Maintenance of adherent cell lines

1. At 70-80 % confluence, the spent medium was aspirated from the culture dish/flask using a sterile Pasteur pipette and the cells were rinsed twice with sterile 1X PBS to remove the traces of the medium.

   The quantity of 1X trypsin sufficient to cover the surface of cell layer was added to the plate (2 ml for 60 mm dish or 4 ml for 100 mm dish). About 80 % of the added trypsin volume was aspirated from the plate leaving behind a thin layer of trypsin. The plate was transferred to the incubator until the cells become spherical in shape.

2. The trypsinized cells were collected in complete medium and transferred to a centrifuge tube using a sterile pipette. The cell suspension was centrifuged at 600g/1000 rpm in a moving angle centrifuge for 3-5 min.
3. The supernatant medium was gently aspirated using a Pasteur pipette without disturbing the cell pellet.
4. The cell pellet was dislodged by gently tapping the tube and the cells were suspended in fresh complete medium. The suspended cells were then transferred to the new culture dish and were seeded at desired confluence.

3.8.2 Maintenance of suspension cell lines

1. After attaining 70-80 % confluence, the cells are dislodged from the surface and the cell suspension was transferred to the centrifuge tube with the help of a Pasteur pipette.
2. The cell suspension was centrifuged at 600g/1000 rpm in a moving angle centrifuge for 3-5 min.

3. The supernatant medium was gently aspirated using a Pasteur pipette without disturbing the cell pellet.
4. The cell pellet was dislodged by gently tapping the tube and the cells were suspended in fresh complete medium. The suspended cells were then transferred to the new culture dish and were seeded at desired confluence.
5. The cell counting of the single cell suspension of both the type of cultures were done using a Neubauer's Haemocytometer.

3.8.3 Cryopreservation and revival of cell cultures

Cryopreservation is a method by which the cells are preserved by cooling them to very low temperature in presence of a preservative for their long-term storage. This helps avoiding loss of cultures due to contamination. The cells could be revived from the frozen stocks whenever required. For the optimal revival of the cell culture, usually healthy cells in log phase of growth are frozen.

Freezing medium: Complete medium supplemented with 10 % Dimethyl sulfoxide (DMSO) was used as a freezing medium. The prechilled freezing medium was used for cryopreservation.

Method for cryopreservation:

1. For cryopreservation, cells are harvested by above mentioned method upon attaining 70-80 % confluence.
2. The cell suspension was centrifuged at *600g/1000 rpm* in a moving angle centrifuge for 3-5 min.

3. The supernatant medium was aspirated using a Pasteur pipette without disturbing the cell pellet. The cell pellet was dislodged by gently tapping the tube and the cells were kept on ice.
4. The cells were immediately suspended in chilled cell freezing medium to form a single cell suspension. The suspended cells were then transferred to labelled and pre-chilled cryopreservation tubes. The cryotubes were then allowed to cool gradually by keeping them in $0^{o}C$ cooler at $-80^{o}C$ overnight. The tubes were further transferred in vapor phase of liquid nitrogen for long term storage. The cryotubes were properly labelled mentioning the cell type, passage number, date and the name of the handling personnel and position of tube storage in the cryo-container was documented.

3.8.4 Method for revival of frozen cell stocks:

1. The cryovial containing the appropriate cell stock was taken out from the cryo-container and the content of the tube was rapidly thawed by immediately placing the tube in water bath maintained at $37^{o}C$. As soon as the cell suspension was thawed, the tubes was removed from the water bath, wiped with 70 % ethanol solution and was then brought inside the laminar flow cabinet.
2. The cell suspension was the immediately transferred to the centrifuge tube containing 4 ml of the complete medium using a Pasteur pipette and mixed well by gentle pipetting.
3. The cell suspension was centrifuged at *600g/1000 rpm* in a moving angle centrifuge for 3-5 min.
4. The supernatant medium was gently aspirated using a Pasteur pipette without disturbing the cell pellet. The cell pellet was dislodged by gently tapping the tube and

the cells were suspended in fresh complete medium. The suspended cells were then transferred to the new culture dish. 24 h after plating, the spent medium was replenished with fresh complete medium and the cells were further passaged after attaining 70-80 % confluence.

3.8.5 Detection of mycoplasma contamination in cell culture:

Mycoplasma has been known since decades as the most common contaminant found in cell cultures throughout the academic laboratories and laboratories of biopharmaceutical industries. Depending on the laboratory, it is estimated that around 15-85% of the cultures are contaminated with mycoplasma. Nevertheless, mycoplasmas can have deleterious effects on eukaryotic cells, as they can alter every cellular function (proliferation, protein synthesis, susceptibility to viral infection, etc.). Thus, such alterations can lead to improper behavior of the cells during the conducted experiments and consequently to the improper results and conclusions from any experiment.

The cell populations used in this study were periodically checked for the mycoplasma free status to ensure true reproducible results. The mycoplasma status was assessed by PCR based assay described earlier [94, 95].

Rapid isolation of genomic DNA from cultured cells

Reagents

1) Solution A (Genomic DNA Extraction Buffer):

Stock solution	For 50 ml	For 10 ml	For 5 ml	For 2 ml	Final conc.
1 M Tris-Cl, pH 9.0	5 ml	1 ml	500 µl	200 µl	100 mM

0.5 M EDTA, pH 8.0	10 ml	2 ml	1 ml	100 µl	100 mM
20 % SDS w/v	2.5 ml	0.5 ml	250 µl	100 µl	1 % w/v
Sterile ultrapure water	32.5 ml	6.5 ml	3.25 ml	1.6 ml	

2) *8 M Potassium acetate*: 39.26 g of potassium acetate was dissolved in 10 ml of ultrapure water and the final volume of the solution was adjusted to 50 ml with ultrapure water. The solution was sterilized by autoclaving and stored at room temperature. (Note: Potassium acetate is highly deliquescent substance, thus weighing should be carried out quickly. The weighed potassium acetate should not be exposed to air for long and must be quickly dissolved in the solvent.)

All centrifugation steps were carried out at room temperature (RT) unless specific temperature required in certain steps is mentioned.

1. After harvesting, the cells were collected in 1.5 ml centrifuge tube. The cells were washed with 1X PBS and centrifuged at *800g/2000 rpm* in a table top centrifuge. The supernatant was discarded and the cell pellet was loosened by gently tapping the tube.
2. 500-1000 µl of solution A (1 ml buffer per 1-5 X 10^6 cells) was added to the cells and was mixed gently by inverting the tubes several times.
3. The lysate was then incubated at 72^{o}C for 30 min with intermittent mixing of the contents every 10 min.
4. 140 µl of 8 M potassium acetate solution was added per 1 ml of the cell lysate, mixed rapidly and incubated on ice for 30 min.
5. The samples were then centrifuged for 10 min at *12000 rpm*.

6. The supernatant was transferred to a fresh 1.5 ml centrifuge tube using a cut pipette tip. The samples were centrifuged for 10 min at *12000 rpm*.
7. The gDNA was precipitated by adding 0.7 volume of isopropanol and centrifugation at *12000 rpm* for 15 min.
8. The DNA pellet was washed twice with 70% ethanol. The pellet was air-dried and dissolved in 50-100 µl of TE buffer containing 1 µg/ml of RNase A. The samples were incubated at 37^{o}C for 1 h to degrade the RNA. The DNA was further used for restriction digestion or as a template in PCR reactions.

PCR for the detection of mycoplasma

For the detection of mycoplasma contamination, PCR reactions were set up using the gDNA extracted from the cells as template. The primers for detection of commonly found strains of mycoplasma and acholeplasma were adopted from [94, 95]. A pool of six forward primers and three reverse primers each added at the concentration of 10 pmol/µl was prepared and used in PCR reactions. Genomic DNA isolated from the cell line previously known to be contaminated with mycoplasma was used as a positive control. Also, to show whether the extracted gDNA was of PCR quality, a PCR reaction was set up for each sample gDNA using a separate known set of primers routinely used in lab.

Primers	Sequence	
Forward	CGCCTGAGTAGTACGTTCGC	Used as primer pool of all forward primers in 10 pmol/µl concentration each
	CGCCTGAGTAGTACGTACGC	
	TGCCTGAGTAGTACATTCGC	
	TGCCTGGGTAGTACATTCGC	
	CGCCTGGGTAGTACATTCGC	
	CGCCTGAGTAGTATGCTCGC	
Reverse	GCGGTGTGTACAAGACCCGA	Used as primer pool of all reverse primers in 10 pmol/µl concentration each
	GCGGTGTGTACAAAACCCGA	
	GCGGTGTGTACAAACCCCGA	

1. All the reagents including 10X Standard Taq Buffer without MgCl2, 10 mM dNTP mix, forward and reverse primer pools, and Taq DNA polymerase were thawed and kept on ice.
2. The PCR reaction was assembled as below:

Component	Volume	Final concentration
10X Taq DNA Polymerase Buffer	2 µl	1X
25 mM $MgCl_2$	1.2 µl	1.5 mM
10 mM dNTP mix	0.4 µl	0.2 mM
Forward primer pool	1 µl	0.2 µM each
Reverse primer pool	1 µl	0.2 µM each
Template DNA (25 ng/µl)	2 µl	50 ng

Taq DNA Polymerase 1U/µl	0.5 µl	0.25 U
Nuclease Free Water	11.9 µl	To make up total volume to 20 µl

Depending upon the number of samples, a master mix was prepared by scaling up the reaction.

3. The PCR cycling parameters were set in the Thermal cycler as follows:

Step	Temperature	Time	No. of cycles
Initial denaturation	95°C	5 min	1
Denaturation	95°C	45 sec	35
Annealing	65°C	30 sec	
Extension	72°C	1 min	
Final extension	72°C	10 min	1
Hold	4°C	∞	

4. 10 µl of each PCR product was electrophoresed on 1 % Agarose gel and the results were assessed based on the presence or absence of the band around 500-520 bp in the samples.

3.8.6 Transient transfection of 293ft cells using BES buffer for lentivirus production:

Transfection of plasmid DNA into HEK293FT cells was carried out using the BES buffer by the method of calcium precipitation. This method of transfection have been used for the

generation of lentiviral particles, stable expression of microRNAs and for the validation of microRNA targets by Luciferase reporter assay that are discussed in the following sections.

Reagents

2 X BBS (BES buffered saline): [50 mM BES, 280 mM NaCl, 1.5 mM Na2HPO4] For 50 ml BBS, 0.533 g BES (Sigma B4554-25G), 0.818 g NaCl (S.D. Fine Chemicals Product No.- 20241 AR) and 0.0134 g Na2HPO4.2H2O (S.D. Fine Chemicals Product No. 20383 AR) were dissolved in 45 ml of autoclaved milli-Q water and the pH was adjusted to 6.95 using 5 M NaOH. The final volume was made up to 50 ml and the pH was checked again. The solution was filtered through a 0.22 μm filter (Millipore) and stored as 0.5 ml aliquots at -20°C.

0.5 M Calcium Chloride [CaCl2]: 3.675 g CaCl2 .2H2O (Sigma C-3306) was dissolved in 45 ml of autoclaved Milli-Q water. The volume was made up to 50 ml and filter sterilized using

0.22 μm filter and stored as aliquots of 0.5 ml at -20°C.

The reagents were thawed at R.T. beforehand. Plasmid DNA used for transfection were purified using QIAGEN plasmid purification midi kit (QIAGEN, Hilden, Germany).

Method

1. 2×10^5 HEK293 cells were seeded in a 35 mm tissue culture plate one day prior to the day of transfection.
2. On the next day, the medium of the plate was changed 4 hrs prior to transfection.

3. The required volume for 6 µg of Qiagen column purified plasmid DNA was added to a sterile eppendorf tube and the volume made up to 50µl with sterile M.Q. water. 50µl of 0.5 M CaCl2 was added dropwise to the tube. 100µl of 2 X BBS was then added dropwise to the tube and mixed by gently pipetting it up and down for 2-3 times. The mixture was then incubated at R.T. for 20 min.
4. The mixture was added on the cells and the plate was swirled gently to allow proper mixing.
5. 16 hrs after transfection, the medium of the plate was changed. The cells were used for further assays or for extraction of RNA. The number of cells and the amount of DNA is scaled up proportionately and used for transfection in 55 mm plates or 90 mm plates.

3.8.7 Generation of lentiviral particles and selection of stable polyclonal populations of medulloblastoma cell lines

The effects of expression of these miRNAs in the medulloblastoma cell lines were studied by generating stable polyclonal populations of medulloblastoma cell lines and studying cell growth and malignant behavior by performing different cull culture assays. Lentiviral particles containing pTRIPZ vector cloned with genomic regions expressing miR-592 or miR-204 or pTRIPZ vector alone were generated and used to transduce medulloblastoma cells which were then selected in the presence of puromycin. The lentiviral particles were generated as follows:

All the procedures involving the use of lentiviral particles were approved by institutional biosafety committee of ACTREC-TMC. All the procedures were performed in certified biosafety level 2 laminar flow cabinet (Esco Technologies, Hatboro, PA, USA). The

infected cell cultures/contaminated plasticware and fluids were decontaminated using 10 % sodium hypochlorite solution and autoclaved in biohazard bags prior to disposal. For generation of lentiviral particles, HEK293FT was used as packaging host cell line and the second-generation packaging plasmids psPAX2 (coat), and pMD2.G (envelope) were used (psPAX2, Addgene plasmid # 12260 and pMD2.G, Addgene plasmid # 12259, was a gift from Dr. Didier Trono). pAdvantage vector (Promega, Madison, WI, USA) was used for enhancing the efficiency of transient protein expression in host cells.

Method:

1. 6-7 X 105 HEK293FT cells were seeded in 60 mm culture dish form a 70-80 % confluent plate one day prior to the transfection. The plate should be 50-60% confluent at the time of transfection.
2. The spent medium was replaced with the fresh complete medium 4 h before the transfection.
5. The cells were transfected with a total 12 µg of plasmid mixture consisting of transfer plasmid, coat plasmid and envelope plasmid in the ratio of 4:3:1. (6 µg of Transfer plasmid-pTRIPz-miR-592/pTRIPz-miR-204/pTRIPz empty, 4.5 µg coat plasmid psPAX2 and 1.5 µg of envelope plasmid pMD2.G)
3. Appropriate volumes of the plasmids were mixed in a sterile 1.5 ml centrifuge tube and the plasmid DNA mixture was diluted up to 100 µl using sterile ultrapure water.
4. 100 µl of 0.5 M CaCl2 solution was added dropwise to the plasmid mixture. (The contents of the tube were not mixed at this step.)

5. 200 µl of 2X BES Buffered Saline (2X BBS) solution was added to the tube dropwise to form a total of 400 µl of the transfection mixture. The content of the tube was mixed gently 2-3 times by pipetting.

6. The mixture was incubated for at least 20 min at room temperature (not more than 40 min).

7. The DNA-calcium phosphate complexes were then added dropwise to the HEK293FT cells, mixed gently by swirling the contents of the plate and then the cells were incubated at 37oC in a CO2 incubator.

8. The medium was replaced with fresh complete medium 16-18 h after transfection.

9. The lentivirus containing cell culture supernatant was collected at 48 h and 72 h post transfection, centrifuged at 600g/1000 rpm at RT for 5 min in a moving angle centrifuge and filtered through 0.45 µ syringe filters.

10. The filtered supernatant was either directly used for transduction or subjected for concentration in the ratios of 5:1 – 10: 1 by ultracentrifugation at 26500 rpm at 4oC for 90 min.

11. For long term storage, the virus containing supernatant was made in to aliquots and stored at -80^{o}C until further use.

12. In order to determine the viral titre 50,000 HEK293 cells were seeded in a 35mm dish. The filtered viral supernatant was serially diluted from 1:10 to 1:1000 and 1 ml of the different dilutions was used for transduction. The medium was changed 16 hrs post transduction and cells were induced with 4 µg / ml of doxycycline. 48 hrs post induction, RFP expression was confirmed by microscopic examination of the cells. The cells were then processed for flow cytometry analysis (FACS Calibur, B.D. Biosciences, USA) to

determine the number of RFP positive cells. The viral titre was determined by the formula [(50,000 × % of RFP positive cells) / 100] × dilution factor.

Selection of the stable polyclonal population of medulloblastoma cells:

1. The selection of miRNA expressing clones was carried out by transduction of the medulloblastoma cell lines with the neat, diluted or concentrated viral supernatant. 1ml of viral supernatant was added to a 35 mm dish containing 50,000 Daoy or D425 cells or 1×10^5 D283 or HD-MB03 cells. 4 μg / ml polybrene was added to the plate to increase the efficiency of transduction. 16 hrs post transduction the medium was changed and fresh complete medium was added to the cells.
2. 48 h after transduction the cells were trypsinised and added to a 55mm dish and the necessary amount of puromycin (250 ng / ml for Daoy, 200 ng / ml for D283, D425 and HD-MB03 cells) was added to select the cells.
3. After 3 doses of puromycin the selected cells were induced with 2-4 μg / ml doxycycline to determine the level of expression of miRNA in the cells. RNA was extracted from the cells and the level of miRNA expression was studied by real time RT-PCR as described in section 3.4. Stable polyclonal populations of pTRIPZ vector alone were also selected in a similar manner. These cells were used for studying the effect of the miRNA expression on the growth characteristics of the cells in the soft agar assay, MTT assay, clonogenic and radiation sensitivity assay, invasion assay and in-vivo tumorigenicity assay.

3.8.8 MTT Cytotoxicity assay:

The effect of expression of miR-592 and miR-204 on the proliferation potential of the medulloblastoma cells was studied by performing the MTT cytotoxicity or cell proliferation assay. It is a colorimetric assay that measures the conversion of the tetrazolium dye to insoluble formazan crystals by living cells. Thus, this assay could be used for the assessment of cytotoxicity, cell growth and proliferation [96].

Reagents

1) MTT solution (5 mg/ml): 50 mg of MTT powder (3-(4,5-dimethylthiazol-2-yl)-2,5-diphenyltetrazolium bromide) was dissolved in 10 ml of 1X PBS. The solution was stored at 4oC protected from light in 1 ml aliquots.

2) Acidified 10% Sodium dodecyl sulfate (SDS) solution: 10 gm of SDS powder was dissolved in 75 m of sterile ultrapure water. The dissolution was assisted by keeping the bottle at 60oC for 1 h. 86.4 µl of concentrated HCl was added to the solution (final concentration of HCl-0.01N). The final volume of the solution was adjusted to 100 ml with sterile ultrapure water. The solution was stored at RT.

Method:

1. The vector control and P1, P2 polyclonal populations of Group 3 medulloblastoma expressing the miRNA were treated with 4 µg/ml of doxycycline for 48 h.

2. 1000 cells of each polyclonal population treated with doxycycline and 500 cells/well of Daoy cells were seeded per well of 96 well plate in 100 µl of complete medium. The cells were seeded at least in triplicate for each time interval.

3. 50 µl of doxycycline containing medium was replenished every 48 hours.

4. 20 µl of MTT solution was added to the wells at the intervals of 48/72 h and the plate was incubated for 4 h at 37^{o}C in CO_2 incubator to allow the formation of formazan crystals.

5. The formazan crystals were dissolved by the addition of 100 µl of acidified 10 % SDS solution to each well with overnight incubation in CO_2 incubator.

6. The optical density of the wells was measured using ELISA plate reader at 540 nm wavelength against the reference wavelength of 690 nm.

7. The growth of the cells was calculated as follows:

Percent Growth = (O.D. Day 8/10 – O.D. Day 0) / O.D. Day 0 *100

8. The Growth curves of the cell populations were plotted as line charts in GraphPad Prism v6.0 software.

3.8.9 Soft Agar colony formation assay:

Soft agar colony formation assay was performed for studying the effects of expression of microRNAs on the anchorage independent growth potential of the cells. The cells were seeded in suspension manner in semi-solid matrix of 0.3 to 0.4 % agarose over a basal layer of 1 % agarose in complete medium.

Materials:

1. <u>2% Low melting point (LMP) agarose solution:</u> 1 gm of low melting point agarose was added to 50 ml of ultrapure water and dissolved by microwaving. The solution was further sterilized by autoclaving. The solution was taken out from the autoclave before solidifying and stored in water bath set at 42^{o}C with constant shaking.

2) <u>2X Complete DMEM/F12 medium</u>: To 80 ml 2X DMEM/F12 medium, 20 ml of FBS and 1 ml of 100X antibiotic-antimycotic solution was added.

3) 1X complete medium supplemented with 10 % FBS:

Method

1. The vector control and miRNA expressing polyclonal populations of medulloblastoma cell lines D283, D425, HD-MB03 and Daoy were treated with doxycycline 72 h before seeding for soft agar colony formation assay.

2. 2X Complete medium and 2 % LMP agarose solution were mixed in equal proportions to make 1X complete medium containing 1% agarose. The basal layer was prepared by pouring 1 ml of this mixture in a 35 mm dish. The medium was uniformly spread by swirling the dish and the basal layer was allowed to solidify at RT for at least 1 h.

3. The cells of each uninduced and doxycycline induced polyclonal population were harvested. The cell suspension was serially diluted with complete medium to obtain 1 X 10^4 viable cells per ml of medium.

4. 1000 cells per plate of each uninduced and doxycycline induced polyclonal population were seeded in a layer containing 0.4 % agarose in 1X complete medium. Cells of each polyclonal population were seeded in triplicate. In case of Daoy cells, 7500 cells were seeded.

5. For cell seeding in triplicate, the components were mixed thoroughly as follows:

400 µl of the cell suspension (1 X 10^4 cell per ml) + 2 ml of 1X complete medium + 800 µl of 2X complete medium + 800 µl of 2 % LMP agarose solution. (4 µg/ ml doxycycline containing medium was used for seeding induced polyclonal populations.)

6. 1 ml of the above mixture was immediately poured and spread over the previously prepared basal layer.

7. The upper layer was allowed to solidify at RT for at least 30 min before transferring the plates to CO2 incubator.

8. The cells were fed with 100-200 µl of 1X complete medium (containing doxycycline for induced populations) after every 48 h.

9. The colonies containing at least 20 cells were counted from each plate after 10-15 days of seeding. The average colony count for each polyclonal population from three sets of experiment was plotted as a bar chart in GraphPad Prism v6.0 software. The significance of the differences was assessed by student's t-test.

3.8.10 Boyden chamber Invasion assay:

Invasion potential of the miRNA expressing medulloblastoma cells as well as the doxycycline treated vector control cells were assessed by studying their potential to invade through the Matrigel coated transwell inserts.

Materials

1. Matrigel: (10 mg/ml-5ml pack size, BD Life Sciences, Cat. No- 356234) This was diluted to 1 mg/ml in plain 1X DMEM and aliquoted as 100 µl volume aliquots and was stored at - 70°C. Fresh aliquot was taken out and diluted and thawed every time. Repeated freeze thawing is not advisable.

2. 8-µm pore size transwell inserts (Cat No-353097, BD Biosciences, San Hose, CA, USA)

3. 24 well plate

4. 96 well dish

5. Calcein AM (1µg/µl in 100% DMSO) (Cat. No- 206700, Calbiochem)

6. Hickman Buds (local make) or Ear buds (Johnson and Johnson Pvt Ltd)

Method:

1. 8 µm pore size transwell insert was placed into the 24 well-plate custom-designed to accommodate these inserts.

2. Membrane on the inner side of the transwell insert was washed 2-3 times with 1X DMEM or 1X DMEM/F12.

3. Matrigel (stock 1 mg/ml) was diluted to 300 µg/ml on ice and 100 µl of the same (30 µg in total) was added over the inner side of the transwell insert carefully so that bubbles are not formed.

4. Plate was incubated at 37^0C for 1 hr to allow matrigel to polymerize.

5. Un-polymerised matrigel is removed and 50000 cells of Daoy or 75000 cells of D283 and HD-MB03 were seeded in 200 µl of 1X DMEM. In case of doxycycline treated cells, cells were treated with doxycycline for 72 hr prior to seeding for invasion assay.

6. 750 µl of complete medium was added in lower chamber which served as chemoattractant. Doxycycline was also added in the upper and lower chamber medium in case of doxycycline induced cells.

7. 5000 cells from the mastermix of cells prepared for seeding in transwell insert were seeded per well of 96 well black plate, in duplicates. This was done to determine initial cell number seeded for invasion assay for each polyclonal population either doxycycline treated or untreated.

8. After ~6-8 hr once these cells have adhered to the plate surface, medium was replaced with fresh medium that is supplemented with Calcein AM (1 µg/µl stock concentration)

with final concentration of 2 µg/ml of medium. The plate was incubated for minimum of 30 min at 37°C.

9. Fluorescence was read with excitation at 485 nm and emission at 535 nm with 0.1 or 0.5 sec as exposure time, Lamp energy 5000, position-top, reading by plate as additional settings, using Mithras LB940 multimode reader (Berthold Technologies, Germany). The average fluorescence measured for 5000 cells of uninduced vector control or respective polyclonal population was taken as control fluorescence reading to normalize the total fluorescence of invaded cells of respective doxycycline induced vector control or polyclonal populations to account for the differences in cell number resulted while seeding.

10. Daoy, D283 and HDMB03 cells were allowed to invade for 36 hr,56 hr and 72 hr respectively. 30-60 min prior to the end of this incubation period, Calcein AM at final concentration of 2 µg/ml was added in the lower chamber medium of transwell insert and incubated for minimum of 30 min at 37°C. For example, 1.6 µl of Calcein AM (1 µg/µl) was first mixed with 50 µl of complete medium, which was then added to lower chamber medium by lifting the insert momentarily.

11. After incubation, membrane of transwell insert was wiped from inside by hickman cotton plug to remove non-invaded cells off the membrane and placed back. Five microscopic images representing all quarters and the centre of each insert were captured using Zeiss Axiovert 200M fluorescence microscope at magnification of 40X (4X objective and 10X of eyepiece).

12. The membrane was then cut with blade gently without disturbing cells on the outer side of the membrane and placed into a well of 96 well plate.100 µl of complete medium was added not to let membrane dry. Fluorescence was read as described in step 9.

13. In case of D283 cells, some proportion of invaded cells does not remain adhered to the membrane but remain in the lower chamber medium. To account for this population of invaded cells, lower chamber medium was centrifuged at 3000 rpm at 5 min to pellet down the cells. Cell pellet was resuspended in 100 µl of complete medium and fluorescence was read as described in step 9. Total fluorescence was calculated from the fluorescence values belonging to lower chamber cells and cells from insert membrane.

14. Total fluorescence measured was normalized to account for the differences in cell seeding as stated in step 9. Difference in normalized fluorescence between doxycycline treated vector control and miRNA expressing population was compared using Student's t test.

3.8.11 Radiation and chemosensitivity assays:

Group 3 medulloblastoma cell lines grow in a semi or non-adherent manner. Therefore, the effect of miRNA expression on the radiation sensitivity or chemosensitivity of the medulloblastoma cell lines were studied by performing MTT assay

For radiation sensitivity assays, the cells were irradiated at different doses and their effects have been observed for the next eight to ten days to analyse if there is a faster cell death or higher sensitization of the miRNA expressing cells to the radiation induced cell death or not.

Method for radiation sensitivity assay:

1. The vector control and miRNA expressing polyclonal populations of Group 3 medulloblastoma cells were treated with 4 µg/ml of doxycycline.

2. 2000-2500 cells of each polyclonal population treated with doxycycline were seeded per well of 96 well plate in 100 µl of complete medium. The cells were seeded at least in triplicate for each time interval.

3. The cells in 96 well plates were irradiated at the doses of 2 Gy, 4 Gy and 6 Gy using Bhabhatron, an indigenously developed telecobalt machine developed by Bhabha Atomic Resarch Center, Mumbai, India. An untreated plate was kept as control.

4. 50 µl of doxycycline containing medium was replenished 24 h post irradiation and 48 h time interval henceforth.

5. 20 µl of MTT solution was added to the wells at 0 day (Immediately after irradiation), 3-day and 6-day time points. After the addition of MTT, the plates were incubated for 4 h at 37^{o}C in CO2 incubator to allow the formation of formazan crystals.

6. The formazan crystals were dissolved by the addition of 100 µl of acidified 10 % SDS solution to each well with overnight incubation in CO_2 incubator.

7. The optical density of the wells was measured using ELISA plate reader at 540 nm wavelength against the reference wavelength of 690 nm.

8. The growth of the cells was calculated

Percent Growth= (O.D. Day 8/10 – O.D. Day 0)/ O.D. Day 0*100

9. The effect of irradiation was calculated by normalizing the growth of irradiated cells with that of the untreated cells. The data was represented as line charts in GraphPad Prism v6.0 software.

10. The D_0 dose of radiation (the dose of radiation required to reduce the surviving population to 37 %) was calculated from the Graph [97].

Method for chemo sensitivity assay:

1. In order to perform the chemosensitivity assays, the common drugs that are used in the treatment of medulloblastoma have been used. The drugs are selected such that their mechanism of action for killing the cells is different.

i) Cisplatin (Kemoplat 10 mg injection from Dabur) crosslinks DNA in several different ways, interfering with cell division by mitosis. The damaged DNA elicits DNA repair mechanisms, which in turn activate apoptosis when repair proves impossible.

ii) Etoposide (POSID 100mg 5 ml injection from Cadila Pharma ltd) forms a ternary complex with DNA and the topoisomerase II enzyme (which aids in DNA unwinding), prevents re-ligation of the DNA strands, and by doing so causes DNA strands to break.

iii) Vincristine (Cytocristin 1mg Cipla) binds to tubulin dimers, inhibiting assembly of microtubule structures and arresting mitosis in metaphase.

2. Group 3 medulloblastoma cell lines D283 and D425 were treated with different doses of the drugs and the dose that led to 40 to 60% cell death was selected for the further experiments. The selected doses were found to be 3µM for cisplatin, 2µM for etoposide and 2 and 0.2µM Vincristin for D283 and D425 cells respectively.

3. The vector control and the miRNA expressing cells were plated at the density of 4000 cells/ well (triplicate) in a 96 well plate. The 0-day MTT reading was taken to ensure equal seeding. Untreated cell populations were also kept to be used as a control with which we can compare the cell death occurring in the vector control as well as the test cells.

4. Drugs were added the next day.

5. After treatment of the cells with cisplatin and etoposide for 48hr and vincristine for 60 hr (the time point at which ~60% cell death takes place), MTT reading was taken by following the protocol of MTT assay (described in section 3.8.8). and the percentage of cell death was measured.

3.8.12 Treatment of the cell lines with Rapamycin, UO126 and chloroquine:

The vector control and miRNA expressing polyclonal populations of medulloblastoma cell lines D283, D425 and HDMB03 were induced with doxycycline for 72 hours and seeded at a density of 1 X 10^5 per 60 mm dish. Next day when they reach almost 70 % confluency, they were treated with 100nM/ml of Rapamycin (Calbiochem, Catalogue no. 553210) for 2 hours for the inhibition of the mTOR activity, 30µM/ml of UO126 (Cell Signaling Technology, Catalogue No. #9903) for 6 hours for the selective inhibition of MEK1 and MEK2. In addition to these cell lines, D341 and Daoy was also treated with 32 µM/ml chloroquine (Lariago injection, IPCA laboratories, Catalogue No. FC6L05) for 1 hour. After the treatment for the given duration of time, protein was extracted from the cells and western blotting analysis for the desired protein was performed.

3.8.13 In vivo tumorigenicity assay

In order to analyze the effect of the expression of miR-592 upon the in-vivo tumorigenic potential of the cells, orthotopic medulloblastoma xenograft in immunodeficient mice was generated by using stereotactic method of intracranial injection. All the experimental procedures involving animals were performed with prior approval of Institutional Animal ethics committee.

Reagents:

1) Anaesthetic agents (Ketamine hydrochloride injection and Xylazine hydrochloride injection)

2) Analgesic agents (Buprenorphine, Neon Laboratories, India, Meloxicam, Intas Pharmaceuticals, India)

3) Sterile ocular lubricant (Neosporin ointment, Neon Laboratories, India)

4) 1X PBS, sterile

5) 70% ethanol

6) Bone cement (Cat. No. W810, Ethicon Inc, Johnson & Johnson Ltd)

7) Tissue adhesive - VetBondTM (n-butyl cyanoacrylate) Cat. No. 1469SB, 3M Animal care

8) products, St Paul, MN, USA)

9) Doxycycline capsules (Biodoxi 100 mg capsules, Biochem Pharmaceuticals, India)

10) 5 % Sucrose solution (w/v)

11) Isoflurane (Forane injection, Abbott Laboratories, India or Aerrane injection, Baxter International, IL, USA)

12) D-luciferin, potassium salt (Cat. No. L8220 Biosynth AG, Switzerland): 3 mg/100 µl solution in 1X sterile PBS. 30 mg of D-luciferin, potassium salt was dissolved in 1 ml of sterile 1X PBS. The solution was stored on ice protected from light until used for injection. The solution was prepared fresh before use.

13) Sterile 1X PBS

14) 70 % Ethanol

Equipments:

1) Small animal stereotaxic frame, Ultra Precise Just for Mouse Stereotaxic Instrument, 51730U, Stoelting, Wood Dale, IL, USA

2) Syringe needle 30G

3) Hamilton Glass syringe, Model 710 SN, 80868, 100uL Customized Syringe Fixed Needle, Needle length: 2 inches, Needle diameter: 26 Gauge, Point style: 4, Angle of Bevel: 45o

4) Sterile cotton buds

5) Surgical instruments including Fine forceps, Iris Scissors, Blunt forceps, sterile scalpel blades.

6) Electric microdrill and non-corrosive surgical grade steel drill bits (Ideal Micro Drill Kit, Cat. No.67-1000, Cell Point Scientific, Gaithersburg, MD, USA)

7) Regulated heating pad/chamber (with thermometer)

8) Electric clippers

Instrument:

1) IVIS Spectrum In Vivo Imaging System, (Caliper Life Sciences) Perkin Elmer, Waltham, MA, USA.

2) Small animal Veterinary Isoflurane Vaporizer

3) Anesthesia induction chamber

Animal type and strain used:

Immunodeficient mice: NOD/SCID (NOD/NcrCrl-Prkdcscid) received from The Jackson Laboratory, Charles River, USA.

Age and gender of animal:

6-8 weeks old both male and female animals were used.

Method:

1) For intracranial orthotopic injections D425 cells expressing empty pTRIPZ or pTRIPZ miR-592a construct were transduced with lentiviral particles of pCS-CG vector (a gift from Dr. Inder Verma), Addgene plasmid #12154 [98] expressing firefly luciferase cDNA FL2 (from pCAG-luciferase vector, a gift from Snorri Thorgeirsson), Addgene plasmid #55764 [90].
2) 2 X 10^5 doxycycline-induced cells were injected into the cerebellum of NOD/SCID mice (NOD CB17-*Prkdc*^{scid}/NCrCrl, Charles River, USA) through 0.5 mm burr hole in the midline, 2 mm posterior to lambda at 2 mm depth, under Ketamine (90 mg/kg body weight) and Xylazine (20 mg/kg body weight) anesthesia using small animal stereotactic frame (Harvard Apparatus, MA, USA) [18].
3) To measure tumor growth, mice were injected of D-Luciferin (Biosynth) (150 mg/kg body weight) intraperitoneally and serial images of the mice were captured under isoflourene anaesthesia (2% in oxygen) using IVIS Spectrum (Perkin- Elmer, MA, USA).

4) For quantification, “Living Image” software was used, the image with peak luciferase activity as seen by the photon output was selected and region of interest (ROI) was drawn manually around the luminescent source and expressed in radiance (photons/sec/cm2/steridian).
5) A pseudo-color image representing light intensity (blue least intense and red most intense) was generated and superimposed over the gray scale reference image.
6) Tumor bearing mice were maintained until they succumbed to the tumor or were about to succumb to the tumor as judged by over 40% loss of weight or other clinical symptoms. Kaplan Meier test was used for analysis of the survival data.
7) After the animals are sacrificed, their whole brain was collected and fixed in neutral buffered formalin and later it was embedded in a paraffin block. Hematoxylin and eosin stained sections of the paraffin blocks were used to determine the tumor margin if it is cohesive or if the cells are loosely spaced, which would give us an idea about the invasive capacity of the cells.

3.8.14 Luciferase reporter assay

The luciferase assay is performed to validate novel miRNA targets or already known targets of the miRNA. The genomic region encoding miR-592 was cloned in the pcDNA4 myc-His B vector (Thermo Fisher Scientific, Waltham, MA, USA) for expressing miR-592 in the HEK293FT cells. 3’-UTR of each of the potential miRNA target genes was amplified from genomic DNA of normal human peripheral blood lymphocytes using Phusion Taq polymerase. The 3’-UTRs were then cloned downstream of firefly luciferase cDNA from pGL3 vector in a pcDNA 3.0 plasmid vector (Method described in section

3.6.2 a). These constructs were used for evaluating the activity of miR-592 promoter by the luciferase reporter assay upon transient transfection into the HEK293FT cells. Further, the miR-592 binding sites in the 3′-UTRs were altered by the site-directed mutagenesis using the overlap extension PCR (as described in section 3.6.2b) [99]. The luciferase reporter constructs were transfected in the HEK293FT cells along with the Green Fluorescent Protein (GFP) expressing vector as a normalization control, with or without the miR-592 expressing construct, using the calcium phosphate BES buffer method. The luciferase activity was evaluated 72 h post-transfection using the Cytation 5 Hybrid Multi-mode reader (BioTek, Winooski, VT, USA).

Reagents for Luciferase assay:

a) Cell lysis Buffer

Component	Volume	Final Concentration
1M Glycine-glycine pH 7.8	1.25 ml	25Mm
1 M MgSO4	0.75 ml	15Mm
250mM EGTA	0.8 ml	4mM
Triton X-100	0.5 ml	1% (v/v)
100mM DTT	*	1 Mm
Autoclaved Milli-Q	Make up to 50ml	

b) Luciferase Assay Buffer

Component	Volume	Final Concentration
1M Potassium phosphate buffer pH 7.8	0.75 ml	15mM

1M Glycine-glycine pH 7.8	1.25 ml	25mM
1M MgSO4	0.75 ml	15mM
250mM EGTA	0.8 ml	4mM
100mM ATP	*	2mM
100mM DTT	*	1mM
Autoclaved Milli-Q	Make up to 50ml	

- *Note:* Add DTT and ATP just before use

c) Luciferin solution

Component	Volume	Final concentration
1M Glycine-glycine pH 7.8	1.25 ml	25mM
1 M MgSO4	0.75 ml	15mM
250mM EGTA	0.8 ml	4mM
20mM D-Luciferin	*	0.2mM
100mM DTT	*	2 mM
Autoclaved Milli-Q	Make up to 50ml	

- *Note:* Add DTT, ATP and D-Luciferin just before use

Method:

1. HEK293 cells were trypsinised, counted and seeded as $1x10^4$ cells per well of 96 well late.

2. 24 hr post seeding, transfection of total of 0.3 μg DNA per well of 96 well was done using BES buffer method (section 3.8.6).

3. DNA mixture was prepared in autoclaved Milli-Q as given below.

Component	Amount (for 1 well of 96 well plate)
3’ UTR reporter plasmid	250 ng

pcDNA4 / pCDNA4-miR-592	500 ng
pCS-CG	250 ng
Autoclaved Milli Q	12.5 µl
0.5M Cacl2	12.5 µl
2X BBS	25.0 µl

4. 72 hr after transfection, medium was removed and cells were washed twice with ice cold 1X PBS.

5. 30 µl of cell lysis buffer was added to each well of a 96 well plate. The cells were scraped from the plate and lysate was made homogenous by pipetting it up and down several times. The lysate was transferred to an eppendorf tube and stored on ice till the lysates for all the wells are prepared.

6. The eppendorf tubes were centrifuged at 16000 rpm at 4^0C for 5 min and the supernatant was transferred to fresh eppendorf tubes.

7. The fluorescence and luminescence were measured using Mithras LB940 multimode reader. 10 µl of sample was added per well of 384 well Optiplate (Cat No. 6007290, Perkin Elmer), and fluorescence was measured at excitation and emission wavelengths of 485 nm and 515 nm. Each sample was assayed in duplicates.

8. 30 µl of assay buffer containing luciferin solution (2:1) was added to each sample and mixed twice by pipetting. The luminescence was read immediately at an exposure time of 1 sec.

9. The readings were then normalized as compared to the normal GFP reading and the percentage decrease in the luciferase activity of the 3'UTR constructs in the presence of miRNA expression was been measured.

3.9 Protein extraction from cultured mammalian cells

Reagents:

10X PBS: (1.5 M NaCl, 89.8 mM Na2HPO4.2H2O, 28.8 mM NaH2PO4.2H2O). 90 g NaCl, 16g $Na_2HPO_4.2H_2O$, 4.5g $NaH_2PO4.2H_2O$ per litre: pH adjusted to 7.5 with 5 N NaOH, autoclaved and stored at room temperature. 10X stock was dilute to 1X with autoclaved Milli-Q water and stored at room temperature.

Lamelli buffer or 1X sample buffer: 62.5 mM Tris-HCl pH 6.8, 2% SDS, 10% glycerol. Total protein was extracted in sample buffer from cultured vector control and miRNA expressing cells that are treated with doxycycline after 72 hours.

Method:

1. The medium was poured off from the culture dishes and the cells were rinsed twice with 1X PBS gently.

2. The PBS was drained off completely and cells were lysed in 1X sample buffer. About 0.5 –0.6 ml sample buffer was used for protein extraction from 90 mm2 dishes with 80-90% confluency. The viscous lysate, due to release of genomic DNA along with proteins from the cells, was collected by swirling the plate several times and transferred into a 1.75 ml microfuge tube.

3. The tubes were immediately kept in a boiling water bath for 7 min, cooled to room temperature and centrifuged in Rota-4 R at 15,000 rpm for 1.5 hr at 20°C to pellet down the genomic DNA. The DNA pellets were discarded.

4. The supernatant lysates containing protein were carefully transferred to fresh tubes and stored at -20°C until further use.

3.9.1 Protein estimation by Folin Lowry method:

The proteins extracted from the cultured medulloblastoma cells were estimated by the Folin-lowry method [100]. The reagents are of AR grade. They are stable, concentrated and can be used for normal as well as micro assays. The protein extracted is used for western blotting. The reagents required and methods are described as follows:

Reagents:

1) 1 mg/ml BSA: 10 mg BSA (sigma) was weighed and dissolved in 1 ml autoclaved Milli-Q water to obtain a stock of 10 mg / ml. This stock was further diluted 1:10 in water to obtain a working stock of 1 mg/ ml. BSA stocks were stored at -20°C.

2) Solution A: Cu-tartrate CO3 (CTC)

a) 20% Na2CO3: 20 g was dissolved in 100 ml Milli-Q water.

b) 0.2 g CuSO4 was dissolved in 40 ml Milli-Q water.

c) 0.4 g potassium tartarate was dissolved in 40 ml Milli-Q water. CuSO4 and potassium tartarate were mixed (b + c) and the volume was made up to 100 ml with Milli-Q water. Final concentration of CuSO4 is 0.2% and potassium tartarate is 0.4%. To this, 100 ml of

20% Na2CO3 (a) was added slowly with constant stirring. This solution A was stored in dark at room temperature.

3) Solution B: 10% SDS. 10 g of SDS was dissolved in 80 ml Milli-Q water, heated at 60°C to assist dissolution. The final volume was adjusted to 100 ml and stored at room temperature.

4) Solution C: (0.8 N NaOH) 16 g of NaOH was dissolved in 100 ml of Milli-Q water, and the volume made up to 500 ml and was stored at room temperature (Note: Do not autoclave).

5) Reagent A: Prepared by mixing solutions A, B, C, and Milli-Q water in a proportion of 1:1:1:1 just before use. (Note: Mixing NaOH with 10% SDS results in a glue like insoluble precipitate. Therefore, dilute the 20%SDS first in the required volume of water and then add NaOH and CTC to it.)

6) Reagent B: Folin-Ciocalteau reagent was diluted 1+5 in Milli-Q water just before use.

Method:

1. 2 µl of protein sample to be estimated was diluted in 1 ml of Milli-Q water in duplicates.

2. BSA standards, ranging from 1 µg to 20 µg were prepared in duplicate by appropriately diluting from 1 mg/ml stock of BSA, in 1 ml of Milli-Q water. 2 µl of the sample buffer used for extraction of protein to be estimated was also added. “Blank” tubes were prepared by adding only 2 µl of the sample buffer.

3. 1 ml of freshly prepared reagent A was added to each tube, immediately mixed on a vortex mixer, and kept in dark at room temperature for 10 min. Then 0.5 ml of freshly

diluted reagent B was added to each tube, immediately mixed on a vortex mixer and incubated in dark at room temperature for 30 min.

4. The absorbance of the blue color developed was read at 750 nm against blank in a spectrophotometer (Shimadzu UV-160A, UV-visible recording spectrophotometer), and the concentration of the unknown protein samples was calculated by using the BSA standard plot.

3.9.2 SDS Polyacrylamide Gel Electrophoresis (SDS-PAGE)

The proteins extracted in sample buffer from doxycycline treated or untreated vector control or miRNA expressing cells are separated by SDS-PAGE for western Blotting.

Reagents:

1) 30% acrylamide solution: 29.2 g acrylamide, 0.8 g bis-acrylamide were dissolved in approximately 50-60 ml autoclaved Milli-Q water and the final volume was made up to 100 ml. Solution was filtered through ordinary filter paper and stored in an amber colored bottle at 4°C.

2) 20% SDS: 20 g SDS was dissolved in 80 ml of Milli-Q water, heated at 60°C to assist the dissolution. The final volume was made up to 100 ml, and stored at room temperature.

3) 1M Tris pH 8.8 and pH 6.8: 60.55 g Tris was dissolved in 400 ml Milli-Q water. pH was adjusted to 8.8 and 6.8 with concentrated HCl, the final volume was made up to 500 ml with Milli-Q water and autoclaved. Solutions were stored at 4°C.

4) 10X electrode buffer: 30 g Tris, 143 g glycine, 20 g SDS were dissolved in approx. 700 ml Milli-Q water and the final volume was made up to 1 L. Stock solution was diluted to 1X with Milli-Q water before use (1X buffer is 25 mM Tris, 190 mM Glycine, 0.2% SDS).

5) 0.5 % Coomassie Blue staining solution: 0.5 g of Coomassie Blue staining dye was dissolved in 50 ml of methanol (LR grade) by constant stirring. The final volume was adjusted to 100 ml by adding 40 ml of Milli-Q water and 10 ml of glacial acetic acid. The staining solution was filtered through filter paper and stored at room temperature for 1 month.

6) Destainer: Methanol (LR), glacial acetic acid (AR) and Milli-Q water mixed in the proportion 5:1:4 and stored at room temperature.

7) Loading Dye: 0.025% Bromophenol Blue was dissolved in 1X Sample Buffer.

Method:

1. Two clean glass plates (one of which was notched), separated by 1.5 mm thick spacers were clamped together. The sides and the bottom of the plates were sealed using 3% agar. The resolving gel of the required percentage (10%) was prepared by mixing the following:

Components	**Final concentration of acrylamide**		
	10%	12%	20%
30% Acrylamide	10 ml	12 ml	20 ml
1M Tris-Cl pH 8.8	11.2 ml	11.2 ml	11.2 ml
20% SDS	0.15 ml	0.15 ml	0.15 ml

Milli-Q water	8.65 ml	6.65 ml	-
TEMED	20 µl	20 µl	20 µl
20% Ammonium persulfate	50 µl	50 µl	50 µl

2. The gel solution was poured between the two glass plates taking care to avoid air bubbles. Water was carefully layered over the gel and it was allowed to polymerize (approximately 20– 30 min).

3. Following polymerization, the water layer was removed and a 5% stacking gel was prepared and overlaid over the resolving gel.

5% stacking gel composition:

Components	**Volume to be added**
30% acrylamide solution	1.67 ml
1 M Tris-HCl pH 6.8	1.75 ml
20% SDS	100 µl
Milli-Q water	6.98 ml
TEMED	10 µl
20% ammonium persulphate	25 µl

A comb of 1.5 mm thickness was inserted immediately into the stacking gel solution between the two plates to form wells. After polymerization of the stacking gel, the comb was gently removed and the wells were cleaned by flushing first with water and then with 1X electrode buffer (using a syringe-needle). The gel plates were clamped to the electrophoresis unit and the upper and lower tanks were filled with 1X electrode buffer.

4. The proteins to be resolved were mixed with 1X sample buffer containing 5% v/v BME and 0.01% bromophenol blue, boiled for 3 min and loaded into the wells of the gel along with pre-stained protein ladder.

5. Electrophoresis was carried out at 22 mA constant current till the dye reached the bottom of the gel. The gel was removed carefully and either stained with Coomassie blue to check equal loading of the proteins or processed for western blotting as described later.

3.9.3 Western Blotting

The proteins separated by SDS-PAGE (Polyacryl Amide Gel Electrophoresis), were transferred to a PVDF membrane by western blotting technique. Various proteins of interest were detected on the blot by the immunodetection method.

Reagents:

1) 1X transfer buffer: 25 mM Tris, 192 mM Glycine, 20% Methanol. 3 g Tris and 14.4 g. Glycine were dissolved in Milli-Q water and volume was made up to 800 ml with Milli-Q water. 200 ml Methanol was added to make 1 L. Buffer was chilled to 4°C before use. (1

L transfer buffer is sufficient for western blotting in Biorad's mini trans-blot electrophoretic transfer cell)

2) 10X Tris-buffered saline (TBS): 0.1 M Tris, 1.5 M NaCl 12.1 g Tris and 87.6 g NaCl were dissolved in Milli-Q water, pH was adjusted to 8.0 with concentrated HCl and the final volume was made up to 1 L. Solution was autoclaved and stored at room temperature.

3) 1X Tris-buffered saline with Tween-20 (TBST): 10X TBS was diluted to 1X with Milli-Q water (1 litre), 1 ml Tween-20 was added to the solution and kept on magnetic stirrer for 1 hr.

4) Ponceau-S staining solution: (0.2% Ponceau-S in 1% glacial acetic acid)

5) SuperSignal® West Pico chemiluminescent substrate

6) Antibodies: Catalogue No and companies mentioned in method.

7) Whatmann Filter paper 3 (Cat No. 4908364)

Method:

1. The protein samples to be blotted were resolved by SDS-PAGE and the gel was kept in 1X

transfer buffer for 15-20 min until the gel was free from the smell of β- mercapto ethanol (BME).

2. The Immobilon PVDF membrane, to be used for blotting, was cut to the size of the gel to be blotted. The membrane was pre-wet in methanol for about 30 seconds, kept in Milli-Q water for 10min. to wash off excess methanol and then placed in 1X transfer buffer for

20 min. Two pieces of a Whatmann 3MM filter paper little bigger than the size of the gel, were also cut.

3. The transfer assembly was prepared according to the manufacturer‟s instructions. The cassette was assembled in a tray containing 1X transfer buffer by arranging the components in the following sequence: First the cassette was placed, with the gray side down in a tray containing transfer buffer. A Scotch-Brite pad was placed over the grey portion of the cassette, and a piece of Whatman paper was placed over it. Then the transfer buffer equilibrated gel was carefully placed over the Whatman paper and the PVDF membrane was juxtaposed to the gel without trapping any air bubbles between the gel and the PVDF membrane. A small cut was given at one corner of the membrane and the gel for correct orientation. Another piece of Whatman paper and a Scotch-Brite pad were placed over the PVDF membrane. The cassette was closed firmly and locked with the white latch on top of the cassette, and slid into the grooves for holding the cassette in place with the grey portion (gel side) towards the cathode (negative electrode) and the transparent portion (membrane side) towards the anode (positive electrode). This whole assembly was placed inside the tank. containing transfer buffer, and the electrodes were connected to the power supply. Transfer was carried out at 40mA constant current at 4°C for 16 hr.

4. After the transfer, the membrane was carefully removed from the cassette using a pair of forceps, rinsed once with Milli-Q water, and kept in destainer for 30 min (to aide in staining with Ponceau-S). Then the membrane was washed twice with TBST for 5 min each and stained with Ponceau-S till the protein bands were visible. The molecular weight marker positions were marked on the membrane with a soft lead pencil and then the

Ponceau-S was completely removed by washing the membrane with TBST. It was either probed immediately or stored at 4°C in TBST, for later use.

5. For probing, the membrane was first blocked with a 5% milk solution prepared in TBST. The membrane was kept in the milk solution for 1 hr at room temperature on a rocker with gentle shaking.

6. The blocking solution was drained off and the membrane was washed 3 times for 5 min each with TBST, on the rocker with vigorous shaking.

7. TBST was drained off completely and the membrane was incubated with appropriately diluted antibody, with gentle shaking on the rocker. The working conditions of various antibodies used are given below:

Name of antibody	**Company/Catalogue No.**	**Type**	**Dilution**	**Duration**
Anti-DEPTOR	Cell Signaling #11816	Rabbit monoclonal	1:1000	O/N 4°C
Anti-Phospho-p70 S6 kinase (Thr 389)	Cell Signaling #9234	Rabbit monoclonal	1:1000	O/N 4°C
Anti- P70 S6 kinase	Cell Signaling #2708	Rabbit monoclonal	1:1000	O/N 4°C
Anti-Phospho 4EBP1 (Thr 37/46)	Cell Signaling #2855	Rabbit monoclonal	1:1000	O/N 4°C
Anti-Phospho- Akt (Ser 473)	Cell Signaling #9271	Rabbit polyclonal	1:1000	O/N 4°C
Anti-Phospho-Akt (Thr 308)	Cell Signaling #9275	Rabbit polyclonal	1:1000	O/N 4°C
Anti-Akt (pan)	Cell Signaling #4685	Rabbit monoclonal	1:1000	O/N 4°C
Anti-P21 WAF1/CIP1	Cell Signaling #2947	Rabbit monoclonal	1:1000	O/N 4°C

Anti-β3 Tubulin	Cell Signaling #5568	Rabbit monoclonal	1:1000	O/N 4°C
Anti- γ tubulin antibody	#T3559 Sigma Aldrich	Rabbit polyclonal	1:5000	O/N 4°C
Anti-ATG5 antibody	Cell Signaling #12994	Rabbit monoclonal	1:1000	O/N 4°C
Anti-LC3B antibody	Cell Signaling #2775	Rabbit polyclonal	1:1000	O/N 4°C
Goat Anti-rabbit IgG	Thermo scientific #31460	Goat polyclonal	1:2000	1hr/RT
Anti-Phospho-p44/42 MAPK (Erk 1/2) (Thr 202/ Tyr 204)	Cell Signaling #4377	Rabbit monoclonal	1:1000	O/N 4°C
p44/42 MAPK (Erk 1/2)	Cell Signaling #9102	Rabbit polyclonal	1:1000	O/N 4°C
Neurofilament- L	Cell Signaling #2837	Rabbit monoclonal	1:1000	O/N 4°C

Table 3.5 List of antibodies used in the study

8. The antibody solution was drained off and the membrane was washed six times for 5 min each with 1X TBST, on the rocker with vigorous shaking.

9. Then the membrane was incubated with appropriately diluted horseradish peroxidase (HRP) conjugated secondary antibody (anti-IgG) for 1 hr at RT on the rocker with gentle shaking. Anti-rabbit HRP-conjugated antibodies (Thermo-Scientific) were diluted 1:2000 in 1% milk-TBST. The antibody solution was drained off and the membrane was washed vigorously six times for 5 min each with 1X TBST and then three times with 1X TBS.

10. The excess buffer was drained off and the blots were developed using a chemiluminescent substrate (Advansta, San Jose, CA, USA), and the images were captured using the Chemidoc gel documentation system of Biorad (Hercules, CA, USA). The

exposure time and type can be set manually and any kind of saturation or over exposure can be controlled. The images were quantified using the Image Lab software of Biorad.

3.9.4 Protein extraction from Fresh tumor tissues

Fresh tumor tissues were cut into tiny pieces and dissolved in at least 500 µl lamelli lysis buffer. It was ensured that the entire tumor tissue gets completely dissolved in the lysis buffer by triturating it with a 1ml tip with edge cut off or by keeping the samples in a rocker to ensure constant mixing and dissolving. The samples are never vortexed or passed through syringe as that would cause the protein samples to get sheared. Then the samples are boiled for 7 minutes. After the sample gets dissolved, the normal protocol for protein extraction and estimation was followed (Section 3.9).

3.10 Transcriptome sequencing

RNA-seq analysis was carried out to identify the change in the expression profile upon miR-592 expression by comparing the expression profile of doxycycline-induced P1, P2 populations expressing miR-592, the parental D283 and the vector control cells. The libraries were prepared from the total RNA using the Illumina TruSeq RNA library preparation kit. The libraries were subjected to 100 nucleotides single-read deep sequencing using the Illumina HiSeq 2500 (San Diego, USA) system to get a minimum of 10 million reads per library. The HISAT2 aligner software (https://ccb.jhu.edu/software/hisat2) was used for aligning the sequence data to the reference human genome hg19 using the default parameters, and the count of the number of reads per gene was derived using the HTSeq-count algorithm (www.bioinformatics.babraham.ac.uk) using the default parameters. The genes

significantly differentially expressed upon miR-592 expression were identified using the DESeq2 R Bioconductor package (https://bioconductor.org/packages/release/bioc/html/DESeq2.html). The data was normalized by variance stabilizing transformation using the DESeq2 software. A heat map of the top 50 significantly (padj < 0.05) downregulated genes (in the decreasing order of log2FoldChange) was plotted using the Multiple Experiment Viewer (http://mev.tm4.org) after median centering the data.

3.11 Protein- protein network analysis

In order to identify the biological pathways enriched upon miR-592 expression, the set of genes significantly differentially expressed were analyzed using the ClueGO version 2.5.5 (http://apps.cytoscape.org/apps/cluego), a Cytoscape plug-in software. This software not only identifies enriched biological pathways but also builds a protein-protein interaction network among the differentially expressed genes that could help to identify the hub proteins. The GO biological processes database, Reactome pathway database and the KEGG database were used for the analysis. The 311 genes significantly (padj < 0.1) upregulated (log2FoldChange ≥ 0.8) upon miR-592 expression were analyzed by the ClueGO software. No additional interacting genes were added to build the network. Two-sided hypergeometric test was used for evaluating the statistical significance of enriched pathways. The p-value corrected using the Bonferroni step down correction method was considered significant at the cut-off of 0.01. For the inclusion in the protein-protein interaction network, a minimum of 2% interacting genes and the Kappa score threshold of 0.47 was used [101].

Chapter – 4:

Role of miR-592 in medulloblastoma pathogenesis

RESULTS AND DISCUSSION

4.1 Role of miR-592 in medulloblastoma pathogenesis

The four molecular subgroups of medulloblastomas are also distinct in the expression profile of microRNAs. MiR-592 is one of the microRNAs that is differentially expressed in the four subgroups, in particular the two non-WNT, non-SHH subgroups. The expression of miR-592 was studied in an Indian cohort and its role in medulloblastoma pathogenesis was studied by evaluating the effect of its expression on the growth and malignant behavior of medulloblastoma cell lines.

4.1.1 MiR-592 is overexpressed in group 4 medulloblastomas and its higher expression correlates with better overall survival and lower incidence of metastasis at diagnosis

The expression of miR-592 was studied in 200 medulloblastomas obtained from the neurosurgery and neuropathology departments of the Tata Memorial Centre, Mumbai. The study was approved by the ethics committee of the Tata Memorial Centre. Both fresh tissues snap-frozen in liquid nitrogen and formalin-fixed paraffin-embedded (FFPE) tumor tissues were included in the study after obtaining informed consent of the patients/parents and assent from children more than 7 years of age. Total RNA was extracted from the FFPE tumor tissues using RecoverAll RNA extraction kit, and from fresh tumors, cultured cell lines by the acid guanidium thiocyanate- phenol-chloroform extraction method. MiR-592 expression levels were analyzed by the real-time RT-PCR assay using the Taqman probe for miR-592. The level of miR-592 was expressed as RQ or Relative Quantity that is calculated by the comparative Ct method using the formula $RQ = 2^{\wedge(-\Delta ct)} X\ 100$ where ΔCt = Ct (miRNA) – Ct (RNU48). RNU48 was used as a house-keeping small RNA control.

MiR-592 expression levels were found to be in the range RQ = 0.05 to 0.5 (0.146 ± 0.156) in the normal cerebellum. In the WNT, SHH and Group 3 subgroups of medulloblastomas, the expression levels of miR-592 were found to be in the range of RQ = 0.01 to 4 (WNT = 0.6 ± 0.148; SHH = 0.74 ± 0.150; Group 3 = 1.6 ± 0.415). However, in Group 4 medulloblastomas, the expression of miR-592 is ~100-fold higher than that of normal cerebellum ranging from 1 to 400 (37.32 ± 7.59). MiR-592 is overexpressed in 95% Group 4 and 13% Group 3 tumors as compared to normal cerebellar tissues (RQ > 1.0) (Figure 4.1.1A). Thus, the expression of miR-592 is a characteristic feature of the Group 4 medulloblastomas. MiR-592 can, therefore, act as a surrogate marker for this subgroup.

The expression levels of miR-592 were correlated with the clinical data routinely updated at the Electronic Medical Records (EMR) of the Tata Memorial Centre. The 116 Group 3/Group 4 patients who received at least one adjuvant therapy after surgery were included in the study. In the combined cohort of Group 3, Group 4 patients having metastasis at diagnosis had lower (RQ ≤ 1.0) miR-592 expression (median RQ = 1.5; 95% CI, -0.28 to 6) than those who did not have metastasis at diagnosis (median RQ = 4.1; 95% CI = -0.47 to 8.43), although the difference did not reach statistical significance (Figure 4.1.1 B). Kaplan Meier survival analysis was also carried out comparing the 'miR-592 high' with the 'miR-592 low' cases in the combined Group 3, Group 4 cohort. Overall survival and progression-free survival was measured from the time of initial diagnosis to the date of death or last follow up and the time of recurrence of the disease or leptomeningeal spread, respectively. The significance of the difference in the survival curves was estimated by the Breslow Wilcoxon test. The hazard ratio was estimated using the log-rank statistics. P-values < 0.05 were considered to be statistically significant. Kaplan Meier survival analysis

showed significantly better (hazard ratio = 0.6087) progression-free survival of the cases having high miR-592 expression. Three-year progression-free survival of 'miR-592 high' cases was 67% (95% CI = 54% - 79%) while that of 'miR-592 low' patients was 51% (95% CI = 34% - 68%). The three-year overall survival of 'miR-592 high' patients was 70% (95% CI = 58%-82%), and 'miR-592 low' patients was 63% (95% CI is 46% - 79%) (Figure 4.1.1 C and D). However, beyond 3 years the difference in the survival diminished

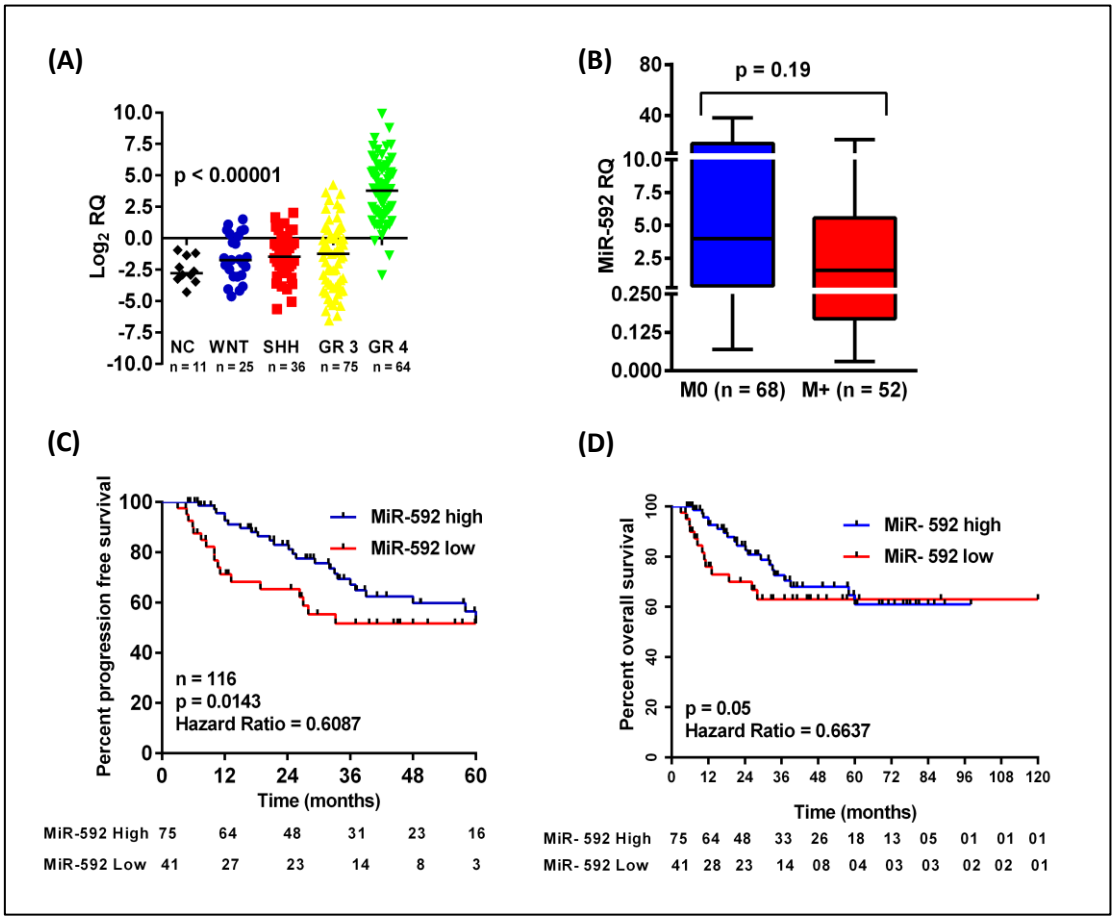

Figure 4.1.1 MiR-592 expression in the four molecular subgroups of medulloblastoma and its correlation with clinical characteristics (A) MiR-592 expression in a cohort of 200 medulloblastomas and normal cerebellar (NC) tissues evaluated by the real-time RT-PCR assay. (B) Expression levels of miR-592 in Group 3/Group 4 medulloblastomas with (M1) or without (M0) metastasis at diagnosis. (C, D) Kaplan Meier survival analysis showing the correlation of miR-592 expression with the progression free and overall survival in 116 Group 3/Group 4 medulloblastoma patients.

as the survival of ‘miR-592 low’ patients that survived beyond this period appeared to be as good as that of ‘miR-592 high’ cases. Thus, miR-592 overexpression is associated with a lower incidence of metastasis at diagnosis and better survival in the non-WNT, non-SHH group of medulloblastomas.

4.1.2 MiR-592 was exogenously expressed in the established medulloblastoma cell lines to the levels similar to that of group 4 medulloblastomas

Medulloblastoma cell lines have been established from the SHH and Group 3 subgroups. No cell line has been established from the WNT and Group 4 subgroups, most likely due to their less aggressive nature. All the cell lines used were validated by short tandem repeat marker profiling and checked for mycoplasma contamination at regular intervals. The cell lines have been characterized and molecularly classified [102]. Their characteristic gene expression profile was also verified using real-time RT-PCR assay in the lab (Ph. D. Thesis, Pooja Panwalkar). Daoy cell belongs to the SHH subgroup. D283, D425, and HD-MB03 cell line belong to Group 3. D283 has an overexpression of MYC but not amplification of the MYC locus whereas D425 and HDMB03, which is a newly established group 3 cell line, overexpress MYC due to amplification of the MYC locus. These three cell lines also have high expression levels of retina-specific genes, which is also a characteristics of group 3 medulloblastomas.

MiR-592 expression was found to be almost 100-fold to 1000-fold lower (RQ = 0.004 to 0.05) in these cell lines as compared to the Group 4 tumors. MiR-592 expression in D283 cells is 0.03 ± 0.007, in D425 it is 0.003 ± 0.001, in HD-MB03 it is 0.0625 ± 0.0067 and in Daoy it is about 0.05 ± 0.008. Therefore, miR-592 was expressed in the cell

lines using a lentiviral vector in a doxycycline- inducible manner to levels similar to that in Group 4 tumors (RQ = 40 to 60). The genomic region encoding miR-592 was cloned in pTRIPZ lentiviral vector downstream the doxycycline-inducible promoter, Lentiviral particles were generated using HEK293FT as the packaging host cell line. The medulloblastoma cell lines were transduced with the pTRIPZ-miR-592 lentiviral particles and polyclonal populations stably expressing the construct were selected in the presence of puromycin. The doxycycline dose and time duration were standardized to achieve the miR-592 expression levels in the range of Group 4 tumors. The dose of 4 µg/ml of doxycycline for 72 h duration was found to be optimal. The vector control population was transduced with the parental pTRIPZ vector.

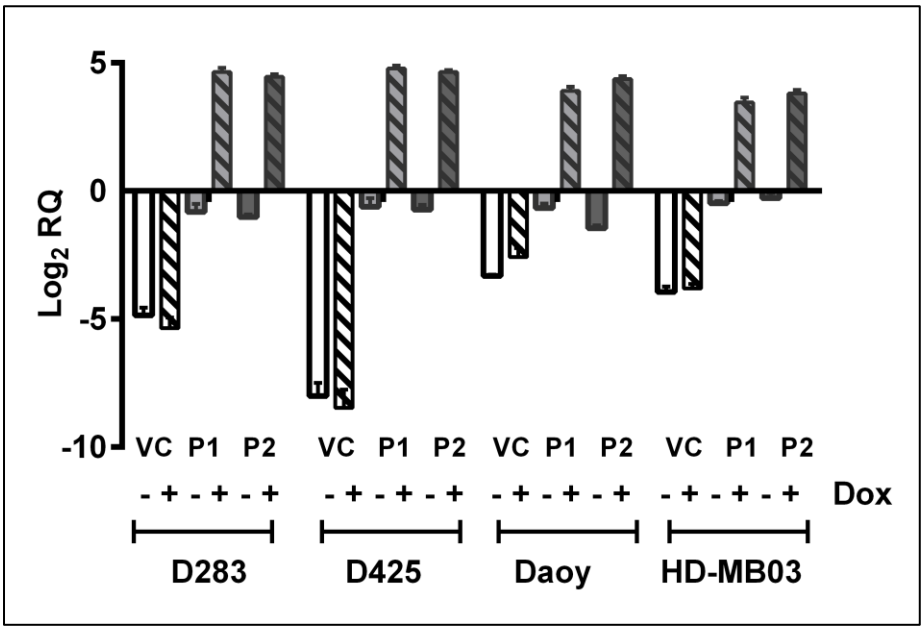

Figure 4.1.2 Level of miR-592 expression in the polyclonal populations of medulloblastoma cells. Expression levels of miR-592 in the indicated medulloblastoma cell line and its stable polyclonal populations (P1, P2) expressing miR-592 before and after doxycycline (+Dox) induction evaluated by the real-time RT-PCR analysis. VC: vector control.

The level of miR-592 expression in the polyclonal populations P1 and P2 of D283 was found to be at the range of RQ 40 - 60, that of D425 was in the range of 55 - 70, in HD-MB03 it was 12-20 and for Daoy it was in the range of 27-42. So, in all the cell lines, the level of miR-592 expression were similar to that observed in the Group 4 medulloblastoma tumors upon induction with 4 µg/ml doxycycline (Figure 4.1.2).

4.1.3 MiR-592 expression did not affect proliferation of the medulloblastoma cells

The effect of miR-592 expression on the proliferation of medulloblastoma cells was studied by the MTT assay. The cells of the polyclonal populations P1/P2 and the vector control populations were seeded in triplicates at a density of 2000 cells in 100 µl medium per well in a 96 well microplate. The medium containing doxycycline was replenished every 48 hours and the cell growth was monitored for 10 days. Figure 4.1.3 (A-D) show the growth curves of miR-592 expressing polyclonal populations P1, P2 which overlap with growth curves of their corresponding uninduced populations. Figure 4.1.3 (E) shows that there is no decrease in the percentage growth of the polyclonal populations expressing miR-592 as compared to the vector control expressing cells. Thus, the expression of miR-592 had no effect on the proliferation of the Group 3 cell lines D283, D425, HD-MB03, and Daoy which is a SHH subgroup medulloblastoma cell line.

4.1.4 The expression of miR-592 reduced the anchorage-independent growth potential of medulloblastoma cells

In order to study the anchorage-independent growth potential of the cells, the soft agar colony formation assay was performed. After doxycycline induction of 72 hours, 1000 cells

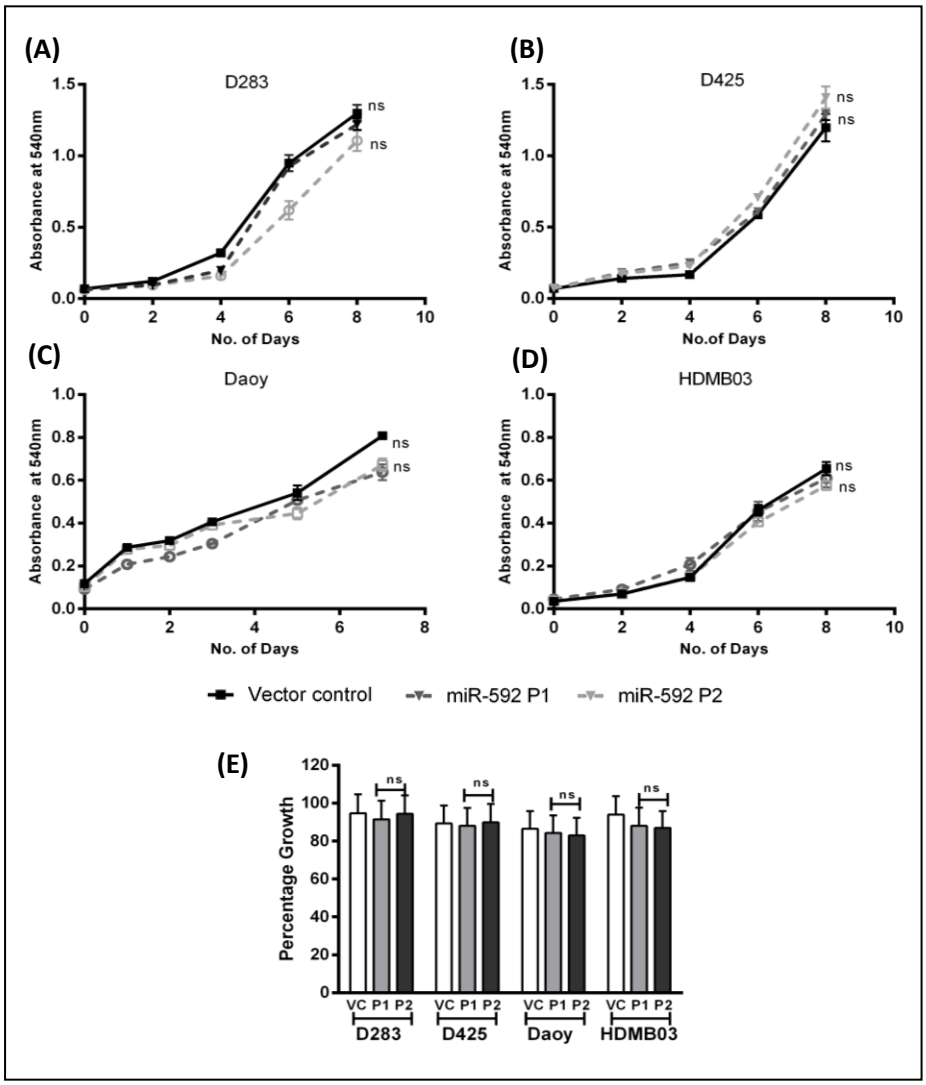

Figure 4.1.3 Effect of miR-592 expression on the proliferation potential of medulloblastoma cells. (A) to (D) show growth curves of the indicated medulloblastoma cell line vector control (VC) and its stable polyclonal populations (P1, P2) expressing miR-592 upon doxycycline induction as studied by the MTT assay. (E) Y-axis denotes the mean growth of the individual clones from three independent experiments as a percentage of the growth of the un-induced population. ns: non-significant.

were seeded in a semi-solid matrix of 0.3% to 0.4 % agarose over a basal layer of 1% agarose in a 35 mm plate and incubated for about 2 weeks for colony formation. The colonies consisting of minimum 5-6 healthy cells were counted manually under a microscope. About 500 -1000 colonies per plate were formed by the four medulloblastoma cell lines. The number of colonies formed by the doxycycline-induced P1, P2 populations

were significantly low as compared to the doxycycline-treated vector control cells in the case of all the medulloblastoma cell lines studied (Fig. 4.1.4A). The percentage decrease in the colony formation of the doxycycline induced vector control and miR-592 expressing clones was calculated with respect to their corresponding uninduced populations. Thus, the anchorage-independent growth potential of the medulloblastoma cell lines was found to be reduced by by 25% to 45% upon expression of miR-592 (Fig. 4.1.4B).

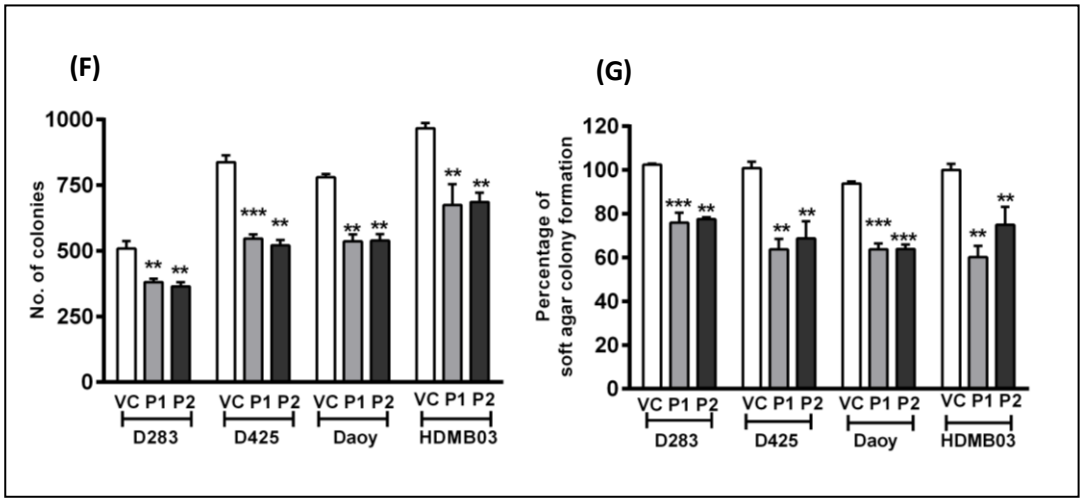

Figure 4.1.4 Effect of miR-592 expression on the anchorage-independent growth potential of the medulloblastoma cells. (A) Y-axis shows the number of soft agar colonies formed by the doxycycline-treated indicated population of the medulloblastoma cell line. (B) Y-axis depicts the colony formation by individual doxycycline-induced clones as a percentage of those formed by their un-induced counterparts from three independent experiments. *, ** and *** indicate $p \leq 0.05$, $p \leq 0.005$, and $p \leq 0.0005$, respectively.

4.1.5 MiR-592 expression decreased tumorigenic potential of medulloblastoma cells

The tumorigenic potential of the medulloblastoma cells was studied by generating orthotopic medulloblastoma xenografts in immunodeficient mice. The polyclonal population expressing miR-592 as well as the un-induced cells of D425 cell line were

engineered to express firefly luciferase. The cells were injected orthotopically into the cerebellum of NOD/SCID mice. The mice were regularly fed with doxycycline so that doxycycline-induced miR-592 expression is maintained.

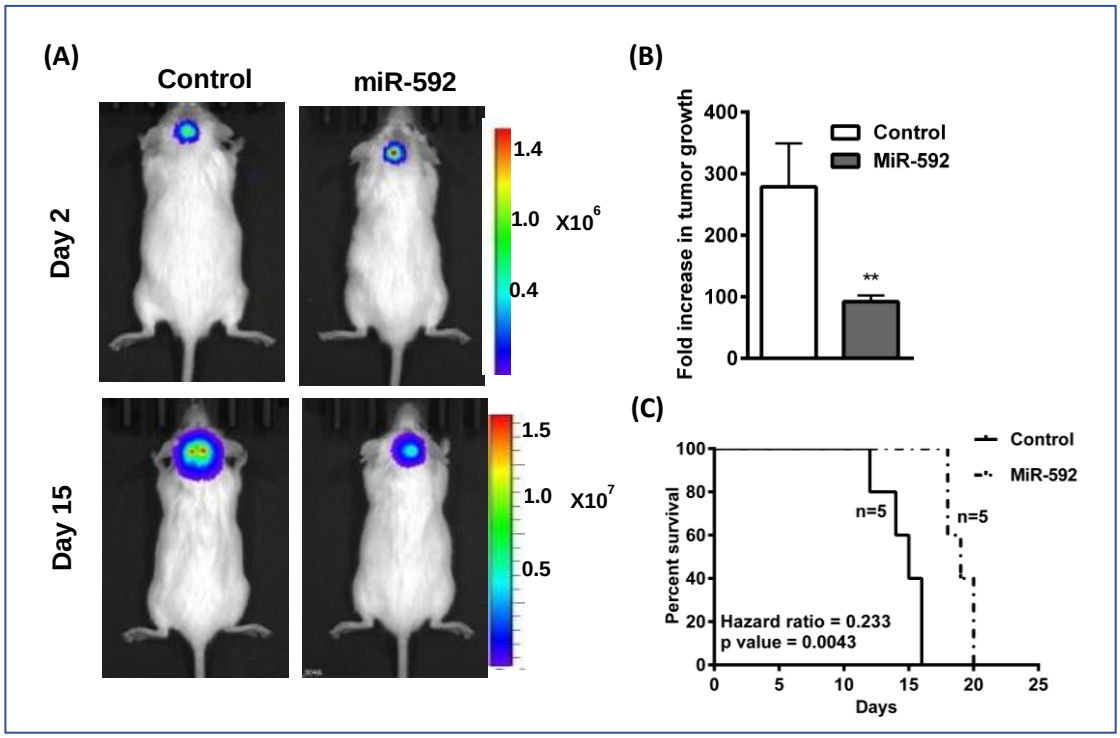

Figure 4.1.5 Effect of miR-592 expression on the tumorigenic potential of medulloblastoma cells. (A) The bioluminescence images of the mice orthotopically injected with doxycycline-treated D425 cells expressing pTRIPZ-miR-592 construct before and after doxycycline-induced miR-592 expression. (B) Y-axis shows the fold increase in the tumor luminescence on day 15 as compared to day two post-injection of the cells. (C) Kaplan Meier Survival analysis of the injected mice. ** indicate $p \leq 0.005$

that the expression of miR-592 is maintained. In order to measure tumor growth, d-luciferin was intra peritoneally injected and serial images of the mice were captured under isoflurane anesthesia. Tumor growth was monitored by using *invitro* bioluminescence imaging. For quantification, “Living Image” software was used, the image with peak luciferase activity

as seen by the photon output was selected and region of interest (ROI) was drawn manually around the luminescent source and expressed in radiance (photons/sec/cm2/steridian). A pseudo-color image representing light intensity (blue least intense and red most intense) was generated and superimposed over the gray scale reference image (Figure 4.1.5 A). This image shows that although at day 2 the number of cells expressing luciferase that has been injected into the cerebellum of the NOD/SCID mice is similar, at day 14 the tumor burden developed by the control cells is much higher compared to that of the miR-592 expressing cells. Five animals were included each in the group of control and test animals. The tumor volume of the animals decreased by 1.5 to 5-fold upon miR-592 expression as calculated from the fluorescence intensity of the tumor formed in the miR-592 expressing cells as compared to the vector control cells (Figure 4.1.5 B). The survival of the miR-592 expressing animals also increased from 16 to 20 days i.e by 25 % as studied by Kaplan Meier survival analysis (Figure 4.1.5 C). Thus miR-592 expression reduced the tumorigenic potential of the medulloblastoma cells and increased their survival.

4.1.6 MiR-592 expression reduced the invasion potential of the medulloblastoma cells:

About 1/3rd of medulloblastomas exhibit metastasis at diagnosis, which means that the medulloblastoma cells have a high invasion potential. Effect of miR-592 expression on the invasion potential of the medulloblastoma cells were studied by the ability of the cells to invade through Matrigel, that is similar to the cellular matrix. 30µg Matrigel was coated over the membrane present at the inner surface of the chamber and incubated for 1 hour. 50,000 cells of vector control and miRNA expressing cells of Daoy and 75,000 cells of D283 that were previously induced with doxycycline were seeded on it. Medium with FBS is added at the lower chamber which can act as a chemoattractant for the cells. The cells

are then allowed to invade through the Matrigel^{TM} coated membrane placed in a trans well insert for 36 h (Daoy cells) to 56 h (D283 cells). Post invasion, the cells are labelled with Calcein, that is a fluorescent labelled dye. The uninvaded cells from the upper surface of the chamber are being wiped out with the help of a cotton bud. Fluorescence was read at the excitation of 485 and the emission of 535nm.

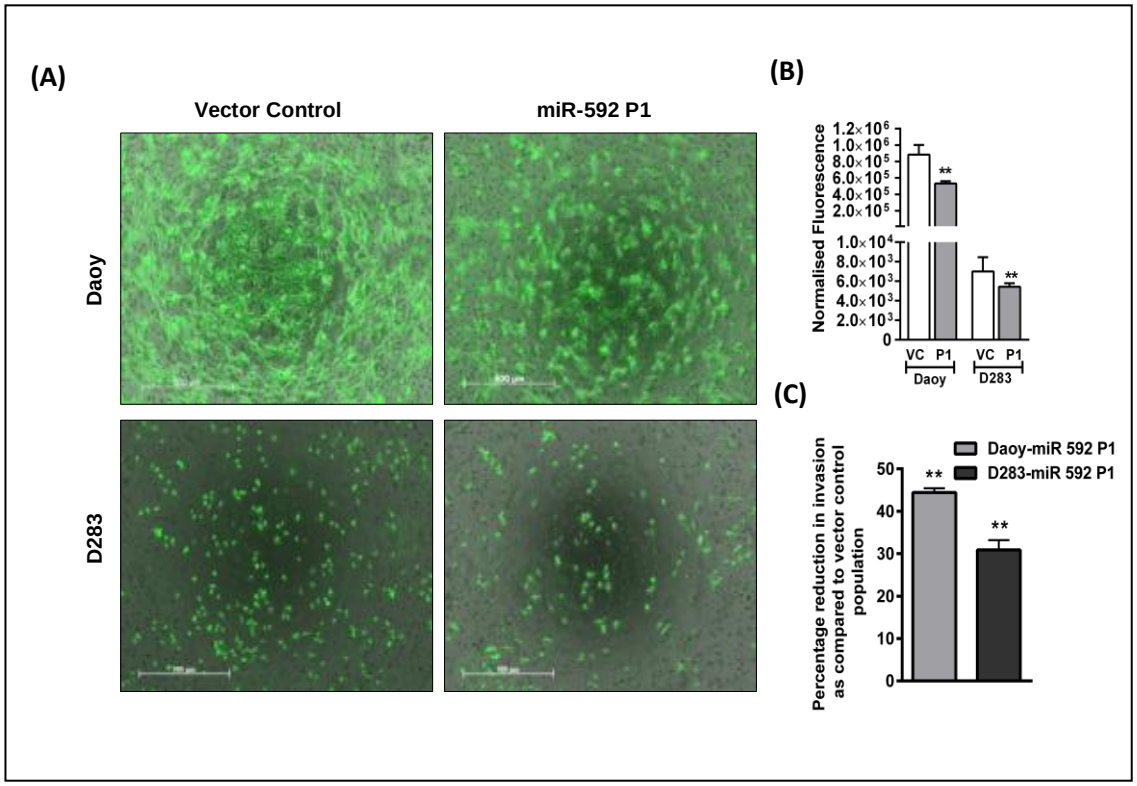

Figure 4.1.6 Effect of miR-592 expression on the invasion potential of medulloblastoma cells. (A) Photomicrographs of the Calcein-labeled vector control or miR-592 expressing P1 population of Daoy and D283 medulloblastoma cells invaded through the matrigel-coated membrane. (B) The normalized fluorescence reading of the individual clones as measured by normalizing the calcein fluorescence of the invaded cells to the initial calcein reading of the cells seeded in the Boyden chamber. (C) Y-axis shows the percentage reduction in the invasive capacity of Daoy and D283 cells upon the miR-592 expression compared to that of the doxycycline induced vector control population from three independent experiments. ** indicate $p \leq 0.005$.

Figure 4.1.6 (A) shows Calcein-labeled cells present on the lower surface of the chamber after the invasion. The fluorescence intensity represented in Figure 4.1.6 (FB) was

normalized with respect to the fluorescence intensity of the cells seeded for the assay. MiR-592 expression resulted in a 30% to 45% reduction in the invasion potential of D283 and Daoy cells as evaluated by the reduction in the normalized fluorescence intensity of the invaded cells from three independent experiments (Fig 4.1.6 C). Thus, miR-592 expression significantly reduced the invasion potential of the medulloblastoma cells.

4.1.7 MiR-592 expression did not sensitize the medulloblastoma cells towards radiation

MiR-592 expression was found to correlate with better survival of medulloblastoma patients, which could be due to better response to radiation therapy. Therefore, the role of miR-592 in radiation sensitivity of medulloblastoma cells was studied. 2000 cells were seeded in triplicates per well of a 96 well plate after 72 h of doxycycline induction. The cells were irradiated at a dose of 4.0 Gy (the dose that killed 50% of cells), medium replaced after 24 hours and then observed for cell growth over the next 6 days by taking the MTT reading at the given time points. However, the growth curves represent similar rate of growth inhibition that was observed in cells expressing miR-592 as compared to the vector control cells (Figure 4.1.7). Thus, radiation has similar effects on the vector control cells as it had on the miR-592 expressing cells or in other words, no further sensitization to radiation has been observed upon miR-592 expression.

4.1.8 MiR-592 expression did not affect chemosensitivity of medulloblastoma cells

Cisplatin, etoposide, vincristine are the drugs are used for the chemotherapy of medulloblastoma patients. For studying chemosensitivity, the dose of the drug that killed 50% of medulloblastoma cells was used in the MTT assay.

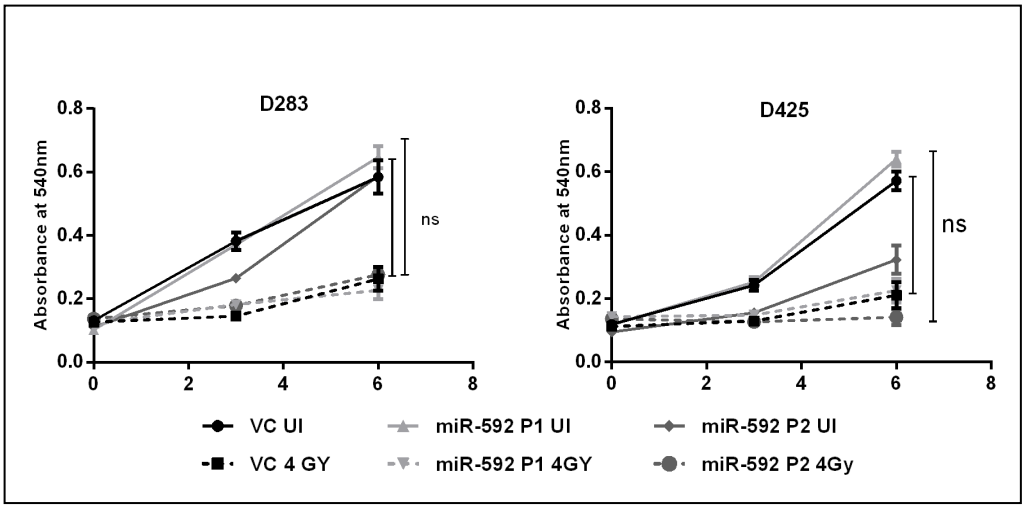

Figure 4.1.7 Effect of miR-592 expression upon sensitivity to radiation of medulloblastoma cells. The figure represents the growth rate of the unirradiated (UI) or growth inhibition observed upon 4 GY irradiation of Vector control (VC) or polyclonal populations of the indicated cell lines (P1 and P2) expressing miR-592 over a period of 6 days. All the cell populations were doxycycline induced. ns refers to non -significant.

The LD50 dose for cisplatin, etoposide, and vincristine was found to be 3.0 µM, 2.0 µM, and 0.2, 2.0 µM for the D283 and D425 cell line, respectively. The three drugs have a different mode of action upon the cells. Cisplatin crosslinks the DNA in ways that interfere with the cell division by mitosis. Etoposide forms a ternary complex with DNA and the topoisomerase II enzyme (which aids in DNA unwinding), prevents re-ligation of the DNA strands, thereby causes DNA strands to break. Vincristine binds to tubulin dimers, inhibiting the assembly of microtubule structures and arresting mitosis in metaphase. Four thousand cells of the vector control (VC) and the miR-592 expressing cells (P1 and P2) were seeded in triplicates per well of a 96 well microtitre plate with or without treatment with doxycycline. The cells were treated with cisplatin and etoposide for 48 h and vincristine for 60 h (the duration that brings about 50% - 60% cell death).

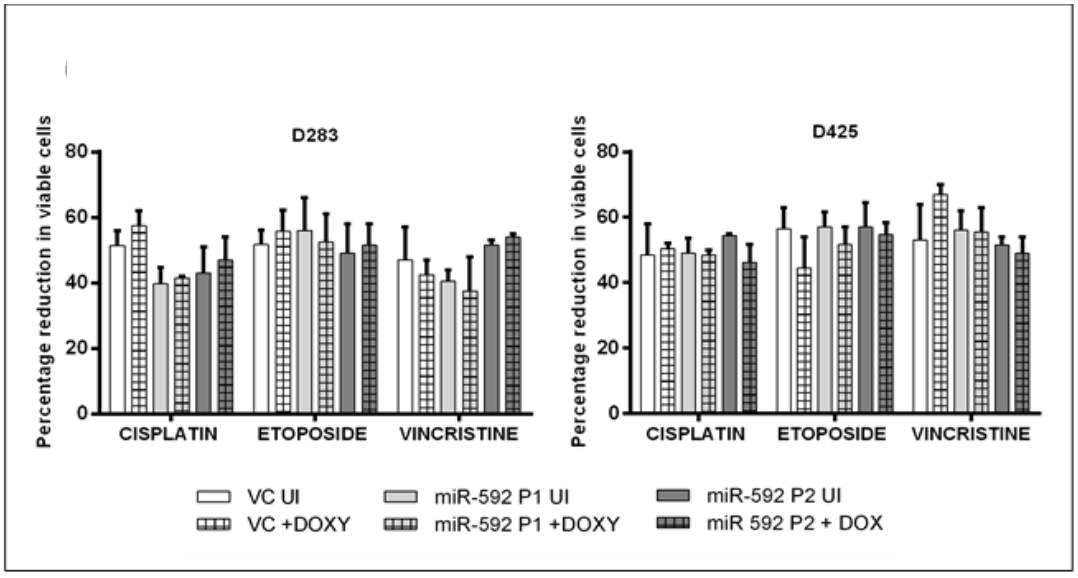

Figure 4.1.8 Effect of miR-592 expression upon sensitivity to chemotherapeutic drugs of medulloblastoma cells. The figure represents the percentage reduction in growth rate upon treatment with the indicated drugs as compared to its untreated counterparts. VC are the vector control cells and P1, P2 are the polyclonal populations expressing miR-592 of the indicated cell lines. The percentage reduction in both the UI (uninduced) or the doxycycline induced (+Doxy) clones have been represented.

and the cell density was evaluated by the MTT assay. The doxycycline-induced miR-592 expression did not increase the cell death brought about by the drug treatment as shown in Figure 4.1.8. Thus, miR-592 expression did not affect chemosensitivity of medulloblastoma cells.

4.1.9 *DEPTOR* and *EML1* are the novel direct targets of miR-592

In order to delineate the molecular mechanism underlying the tumor-suppressive effect of miR-592 expression in medulloblastoma cells, RNA-seq analysis was performed. The genes significantly differentially expressed upon miR-592 expression were identified by the RNA-seq analysis of miR-592 expressing polyclonal populations P1, P2, the vector control, and the parental D283 cells. The heatmap in Figure 4.1.9 (A) shows the top 50

genes that were significantly downregulated in the miR-592 expressing polyclonal populations of D283 cells. *DEPTOR* and *EML1* were identified as putative miR-592 target genes among these top 50 downregulated genes using the Targetscan software (www. targetscan.org). *DEPTOR*, an endogenous mTOR inhibitor, contains a 8-mer binding site for miR-592 with a weighted context score of 99, making it one of the most likely miR-592 targets. *EML1*, which encodes for a microtubule like protein has two 7-mer binding sites for miR-592 with a weighted context score of 88. The *DEPTOR* and *EML1* expression levels were evaluated by a real-time RT-PCR assay. Upon miR-592 expression, DEPTOR levels decreased by 15-fold to 50-fold while *EML1* levels decreased by 1.5 to 4-fold in D283 and D425 cells, upon miR-592 expression (Figure 4.1.9 B). Furthermore, the levels of *DEPTOR* and *EML1* were also found to be lower in the Group 4 tumors as compared to the Group 3 tumors in a study performed by *Cavalli* et al [45] (Figure 4.1.9 C). The downregulation of DEPTOR at the protein level in the polyclonal populations expressing miR-592 was also confirmed by the western blotting (Figure 4.1.9 D). Luciferase assay was performed by cloning the 3'UTR region of the potential miR-592 targets downstream of the firefly luciferase cDNA from pGL3 vector into pCDNA3.0 plasmid vector and transiently transfecting into the 293FT cells in presence or absence of a vector expressing miR-592. If the miRNA binds to its target sequence in the 3' UTR, then the transcription of the luciferase gene would get affected, and the luciferase activity would decrease which was read by a multimode reader instrument. Luciferase reading was taken after 72 h of transfection and upon addition of D-Luciferin substrate to the cell lysates. The luminescence was normalized to the fluorescence of GFP expressing construct, which was co transfected to serve as a control for the transfection efficiency. The luciferase reporter

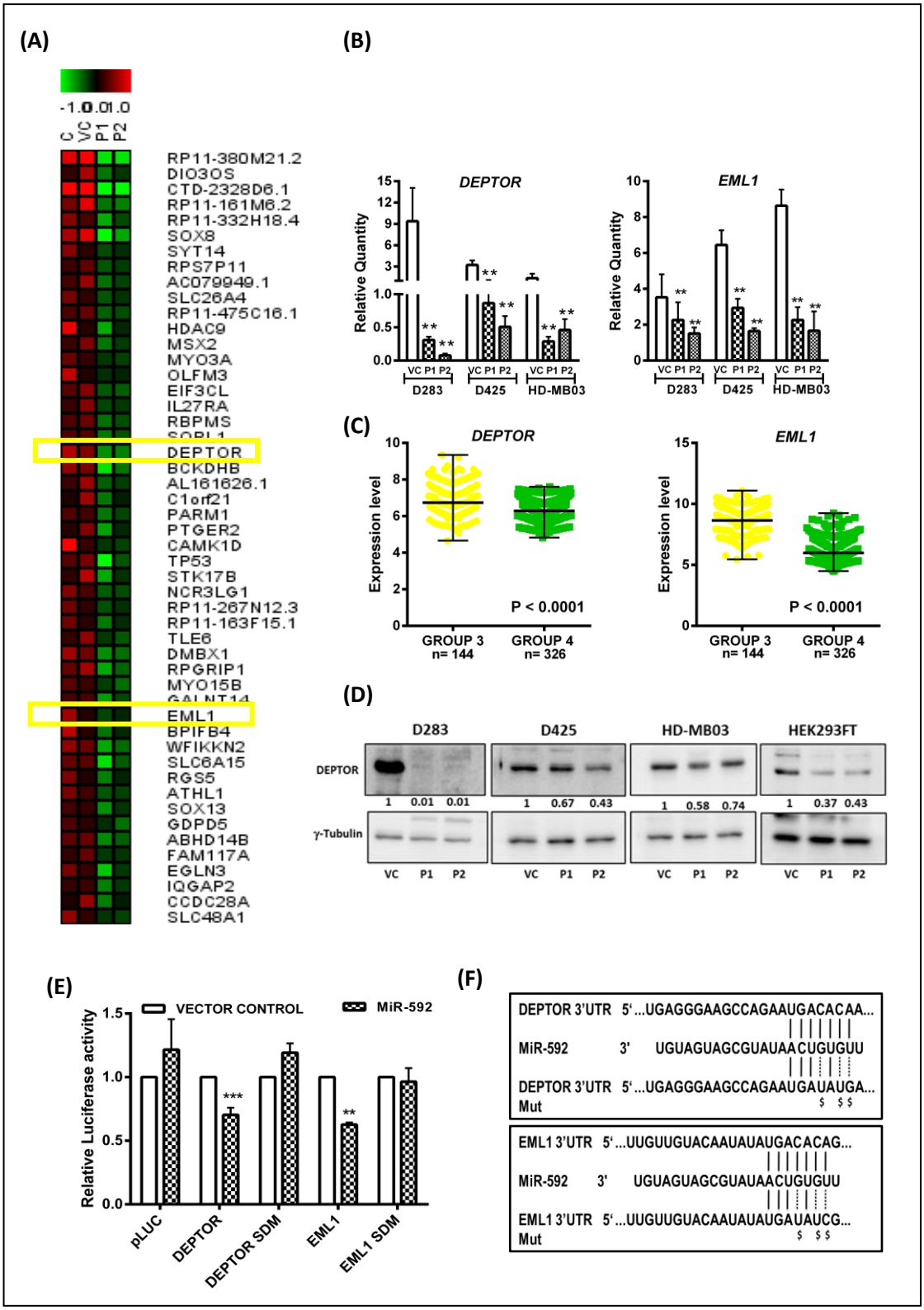

Figure 4.1.9 Identification and validation of DEPTOR and EML1 as the novel targets of miR-592. (A) Heat map showing the top 50 genes downregulated significantly (padj <

0.05) upon miR-592 expression in D283 cells, identified by the DESeq2 analysis. (B) Real-time RT-PCR analysis of the expression levels of DEPTOR, EML1 in vector control (VC) and miR-592 expressing P1, P2 populations of D283, D425 and HD-MB03 cells upon doxycycline induction. (C) The expression levels of DEPTOR, EML1 in Group 3, Group 4 medulloblastomas of the MAGIC cohort. (D) Validation of downregulation of DEPTOR at the protein level in the polyclonal populations expressing miR-592 of the indicated cell lines. The numbers below each blot indicate fold changes in the protein levels as compared to that in the vector after normalization using the protein γ-tubulin. (E) Y-axis shows luciferase reporter activity of the indicated construct upon miR-592 expression relative to that in the control. (F) The nucleotide sequence of the miR-592 target site in the 3' UTR of DEPTOR and EML1 gene. The mutations introduced by the site-directed mutagenesis are indicated by $. Mut:mutant; **, *** indicates $p \leq 0.05$, $p \leq 0.005$ respectively.

activity of the *DEPTOR* and *EML1* constructs decreased upon miR-592 expression by 35% to 45%, thereby confirming them as the direct targets of miR-592 (Figure 4.1.9 E). Furthermore, site-directed mutations were introduced into the 3' UTR of these constructs to alter the nucleotides of the miR-592 binding site.

These 3'UTR-mutant constructs were transfected into the HEK293FT cells and checked for the luciferase activity in the presence and absence of miR-592 expression. The alterations introduced in the potential miR-592 binding site in the 3'-UTR constructs abrogated miR-592 mediated reduction in the luciferase activity, thereby further validating *DEPTOR* and *EML1* as the direct targets of miR-592 (Figure 4.1.9 E and F). Thus, miR-592 directly targets *DEPTOR* and *EML1* by binding to their 3' UTRs and brings about downregulation of their expression. A western blot analysis also confirmed the downregulation of DEPTOR protein levels in all three medulloblastoma cell lines D283, D425, and HD-MB03, as well as in the HEK293FT cells, upon miR-592 expression. This finding is consistent with the lower expression of *DEPTOR* and *EML1* in the Group 4 tumors compared to Group 3 tumors.

4.1.10 MiR-592 mediated downregulation of DEPTOR activates both mTORC1 and mTORC2 complexes

DEPTOR is an endogenous inhibitor of mTOR kinase which is a component of both mTORC1 and mTORC2 complexes. The mTOR kinase signaling pathway plays a central role in cell growth, cell survival, and cell metabolism. The ribosomal protein S6 Kinase 1 (S6K1) and the translation repressor protein 4E-BP1 are well known downstream targets of mTORC1 complex. The mTORC2 complex is known to activate the AKT kinase by phosphorylating its S473 amino acid residue. The expression of miR-592 increased the levels of phospho-S6 kinase, phospho-4E-BP, and phospho-AKT(S473) (Fig. 4.1.10) in D283, D425, and HD-MB03 medulloblastoma cell lines as well as in HEK293FT cells, concomitantly with the downregulation of DEPTOR, upon doxycycline-induced miR-592 expression. Thus, the downregulation of DEPTOR, an endogenous inhibitor of mTOR kinase, by miR-592 leads to an increase in the activity of both mTORC1 and mTORC2 complexes.

4.1.11 Expression of miR-592 reduced the level of the active form of AKT kinase

The activation of mTOR kinase is also known to activate an inhibitory feedback loop that downregulates the activity of AKT kinase. For activation of the AKT kinase its phosphorylation on T308 residue is essential. Therefore, the expression levels of phosphor-AKT(T308) and the cell cycle inhibitor p21 (CDKN1A), an AKT substrate, were studied upon the expression of miR-592. The miR-592 expression increased the levels of the AKT kinase, phosphorylated on S473 residue (Fig. 4.1.10), but decreased the levels of AKT kinase phosphorylated on the T308 residue (Fig 4.1.11), in all 3 Group 3 medulloblastoma

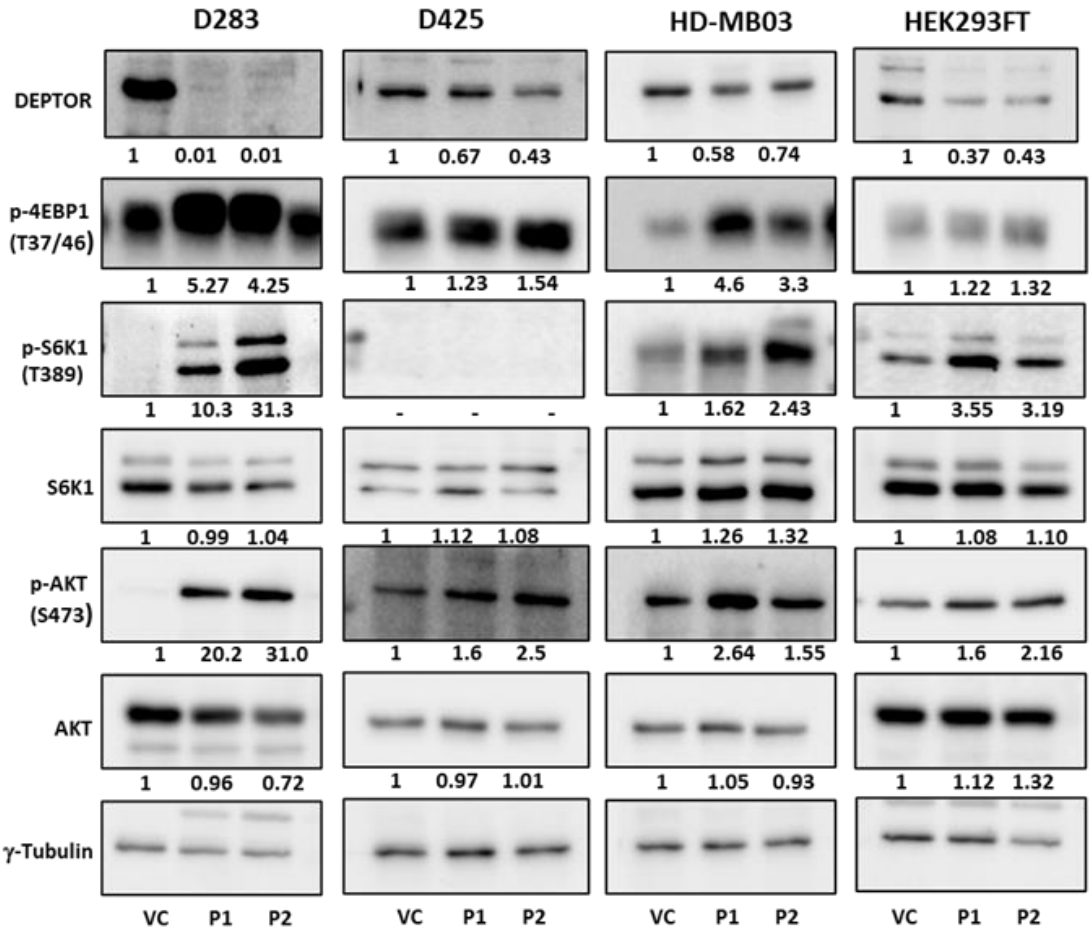

Figure 4.1.10 Western blot analysis showing the protein levels of DEPTOR and the substrates of mTORC1 and mTORC2 complexes upon expression of miR-592. The expression levels of total and phosphorylated forms of mTORC1 substrate S6K1, phosphorylated form of 4E-BP1, and total and phospho-AKT, a mTORC2 substrate were analyzed in the indicated cell line before or after miR-592 expression. VC: vector control cells; P1, P2: polyclonal expressing miR-592. The numbers below each blot indicate fold changes in the protein levels compared to that in the vector control cells after normalization using the house-keeping protein γ-tubulin.

cell lines as well as in the HEK293FT cells. The downregulation of the activity of the AKT kinase was further confirmed by the upregulation of the levels of p21, its substrate, which it targets for degradation (Fig. 4.1.11).

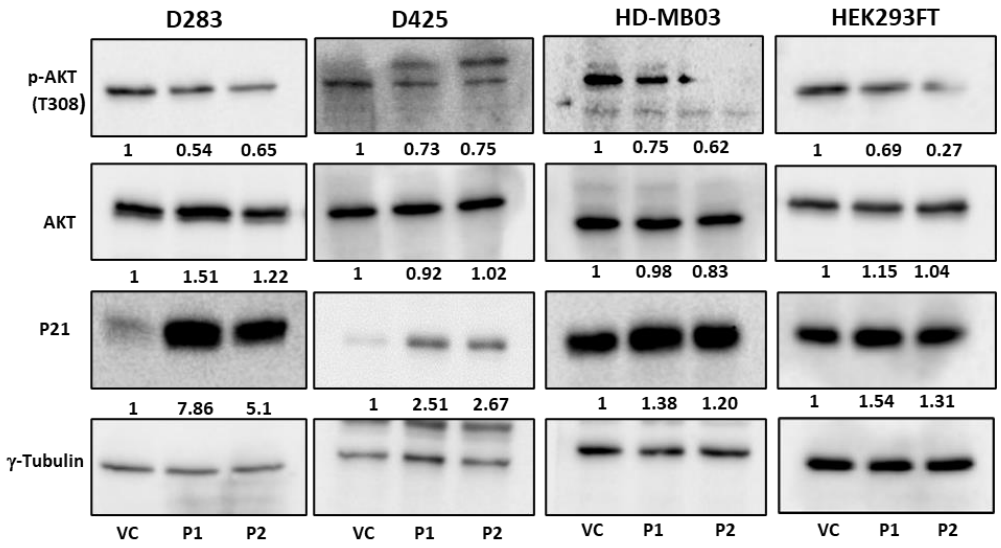

Figure 4.1.11 The western blot analysis showing the protein levels of the active form of the AKT kinase and its target p21 upon expression of miR-592. The expression levels of the active form of AKT kinase were studied by the western blot analysis using an antibody specific for the p-AKT (T308), and p21 (CDKN1A which is a target of the AKT kinase. The vector control (VC) cells as well as the polyclonal populations (P1, P2) expressing miR-592 of the indicated cell lines were treated with doxycycline. The numbers below each blot indicate the fold change in the protein levels compared to that in the vector control after normalization using the housekeeping protein γ-tubulin.

4.1.12 MiR-592 expression imparted a Group 4 characteristic neuronal differentiation-related signature to Group 3 medulloblastoma cell lines

RNA sequencing was performed to identify the genes differentially regulated upon miR-592 expression. Protein-protein interaction network analysis was performed by using the ClueGO plug in of the Cytoscape software which identified the pathways significantly enriched (by KEGG and Reactome pathway databases) upon miR-592 expression. The analysis performed on the 311 genes significantly (padj < 0.1) upregulated (log2FoldChange ≥ 0.8) upon miR-592 expression in D283 cells, showed enrichment of several neuronal differentiation-related genes (Figure 4.1.12A). The upregulation of insulin

resistance related type II diabetes mellitus pathway (highlighted) was also found to be enriched in the genes upregulated upon miR-592 expression. The enrichment of this pathway indicates the activation of the inhibitory feedback loop of mTOR signalling pathway that imparts insulin resistance due to downregulation of the PI3K/AKT signalling pathway. The enrichment of the activation of the inhibitory feedback loop of the mTOR signalling pathway is also consistent with the decrease in level of activated AKT, upon miR-592 expression. The pathway enrichment also showed the MAPK3 (highlighted) as a hub protein connected to several pathways involved in neuronal differentiation like axonal guidance, neuronal system, neurotransmitter receptors, transmission across chemical synapses. The upregulation of neuronal differentiation-related genes is a characteristic of Group 4 medulloblastomas as shown in the pathway enrichment analysis of the genes upregulated in Group 4 medulloblastomas. The figure 4.1.12 (B) shows the enrichment of several pathways involved in neuronal differentiation, neurogenesis and synaptic signalling is observed in Group 4 medulloblastomas.

4.1.13 Expression of miR-592 imparted neuronal differentiation related signature by activating mTOR and MAPK pathways in medulloblastoma cells

The miR-592 mediated downregulation of DEPTOR resulted in the activation of the mTOR kinase signalling pathway in the medulloblastoma cell lines as discussed above. MiR-592 also brought about upregulation of neuronal differentiation-related genes in D283 Group 3 cell line as identified by the RNA-seq analysis. The RNA-seq analysis also identified MAPK3 or ERK1 as a hub protein connected to various neuronal differentiation-related genes. Therefore, the effect of miR-592 expression on the activity of ERK1/ERK2 kinases

and the effect of inhibition of mTOR kinase and ERK1/ERK2 kinases on the upregulation of the neuronal differentiation-related genes was studied by the western blot analysis.

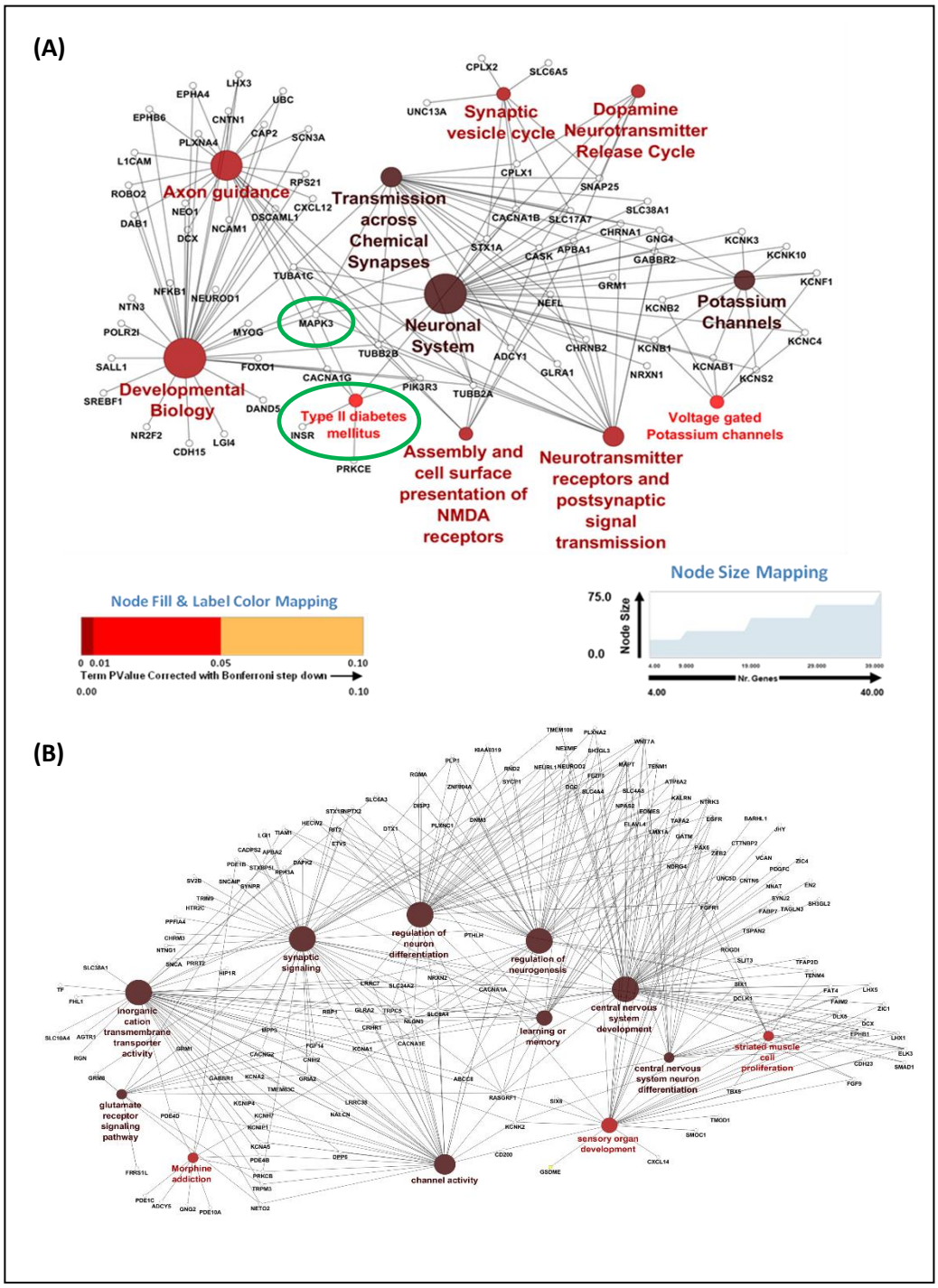

Figure 4.1.12 Pathways enriched upon miR-592 expression in the medulloblastoma cells Protein-protein interaction network analysis of the genes significantly upregulated

(log_2FoldChange ≥ 0.8) upon miR-592 expression in D283 cells (A) and in Group 4 medulloblastomas (B). The network was built from the genes significantly enriched (padj < 0.01) in the pathways from the KEGG and Reactome databases without any additional interactors. padj = p value corrected by the Bonferroni step down method.

The treatment with 100 nM rapamycin abolished the activity of the mTORC1 complex as judged by the downregulation of the levels of phospho-4E-BP1 in the vector control and P1, P2 populations of D283 cell line expressing miR-592 (Figure 4.1.13). The treatment with the ERK1/ERK2 inhibitor UO126 downregulated the levels of phospho-ERK1/ERK2 in the vector control and the miR-592 expressing P1, P2 populations of D283 cells. The inhibition of mTOR kinase signalling by rapamycin or inhibition of ERK1/ERK2 signaling by UO126 inhibitor, inhibited the miR-592 mediated upregulation of the neurofilament protein NF-L, a marker of neuronal differentiation in D283 cells. Thus, both mTOR kinase signalling and the MAPK signalling appear to contribute to the miR-592 mediated upregulation of neuronal differentiation-related genes in D283 cells. Interestingly, treatment with rapamycin inhibited MAPK signaling in addition to the mTOR signaling. The miR-592 mediated activation of the MAPK signaling pathway was also confirmed in D425 and HD-MB03 Group 3 medulloblastoma cell lines (Figure 4.1.13 B). Furthermore, upregulation of the neuronal differentiation markers NF-L and TUBB3 was also confirmed by western blotting in D283 and D425 cells (Figure 4.1.13 C). Interestingly, upegulation of the mTOR signaling, MAPK signaling and the neuronal differentiation marker TUBB3 was also confirmed in a set of Group 4 tumors compared to Group 3 tumors (Figure 4.1.13 D). Figure 4.1.13 (E) shows uniform protein loading from the fresh tumor tissues belonging to group 3/ group4 medulloblastomas

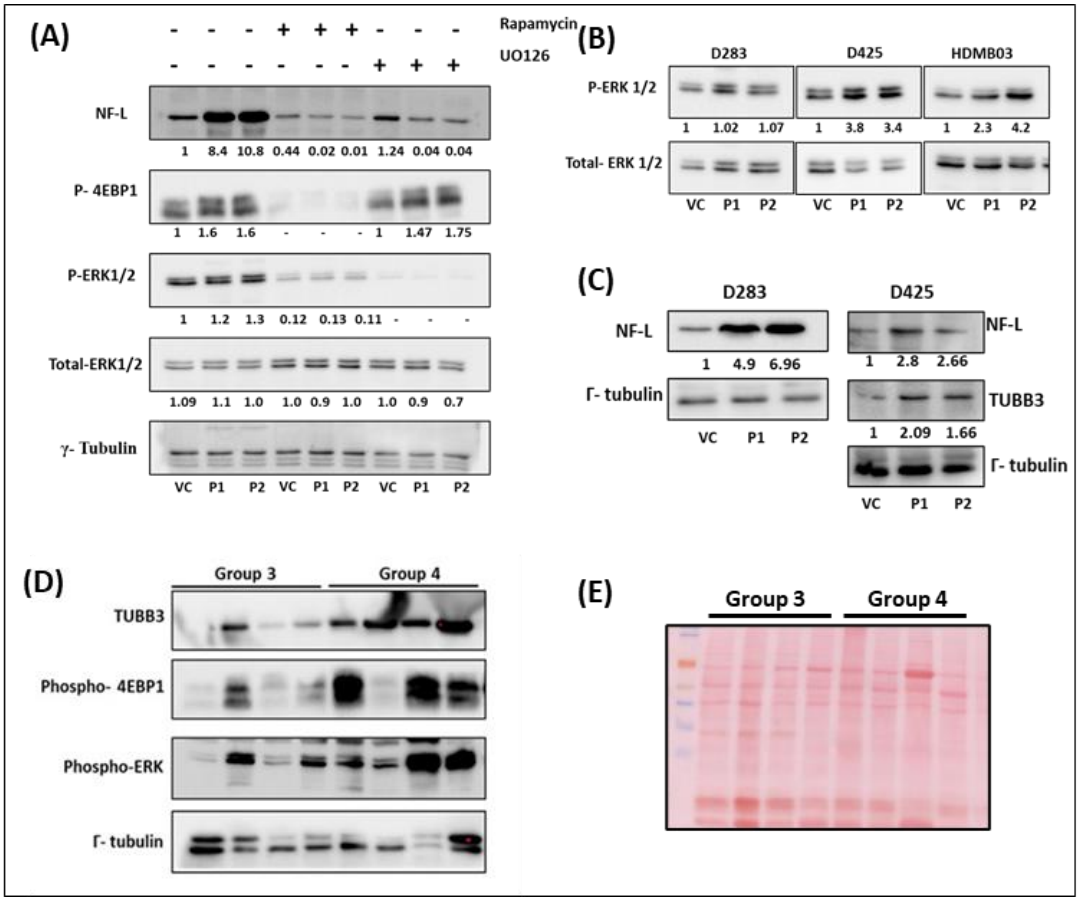

Figure 4.1.13 Western Blot analysis showing protein levels of neuronal differentiation-related markers and targets of the mTOR, MAPK signaling pathways
(A) Protein levels of neuronal differentiation related markers (NF-L) and targets of mTORC1 signaling (phospho-4E-BP1), MAPK signaling (phospho-ERK 1/2) in the vector control (VC) and miR-592 expressing polyclonal populations (P1 and P2) of D283 cells with (+) or without (-) treatment with rapamycin and UO126. (B) the protein levels of phospho-ERK1/ERK2 and total levels of ERK1/ERK2 and (C) the neuronal differentiation marker NF-L and TUBB3 in VC: vector control and P1, P2: miR-592 expressing polyclonal populations of the indicated cell line. All the cell populations were treated with doxycycline. (D) The expression levels of the indicated protein in four tumor tissues each of Group 3 and Group 4 medulloblastomas and the (E) Ponceau staining of the blot showing equal loading of the protein extracts. The numbers below each blot indicate fold changes in the protein levels as compared to that in the vector control after normalization using the house-keeping protein γ-tubulin.

Thus, miR-592, a group 4 specific microRNA, appears to contribute to the activation of the mTOR signaling as well as the MAPK signaling and thereby upregulates the neuronal differentiation-related genes in Group 4 medulloblastomas.

4.2 Discussion:

MiR-592 is differentially expressed across the four subgroups of medulloblastoma. While it has low level of expression in the WNT, SHH and Group 3 subgroup medulloblastomas, it is over expressed in almost every Group 4 tumors. Group 3 and Group 4 tumors have an overlap in their genetic profile as well as in their underlying chromosomal aberrations [46]. MiR-592 overexpression was found to be a characteristic feature of the Group 4 medulloblastoma and hence can serve as a useful marker to distinguish Group 4 tumors from Group 3 tumors. MiR-592 is co-expressed with its host gene GRM8 in medulloblastoma. GRM8 encodes a metabotropic glutamate receptor. Recently, a single cell RNA - sequencing analysis of the posterior fossa brain regions showed that the transcriptome of Group 4 medulloblastomas closely resembles that of the progenitor and differentiated cells of the unipolar brush neurons from the cerebellar region of the brain [103]. Unipolar brush cells are glutamatergic interneurons enriched in both ionotropic and metabotropic glutamate receptors. MiR-592 expression, therefore, seems to be a characteristic of the Group 4 medulloblastomas as the cell of origin for the Group 4 medulloblastomas is a glutamatergic neuronal progenitor cell.

Deregulation of microRNAs expression is common in various cancers and known to play a role in the disease pathogenesis [16]. MiR-592 has been reported as both an oncogene and as a tumor suppressor. One of the earliest reports states that the increasing level of miR-592 expression is associated with the transition of normal colon to carcinoma [82]. MiR-592 also represses FOXO3 expression and promotes proliferation of the prostate cancer cells [83]. On the other hand, MiR-592 targets DEK oncogene and suppresses cell growth in hepatocellular carcinoma cell line HepG2 [19]. MiR-592 functions as a tumor

suppressor in glioma by targeting IGFBP2 [85]. MiR-592 has also been reported to suppress the development of glioma by regulating Rho-associated protein kinase [84]. In breast cancer, miR-592 is reported to act as a tumor suppressor by downregulating TGF-beta2 [86]. In the present study, the expression of miR-592 in multiple Group 3 cell lines and a SHH subgroup cell line was found to decrease anchorage-independent growth, invasion potential, and tumorigenicity of medulloblastoma cells by about 25% -30%. Thus, miR-592 seems to decrease the malignant potential of the medulloblastoma cells, which is consistent with its reported tumor-suppressive role in other cancers like hepatocellular carcinoma, glioma and breast cancer. However, it is to be noted that its expression is ~ 100-fold high in Group 4 tumors as compared to normal cerebellar tissues, which fail to inhibit growth of these tumors. MiR-592 expression to levels similar to those in Group 4 tumors in established medulloblastoma cell lines could not inhibit proliferation or increase radiation or chemosensitivity and had moderate effect on their malignant characteristics like anchorage-independent growth and invasion potential.

EML1 and DEPTOR were identified as novel targets of miR-592 in the present study. MiR-592 expression downregulated both these targets in medulloblastoma cells and the luciferase reported assay unequivocally demonstrated the presence of miR-592 binding site in their 3'-UTRs. Both the genes are expressed at lower levels in Group 4 tumors as compared to Group 3 tumors as analyzed in a large cohort of medulloblastomas. Therefore, the high miR-592 expression is likely to contribute to lower expression of EML1 and DEPTOR in Group 4 medulloblastomas.

EML1 encodes for 'Echinoderm microtubule-associated protein like 1' that has been found to play a role in microtubule dynamics in interphase as well as mitotic phase cells

[104]. Loss of EML1 has been reported to result in abnormal spindle orientation in neural progenitor cells and the proliferation of ectopic neural progenitor cells in mouse and human brain [105]. A recent report has suggested that homozygous missense mutation or partial homozygous deletion of EML1 gene results in complex brain malformations in families having biallelic EML1 mutations leading to decreased protein activity [106]. The downregulation of EML1 upon miR-592 expression could disturb the microtubule dynamics, thereby contribute to medulloblastoma pathogenesis. On the other hand, a novel EML1-ABL1 fusion in the T-cell acute lymphoblastic leukemia (T-ALL) patient has been reported to act as an oncogene by constitutively activating the tyrosine kinase activity of ABL1 [107].

DEPTOR, or the DEP domain-containing mTOR-interacting protein was also identified as a novel miR-592 target in the present study. It is an endogenous inhibitor of the mTOR (mechanistic Target of Rapamycin) signaling. mTOR, a kinase forms two different complexes, mTORC1 and mTORC2. These complexes play a crucial role in regulating growth, metabolism, and immunity in response to nutrients, growth factors, and cytokines [108]. Deregulation of the mTOR signaling can result in several diseases like cancer, diabetes, making mTOR activity an attractive therapeutic target [109]. Since mTOR is involved in regulating several biological processes like mRNA translation, ribosome biogenesis, cell growth, and proliferation, the ability of DEPTOR to regulate this kinase suggests an important role of this protein in maintaining cellular homeostasis and normal cell functioning.

The mTOR is a serine/threonine protein kinase in the PI3K-related kinase family that forms the catalytic subunit of two distinct protein complexes, mTOR complex 1

(mTORC1) and 2 (mTORC2). Along with its core subunits – mTOR, Raptor and mLST8, mTORC1 also contains two inhibitory subunits – PRAS40 and DEPTOR [110, 111]. mTORC1 complex is inhibited by rapamycin. On the other hand, mTORC2 is characterized by insensitivity to acute rapamycin treatment [112]. Like mTORC1, mTORC2 also contains mTOR and mLST8, but instead of Raptor, it contains Rictor, that possesses analogous function. mTORC2 also contains DEPTOR along with other regulatory subunits like mSin1 and Protor1/2. mTORC1 promotes protein synthesis through the phosphorylation of two key effector molecules, p70 S6K1, which is a ribosomal protein kinase, and the eIF4E binding protein (4EBP). mTORC1 directly phosphorylates S6K1 on its hydrophobic motif side, Thr389, enabling its subsequent phosphorylation and activation by PDK1 [113]. S6K1 thereby phosphorylates and activates several substrates that promote mRNA translation. While mTORC1 is involved in controlling cell growth and metabolism, mTORC2 controls cell proliferation mostly by phosphorylating several members of the AGC family of protein kinases. The most important role of mTORC2 is the phosphorylation and activation of AKT, a key effector molecule of insulin/PI3K signaling pathway. mTORC2 phosphorylates AKT at Serine 473 (Ser473), present in the C-terminal hydrophobic motif of the molecule which is one of the requirements for activation of the kinase activity of AKT [114]. Once active, AKT promotes cell growth, proliferation, and migration through the phosphorylation or inhibition of several key substrates such as FOXO1/3a transcription factor, metabolic regulator GSK3β, and mTORC1 inhibitor TSC2 [115].

Upon expression of miR-592, the expression level of DEPTOR was downregulated in the polyclonal populations of several medulloblastoma cell lines. As DEPTOR was

downregulated, the inhibition upon mTORC1 and mTORC2 complexes was relieved resulting in activation of both these complexes. The increase in the levels phospho-S6K1, phospho4EBP1, and phosphor (Ser 473)-AKT, which are the substrates of the two mTOR complexes, respectively showed activation of both mTOR complexes upon miR-592 expression in medulloblastoma cells. The activation mTOR kinase activity mediated by downregulation of DEPTOR upon miR-592 expression indicates that miR-592 expression could result in increased protein synthesis and cell growth in medulloblastoma cells. Thus, miR-592 could act as oncogene in Group 4 medulloblastomas, thereby contributing to the pathogenesis of Group 4 medulloblastomas. A recent study on the proteomic and phospho-proteomic analysis of medulloblastomas has shown the enrichment of the Receptor Tyrosine kinase (RTK) signaling pathway as well as its downstream the Mitogen Activated Protein Kinase (MAPK) signaling and the mTOR signaling pathway in Group 4 medulloblastoma. The study claims ERBB4/SRC signaling as a hallmark of Group 4 medulloblastomas [69]. Besides the study has also found the expression of DEPTOR at both RNA and protein level to be lower in Group 4 medulloblastomas as compared to Group 3 tumors. These findings are consistent with our study that has shown miR-592, a miRNA overexpressed in Group 4 tumors, to target DEPTOR and thereby activate the mTOR signaling pathway. Thus, by activating mTOR signaling miR-592 appears to contribute to the pathogenesis of Group 4 medulloblastomas.

However, several studies carried out by using in vitro cell culture assays revealed that the effect of DEPTOR on mTOR signaling is much more complicated than what is anticipated. Although the depletion of DEPTOR promotes mTORC1 activity, several negative feedback loops emerge from mTORC1, the activation of which affects the PI3K

signaling [109]. Overactivation of mTORC1 triggers several negative feedbacks that also inhibit growth factor signaling pathway. The activation of S6K1, downstream of mTORC1 complex induces the phosphorylation of Insulin receptor substrate-1 (IRS1) on specific serine residues, which destabilizes IRS1 and reduces the ability of the growth factors to activate the signaling [116]. mTORC1 itself can also directly target IRS1 for its degradation [117]. Another mTORC1 mediated feedback loop involves growth factor receptor-bound 10 (GRB10), an endogenous inhibitor of the receptor tyrosine kinases. mTORC1 mediated phosphorylation stabilizes Grb10, leading to feedback inhibition of the phosphatidyl inositol 3-kinase (PI3K), and extracellular signal-regulated, mitogen-activated protein kinase (ERK-MAPK) pathways [118]. The activation of Akt at its Thr-308 residue by PDK1 takes place in response to IGF-1 (Insulin like Growth factor-1), a pathway in which the IRS proteins becomes obligatory [119]. AKT activation involves phosphorylation of two residues: threonine 308 (Thr308) in the activation loop and serine 473 (Ser473) in the C-terminal hydrophobic motif. Although the Ser473 phosphorylated AKT is studied in most of the tumors as a correlation of AKT activity, phosphoThr308-AKT also should be studied for evaluating activation of AKT kinase. Studies that compared these two phosphorylated AKT levels with the phosphorylation of three different AKT substrates, PRAS40, TSC2, and TBCID4 showed that AKT Thr308 phosphorylation correlated with the phosphorylation of each AKT substrates tested, whereas AKT-Ser473 phosphorylation did not correlate with the phosphorylation of any of the substrates examined [120]. Thus, the study concluded that phosphorylation of Thr308 is a more reliable marker of AKT activity, than Ser473. In the polyclonal populations expressing miR-592, the levels of Phospho-Thr308-AKT were downregulated which could be due to

the activation of the mTORC1 mediated feedback loop. The activation of the feedback loop is also supported by the enrichment of type II Diabetes pathway in the genes significantly upregulated upon miR-592 expression in medulloblastoma cells. Activation of the feedback loop by mTORC1 leads to the degradation of Insulin receptor substrate (IRS1), which is situated proximal to the insulin receptor, thereby desensitizing the cells to insulin, that can occur in Type II Diabetes [121]. Furthermore, activated AKT mediated metabolic activities of insulin like augmenting the glucose transport will be hampered under this scenario [122]. Akt is also a well-known inhibitor of the $p21^{Cip1/WAF1}$ molecule where in activated Akt phosphorylates p21 at Thr145 [123] , resulting in its nuclear export and proteasomal degradation. The increased levels of p21 further support the decreased AKT activity upon miR-592 expression in the medulloblastoma cells. AKT is a central player that promotes cell growth, motility, cell metabolism, and cell survival by phosphorylating several downstream targets. AKT phosphorylated cell cycle inhibitors like p21, FOXO family proteins, MDM2, GSK-3β thereby inhibiting p53 signaling, NF-kB signaling, and activating WNT signaling. AKT, therefore, is one of the most potent oncogenes. The downregulation of AKT activity as a result of the activation of the feedback-inhibitory loop of the mTOR signaling pathway could thus contribute to the decrease in the malignant potential of the medulloblastoma cells upon miR-592 expression. Thus, miR-592 mediated downregulation of DEPTOR levels activated the activity of both mTORC1 and mTORC2 kinases. However, activation of the feedback inhibitory loop of the mTOR signaling pathway led to an overall decrease in the activity of AKT kinase consistent with the reduction in the anchorage-independent growth, invasion potential, and tumorigenicity of medulloblastoma cells observed upon miR-592 expression. MiR-592 expression in Group

4 medulloblastomas, therefore, appears to contribute to the pathogenesis by activating mTOR signaling pathway but at the same by inhibiting the activation of AKT kinase thereby dampening the overall oncogenic effect consistent with the relatively indolent nature of Group 4 tumors.

Protein-protein interaction network analysis of the genes significantly upregulated by the expression of miR-592 in D283 medulloblastoma cells showed enrichment of several neuronal differentiation-related genes, which is a characteristic of the Group 4 tumors. TUBB3 is a neuron-specific β tubulin isoform type III while Neurofilament-L is a major intermediate filament of neurons. TUBB3 and Neurofilament-L showed an increase in the expression levels, validating the neuronal differentiation-related expression profile of miR-592 expressing medulloblastoma cells. Interestingly, inhibition of mTOR signaling by rapamycin abrogated the increase in the expression of neuronal differentiation-related protein NF-L upon miR-592 expression. Thus, by targeting DEPTOR and thereby activating mTOR kinase, miR-592 imparted the neuronal-differentiation related expression profile to D283, D425 Group 3 medulloblastoma cells. Notably, mTOR activation also promotes neural stem cell differentiation, and increased mTORC1 signaling by downregulation of the levels of TSC2, brings about a global increase in the rate of protein synthesis and also loss of stemness [124, 125]. Activation of mTOR kinase has been reported to be essential for oligodendrocyte differentiation and neuronal differentiation of neuroblastoma cells [126]. The mTOR signaling is reported to promote both proliferation and differentiation of several cell types [127]. Interestingly, *DEPTOR* is also a stemness factor that regulates pluripotency and reduction in its levels is sufficient to promote differentiation as observed in mouse embryonic stem cells [128]. However, as in the case

of Group 4 tumors, miR-592 expressing medulloblastoma cells do not show neuronal morphology despite the expression of several differentiation-related proteins.

The protein-protein interaction network analysis showed MAPK as a hub protein connected to several neuronal differentiation-related proteins upon miR-592 expression in the D283 medulloblastoma cells. MiR-592 expression upregulated the activity of ERK1/ERK2 in all the medulloblastoma cell lines studied. The treatment with ERK1/ERK2 inhibitor abrogated the increase in the level of neuronal differentiation marker NF-L in D283 cells. Interestingly, inhibition of the mTOR kinase activity by rapamycin also inhibited ERK kinase activity in miR-592 expressing medulloblastoma cells.

In summary, miR-592 is overexpressed in over 95% of Group 4 medulloblastomas and correlates with better survival in the non-WNT, non-SHH subgroup medulloblastomas. The expression of miR-592 decreased the anchorage-independent growth, invasion potential and tumorigenicity of MYC overexpressing Group 3 medulloblastoma cells. EML1 and DEPTOR were identified as novel targets of miR-592. MiR-592 mediated reduction in the expression levels of EML1 and DEPTOR could contribute to the pathogenesis of Group 4 medulloblastomas by disturbing microtubule dynamics and activating mTORC1, mTORC2 complexes, respectively. The feedback inhibitory loop of the mTOR signaling appears to be activated upon miR-592 expression as well resulting in a decrease in the activity of AKT, a highly potent oncogene. Thus, miR-592 could also contribute to the indolent nature of Group 4 medulloblastomas. Furthermore, miR-592 brought about significant increase in the expression of neuronal differentiation-related genes, a characteristic of Group 4 medulloblastomas that was abrogated upon treatment with rapamycin, a mTOR kinase inhibitor. In conclusion, miR-

592 by downregulating DEPTOR activates activity of mTORC1, mTORC2 complexes and thereby contributes to the pathogenesis and characteristic neuronal-differentiation related expression profile and indolent nature of Group 4 medulloblastomas.

Chapter – 5:

Role of miR-204 in medulloblastoma pathogenesis

RESULTS AND DISCUSSION

5.1 Role of miR-204 in medulloblastoma pathogenesis

There is a considerable level of heterogeneity that exists within the four subgroups of medulloblastoma with respect to overall survival. Therefore, molecular markers are required for further risk stratification in each subgroup particularly in the three non-WNT subgroups. Group 3, Group 4 medulloblastomas have an overlap in their expression profile and underlying genetic alterations. However, the two subgroups differ in the overall survival rates with Group 3 having the worst five-year survival among all the four subgroups. MiR-204 is differentially expressed in the four molecular subgroups and in particular in Group 3, Group 4 medulloblastomas. The expression of miR-204 was studied in a cohort of 260 medulloblastoma patients by the method of the Taqman probe based real-time RT-PCR as described earlier (section 3.2.2) and correlated with the clinical features like metastasis and overall survival of the group 3/ expressing the microRNA in the established medulloblastoma cell lines and the molecular mechanism underlying the effects of miR-204 was also investigated.

5.1.1 MiR-204 is differentially expressed across the four subgroups of medulloblastoma in the Indian cohort and the western MAGIC cohort and also in the different subtypes of medulloblastoma as identified by integrative genomics

In the present study, 260 medulloblastomas were classified into their molecular subgroups by real-time PCR assay based on the expression level of 12 genes and 9 microRNAs (described in section 3.2.2d). The cohort comprised of 44 WNT, 75 SHH, 67 Group 3 and 74 Group 4 medulloblastomas. The expression level of miR-204 was studied in these tumor tissues as well as in the normal posterior fossa brain regions: cerebellum, mid-brains, pons,

and medulla which are believed to be the sites of origin for the four molecular subgroups of medulloblastoma. In the normal posterior fossa region, the expression level of miR-204 was found to be in the range of RQ = 21 to 93 (Fig 5.1.1 A). MiR-204 was differentially expressed across the four subgroups of medulloblastoma. In WNT subgroup the mean ± SE RQ of miR-204 expression is 95.3± 10.3, in SHH subgroup it is 5.2 ± 1.2, in group 3 it is 39.9 ± 9.0 and in group 4 it is 130.3 ± 16.5. Thus, miR-204 has high (RQ > 20) expression levels in WNT and 75% Group 4 medulloblastomas and low level of expression in almost all SHH and 54% Group 3 medulloblastomas (Figure 5.1.1 B). Thus, miR-204 is downregulated in all SHH medulloblastomas and in a subset of Group 3/ Group 4 tumors. MiR-204 expression was studied in an independent cohort of 763 medulloblastomas (MAGIC cohort) with the kind help of Dr. Vijay Ramaswamy from SickKids, Canada. The MAGIC cohort consisted of 70 WNT, 223 SHH, 144 Group 3 and 326 Group 4 medulloblastomas. MiR-204 showed differential expression profile across the four core medulloblastoma subgroups of the MAGIC cohort similar to that in the Indian cohort. It has high expression levels in the WNT tumors, low expression level in the SHH subgroup and low level of expression in a subset of group 3/ group 4 tumors (Figure 5.1.1 C). We have already discussed the broad continuum of subtypes within these subgroups that are recently defined in the previous chapters. Upon studying the genome wide DNA methylation data, gene expression data and copy number alteration data, the integrated analysis has identified 12 subtypes corresponding to the four core molecular subgroups of medulloblastoma [42]. MiR-204 expression level was found to be high in both the WNT subtypes, low in all four SHH subtypes, low in all 3 Group 3 subtypes and low to moderate in two out of three subtypes of Group 4. Group 3γ having the worst outcome had the lowest

level of mir-204 expression among the Group 3/ Group 4 subtypes (Figure 5.1.1 D). Analysis that integrated somatic mutation data analysis in addition to the genome wide methylation, transcriptome and copy number variation data has reported 8 subtypes within the Group 3/ Group 4 medulloblastomas [43]. Analysis of miR-204 in these eight subtypes showed that MiR-204 expression in these 8 subtypes shows considerable variation with the least expression in the 3 subtypes (ii, iii and iv) that contain only Group 3 tumors, in concordance with the fact that miR-204 is downregulated in most of the Group 3 medulloblastomas even in the Indian cohort. Furthermore, the subtype ii enriched for MYC amplification has the least miR-204 expression levels (Figure 5.1.1 E).

5.1.2 Lower level of miR-204 expression correlated with higher incidence of metastasis at diagnosis and poor overall survival in the non-WNT, non-SHH medulloblastomas and this clinical correlation was validated in an independent, non-overlapping cohort of patients

In the combined cohort of Group 3/ Group 4 medulloblastomas, the patients having metastasis at diagnosis had a median miR-204 RQ of 23.5 whereas patients who did not have metastasis at diagnosis had a median RQ of 54.52. Thus, patients with lower level of miR-204 had significantly ($p = 0.024$) higher incidence of metastasis at diagnosis as compared to the patients having a high expression of miR-204 (Figure 5.1.2 A). In the western 'MAGIC' cohort as well, patients having metastasis at diagnosis had a lower expression of miR-204 as compared to patients who did not have metastasis at diagnosis. However, this difference was not statistically significant (Figure 5.1.2 B).

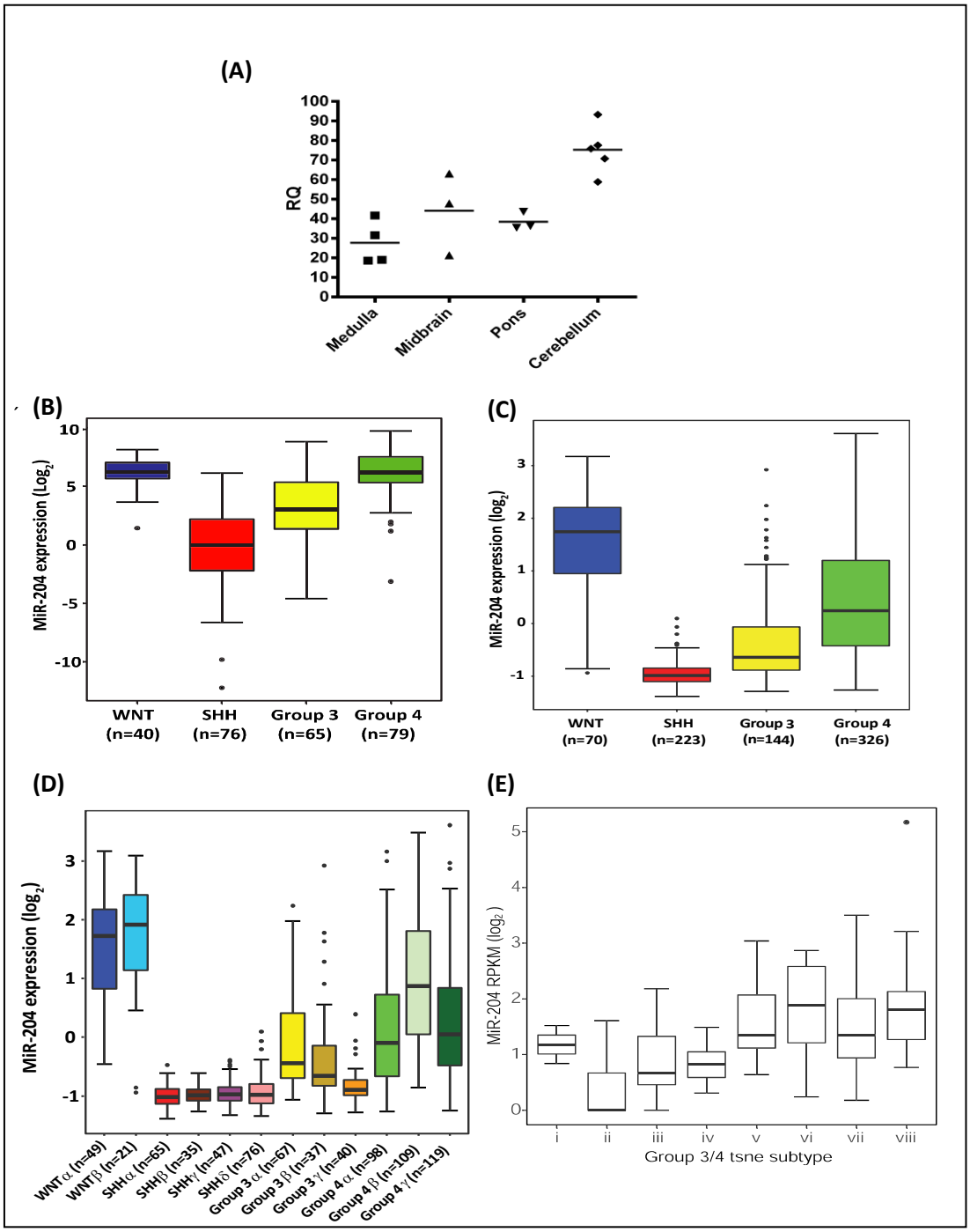

Figure 5.1.1 The expression level of miR-204 across the molecular subgroups in Indian cohort of 260 and a non-overlapping western cohort of 763 medulloblastoma
(A) The miR-204 expression level in posterior fossa regions of the normal brain. The expression level of miR-204 across the four medulloblastoma subgroups of the Indian cohort (B) and MAGIC cohort (C). Expression level of miR-204 across the 12 medulloblastoma subtypes from the MAGIC cohort (D) and the 8 subtypes of Group 3/ Group 4 medulloblastoma from the Northcott et al. dataset (E) [46] .

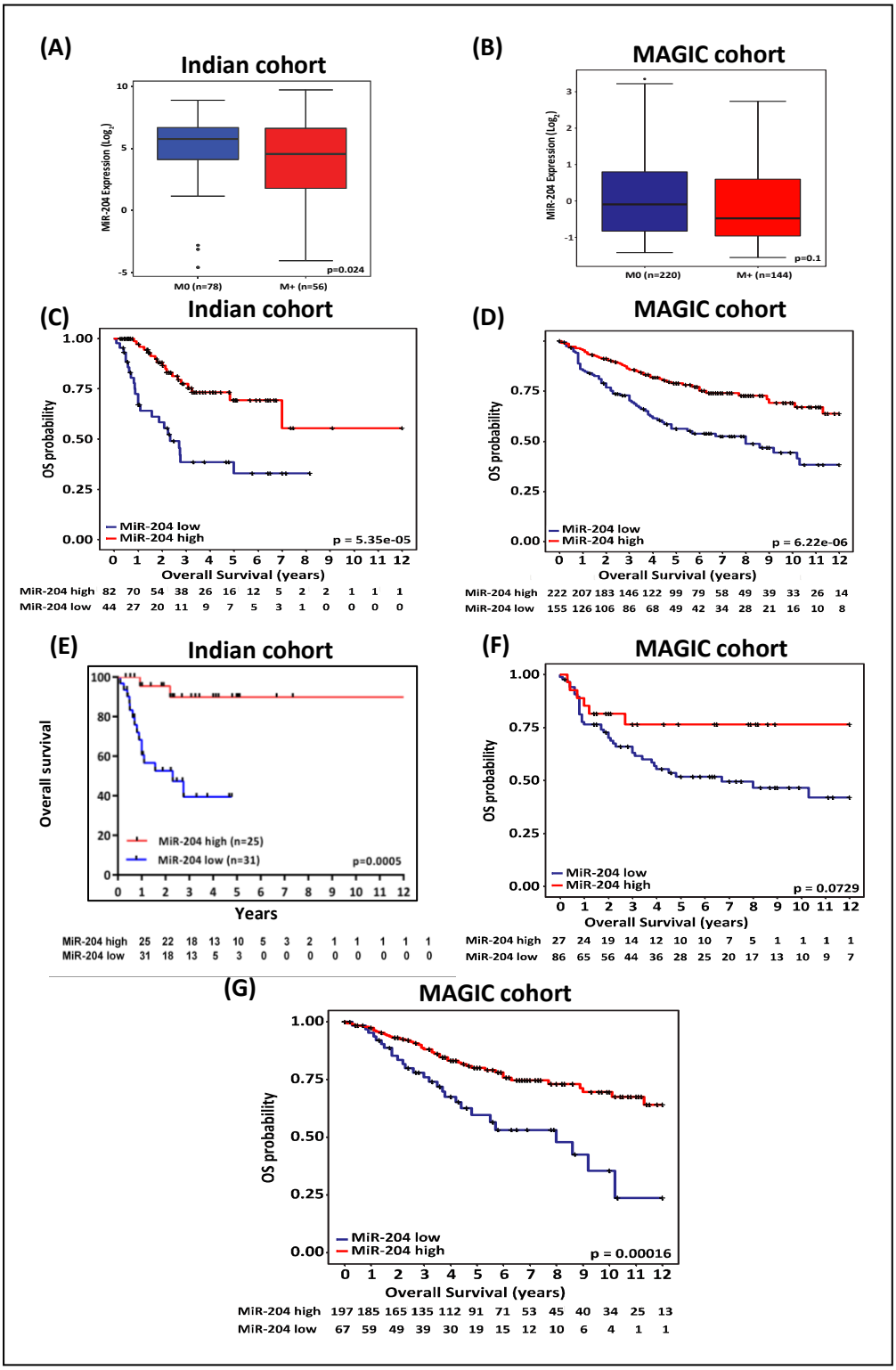

Figure 5.1.2 Correlation of miR-204 expression with the incidence of metastasis and overall survival Correlation of miR-204 expression with the presence (M+) or absence

(M0) of metastasis at diagnosis in the combined cohort of Group 3/Group 4 medulloblastomas of Indian cohort (A) and the western MAGIC cohort (B). Kaplan Meier survival analysis comparing the overall survival of 'miR-204 high' patients to 'miR-204 low' patients in the combined Group 3/Group 4 patients of the Indian cohort (C) and the MAGIC cohort (D). Kaplan Meier survival analysis comparing 'miR-204 high' patients to that of 'miR-204 low' patients only in the Group 3 medulloblastomas of the Indian cohort (E) and MAGIC cohort (F) and that in the Group 4 medulloblastomas of the MAGIC cohort only (G*).*

Kaplan Meier analysis was performed to evaluate the difference in the survival rates of 'miR-204 high' and 'miR-204 low' patients. The Log-rank test was used to determine the statistical significance of the difference in the survival curves and p values < 0.01 was considered to be statistically significant. Group 3/ Group 4 tumors having a low expression of miR-204 had a significantly ($p = 0.00005$) poor overall survival as compared to the patients with high expression of miR-204. Five-year overall survival of the 'miR-204 low' subset in the Indian cohort is 33% (95% CI, 16.8% -50.2%) as compared to 69.4% (95% CI, 54.1% -80.4%) of the 'miR-204 high' subset (Figure 5.1.2 C). Thus, low miR-204 expression correlated with higher incidence of metastasis at diagnosis and poor overall survival in the Indian cohort. In case of overall survival, the subset with lower expression of miR-204 in the combined Group 3/ Group 4 medulloblastomas ($n = 377$) of the MAGIC cohort, had significantly poorer overall survival that the subset with a higher expression level of miR-204. Five-year overall survival of the 'miR-204 low' subset is lower at 56.3% (95% CI, 48.1% - 65. 9%) as compared to 78.9% (95% CI, 73.1-85.2%) of the 'miR-204 high' subset (Figure 5.1.2 D). It was then studied if miR-204 expression level can identify a high-risk subset of patients in the Group 3 and Group 4 subgroup medulloblastomas individually. In the Indian cohort miR-204 expression level could successfully distinguish the 'low-risk' patients from the 'high-risk' patients within the Group 3 patients (Figure

5.1.2 E). In case of the MAGIC cohort, within the Group 3 tumors, patients having lower level of miR-204 expression (n = 86) had a tendency towards poorer survival than the patients with a higher level of miR-204 expression (n = 27). However, the difference did not reach statistical significance because of the lower fraction of the 'miR-204 high' patients (Figure 5.1.2 F). The subset of miR-204 low patients in the Group 4 medulloblastomas being extremely low, the survival analysis for Group 4 medulloblastomas on the basis of miR-204 expression was performed only in the MAGIC cohort. Within Group 4 tumors, the 'miR-204 high' subset had a five-year survival rate of 80% (95% CI 74% - 86.6%) while the 'miR-204 low' subset had a five-year survival of 59.7% (95% CI 47.2 – 75.4%) in the MAGIC cohort (Figure 5.1.2 G). Thus, we can conclude that miR-204 can act as a marker for good prognosis not only in the combined cohort of non-WNT, non-SHH medulloblastomas, but also within Group 3 and Group 4 tumors individually within the Indian as well as in an independent, non- overlapping MAGIC cohort. Thus, it was observed that both in the Indian as well as the western cohort, lower expression level of miR-204 identifies a highly aggressive subset of tumors that has a poor overall survival.

5.1.3 Restoration of miR-204 expression in Group 3 medulloblastoma cell lines to levels similar to that in normal cerebellum

The expression level of miR-204 in the established Group 3 cell lines D425, HD-MB03 and D283 was evaluated by the real-time RT-PCR assay. D425 and HD-MB03a recently established Group 3 cell line have the miR-204 expression level in the range of RQ = 0.02 to 0.14, which is almost 1000-fold lower than that of normal cerebellum. D283, which has a characteristic intermediate between Group 3, Group 4 tumors [102] had miR-204

expression in the range of RQ = 9.4 ± 1, which is 3-5-fold lower than the normal cerebellum levels (Fig 5.1.3 A).

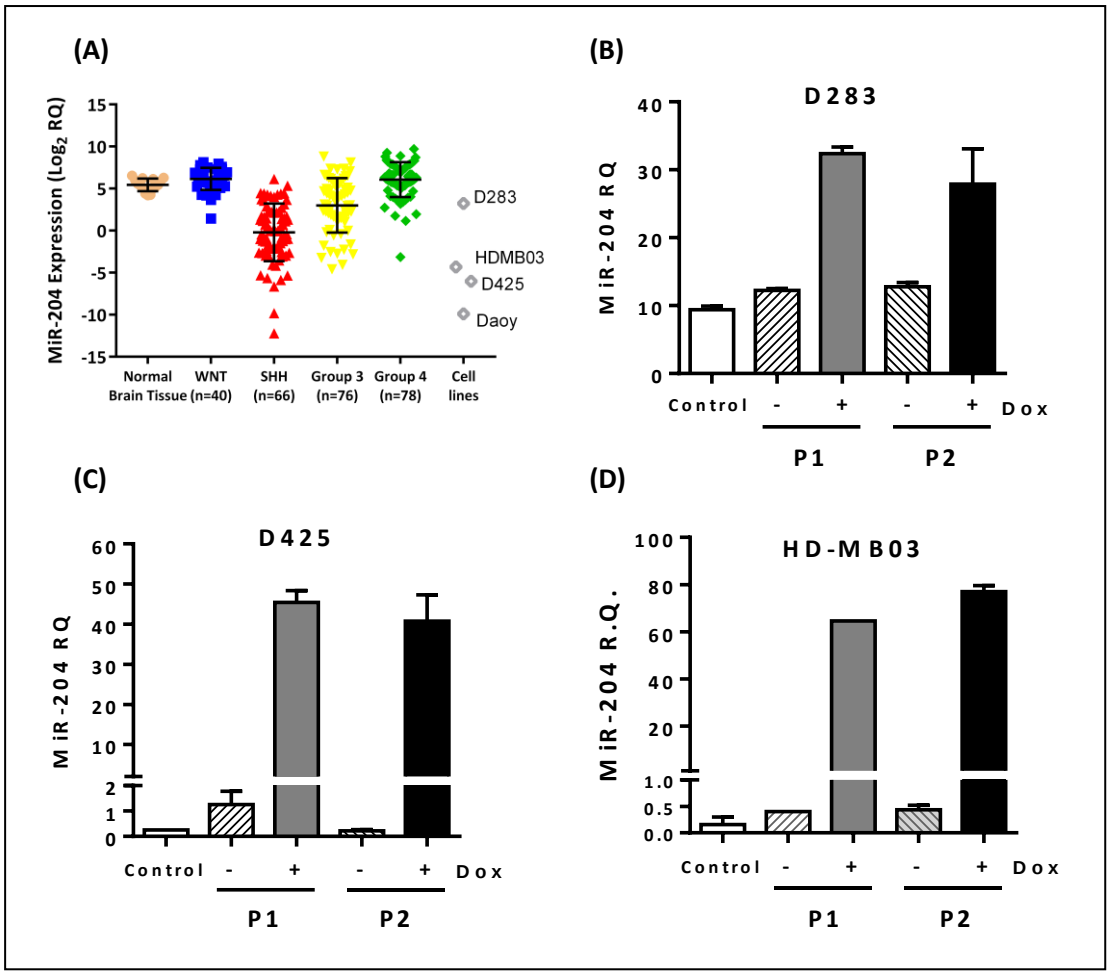

Figure 5.1.3 Expression levels of miR-204 in normal cerebellum, cell lines and the polyclonal populations of medulloblastoma cell lines expressing pTRIPZ-miR-204 construct. (A) MiR-204 levels across the normal cerebellum, medulloblastoma subgroups and established medulloblastoma cell lines. (B to D) MiR-204 expression levels in the established polyclonal populations (P1 and P2) of the indicated medulloblastoma cell lines before (-) and after (+) doxycycline induction.

For the expression of miR-204 in doxycycline-inducible manner, the genomic region encoding miR-204 was cloned into a lentiviral pTRIPZ vector and viral particles were generated by transfecting HEK293FT as a host cell line. Medulloblastoma cell lines were

transduced with this pTRIPZ-miR-204 construct and stable polyclonal populations were selected in the presence of puromycin. The polyclonal populations P1, P2 expressed miR-204 in the range of RQ = 25 to 70 comparable to the expression in the normal cerebellar tissues, upon induction with 4 µg/ml doxycycline for 72 h. (Figure 5.1.3 B to D). The polyclonal populations expressing miR-204 in Daoy cell line, which belongs to the SHH subgroup medulloblastoma and D341 belonging to Group 3 medulloblastoma were already available in the lab (Ph. D. thesis, Pooja Panwalkar). The medulloblastoma cell lines transduced with parental vector pTRIPZ vector alone were used as the as the vector control populations.

5.1.4 Restoration of miR-204 expression inhibited the proliferation and anchorage–independent growth potential of the medulloblastoma cells

The effect of miR-204 expression on the proliferation of medulloblastoma cells was studied by the MTT assay. The cells were seeded in triplicates at a density of 2000 cells in 100 µl medium per well in a 96 well plate. The medium containing doxycycline was replenished every 48 h. Percentage growth was calculated by measuring the total growth of individual clones from day 0 to day 10. Figure 5.1.4 A shows the growth pattern of vector control cells and cells expressing miR-204 in the indicated cell lines. In case of D283 and D425 cells, the proliferation potential of the cells was brought down by about 25% to 40% (Figure 5.1.4 B). However, no significant reduction was observed in case of the HD-MB03 cells. This indicates that the expression level of miR-204 brought about a significant reduction in the proliferation potential of D283 and D425 cell lines. The anchorage-independent growth potential of the cell is the one of the best representations of its malignant potential

and it is measured by the number of colonies formed in the soft agar colony-formation assay. After a doxycycline induction of 72 h, 2000 cells were seeded in semi-solid matrix

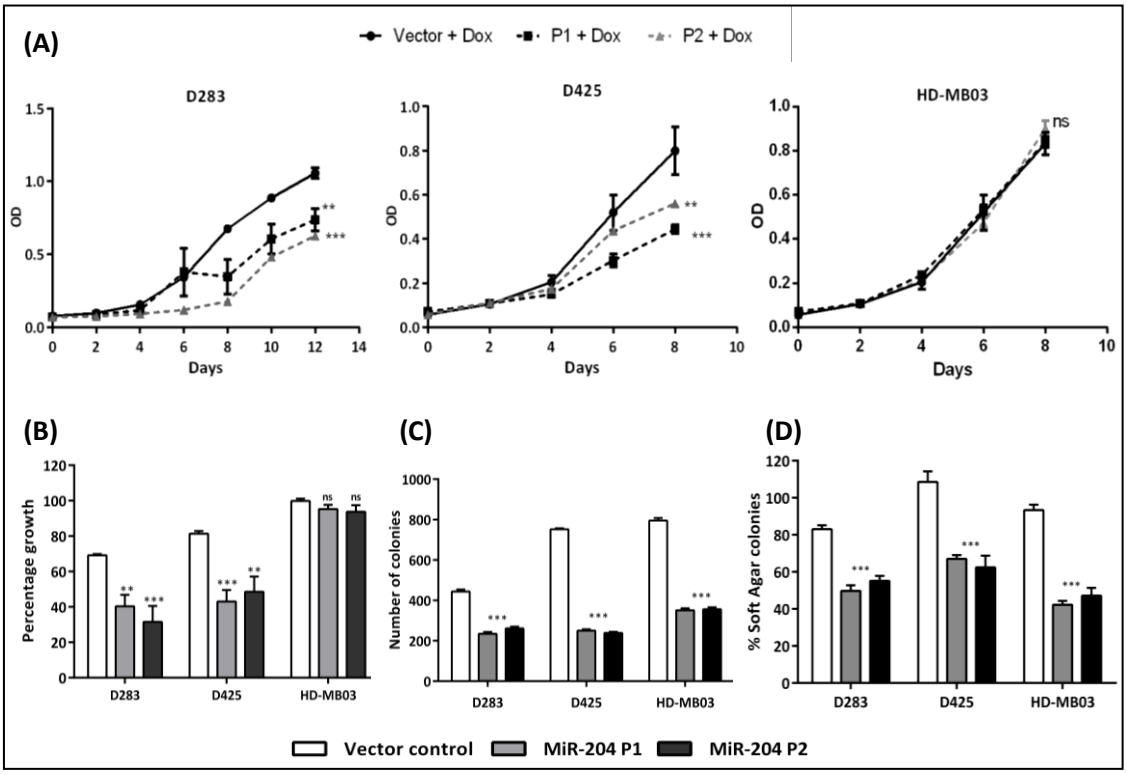

Figure 5.1.4 Effect of miR-204 expression on the proliferation and anchorage-independent growth potential of medulloblastoma cell lines. (A) Growth curves of the polyclonal populations (P1 and P2) expressing miR-204 and the vector control populations of the indicated cell lines upon doxycycline induction as studied by the MTT assay (B) Y-axis denotes the growth of the doxycycline-induced vector control and P1, P2 populations as a percentage of the growth of the corresponding un-induced populations, studied by the MTT assay. (C, D) Effect of miR-204 expression on the anchorage-independent growth of the medulloblastoma cells as studied by the soft-agar colony formation assay. Y-axis denotes the number of colonies (C) formed in the doxycycline-induced vector control cells and the P1, P2 populations in the indicated cell lines and as a percentage (D) of those formed in the corresponding un-induced populations from three independent experiments. ** and *** indicates $p \leq 0.001$ and $p \leq 0.0001$, respectively.

of 0.3 to 0.4 % agarose over a basal layer of 1% agarose in a 35mm plate. The polyclonal populations treated with doxycycline for the induction of miR-204 expression consistently

formed lower number of colonies as compared to their un-induced counterparts. The number of colonies reduced from ~400 to ~250 in D283 cells, ~750 to ~300 in D425 cells and from ~800 to ~300 in HD-MB03 cells. Thus, there was a significant inhibition (35 to 55%, $p < 0.001$) in the soft agar colony formation capacity of all the three cell lines studied (Figure 5.1.4 C and D). Therefore, the restoration of miR-204 expression could significantly inhibit the anchorage-independent growth potential, thereby the malignant potential of the medulloblastoma cells.

5.1.5 Expression of miR-204 increased the radiation sensitivity of the medulloblastoma cells

Patients with high miR-204 expression had a significantly better prognosis than the patients having low miR-204 expression, which could be possibly due to a better response to the treatment. Radiation therapy, as discussed previously, comprises of an indispensable part of medulloblastoma treatment. Therefore, the effect of miR-204 expression on the radiation sensitivity of the medulloblastoma cells was studied. D283 and HD-MB03 cells grow in a semi-adherent manner. Therefore, their radiation sensitivity was evaluated by the MTT assay. Two thousand cells of the miR-204 expressing polyclonal populations and the vector control were seeded in triplicates in a 96 well plate after 72 h of doxycycline induction. The cells were irradiated at a dose of 2, 4, or 6 Gy, the medium replaced after 24 h, their growth was followed by the MTT assay at 2-day intervals. The D0 dose is the dose of radiation required to reduce the population of living cells to 37%. Thus, it is a measurement of the relative radiation sensitivity of different cell populations. Upon expression of miR-204, there was a significant reduction in the D0 dose by 0.8 Gy to 1.6 Gy in D283 and HD-MB03 cells, respectively (Figure 5.1.5).,

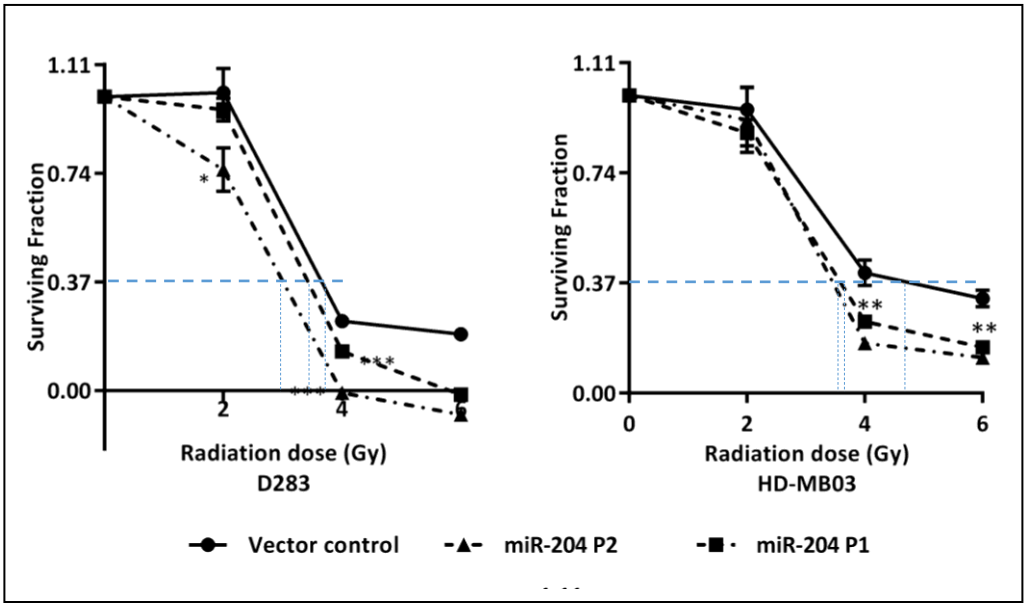

Figure 5.1.5 Effect of miR-204 expression on the radiation sensitivity of the medulloblastoma cells. The survival curves of doxycycline-treated P1, P2 populations expressing miR-204 and the vector control of D283 and HDMB03 cell line upon the indicated dose of radiation, studied by the MTT assay. Surviving fraction is the growth of the irradiated cells as a percentage of the growth of the un-irradiated cells.

Thus, the miR-204 expressing medulloblastoma cells required a lower dose of radiation to bring down its surviving population to 37%, indicating that the microRNA expression has increased radiation sensitivity of the medulloblastoma cells.

5.1.6 Expression of miR-204 inhibited the invasion potential of medulloblastoma cells

Medulloblastomas have the propensity to invade through the cerebrospinal fluid and spread either to the spinal cord or into the leptomeningeal space. About one-third medulloblastoma patients present metastasis at the time of diagnosis. The patients with metastasis at diagnosis were found to have a low level of miR-204 expression as compared to the patients who did not have the metastasis. Therefore, the effect of miR-204 expression on the invasion potential of medulloblastoma cells was investigated by evaluating the

potential of the cells to invade through the Matrigel-coated membrane in a transwell insert. Doxycycline-treated 50,000 cells of Daoy cell line and 75,000 cells of D283 and HD-MB03 cell line were seeded on the Matrigel-coated membrane in a serum-free medium. The medium containing FBS was added in the lower chamber which could act as a chemoattractant for the cells. The cells were then allowed to invade through the Matrigel-coated membrane in the transwell insert for 36 h (Daoy cells), 56 h (D283 cells) or 72 h (HD-MB03). Post invasion, the cells were labeled with Calcein, a fluorescent dye for 1 h. The un-invaded cells from the upper surface of the membrane were wiped out with the help of a cotton bud. Fluorescence intensity of the Calcein-labeled cells invaded onto the lower surface of the membrane was read at the excitation of 485 nm and the emission of 535 nm.

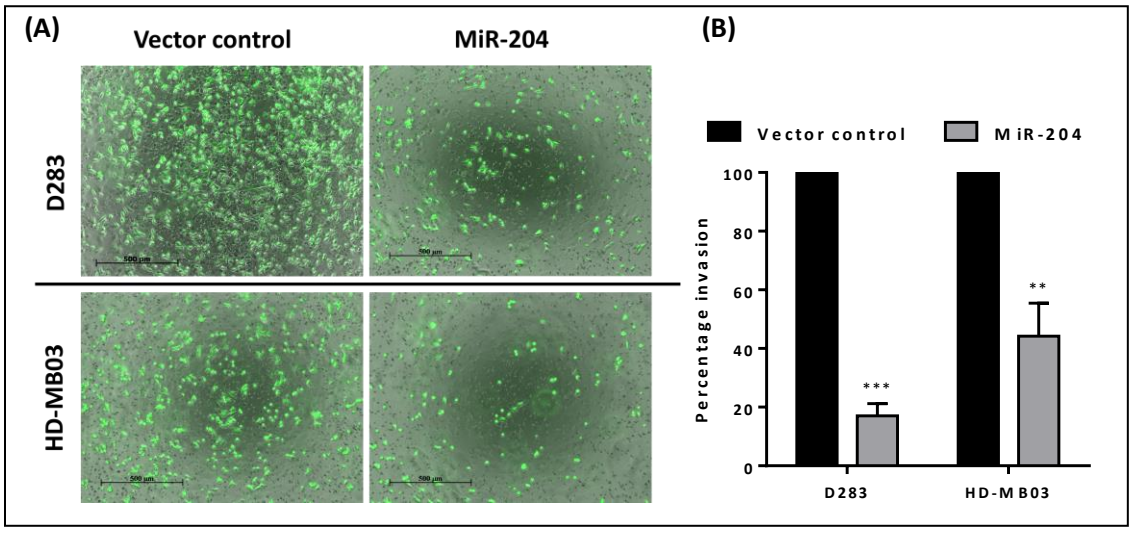

Figure 5.1.6 Effect of miR-204 expression on the invasion potential of medulloblastoma cells (A) Photomicrographs of the Matrigel-coated chamber post-invasion of the doxycycline-induced vector control or miR-204 expressing cells of the indicated cell line labeled with Calcein. (B) Y-axis indicates the invasion of the miR-204 expressing cells of indicated cell line as a percentage of the invasion of the corresponding vector control cells as evaluated by measuring fluorescence intensities of the calcein-labeled invaded cells. **, *** indicate $p \leq 0.001$ and $p \leq 0.0001$ respectively.

Figure 5.1.6 (A) shows the images of the calcein-labeled cells on the lower side of Matrigel-coated membrane post-invasion. The fluorescence intensity of the invaded cells was normalized with respect to the total intensity of the number of cells seeded for the invasion assay. The fluorescence intensity of the invaded cells of the P1/P2 populations expressing miR-204 was found to be 60%-80% less than that of the vector control population (Figure 5.1.6 B).

5.1.7 MiR-204 inhibited autophagy in medulloblastoma cells by targeting LC3B

MiR-204 is known to inhibit autophagy by directly targeting MAP1LC3B (LC3B) in clear cell renal cell carcinoma cells [129]. LC3B is a well-known marker of autophagy that plays a crucial role in the process. Hence, the effect of miR-204 expression on the basal level of autophagy in the medulloblastoma cells was investigated by studying LC3B flux and the expression levels of SQSTM1/p62 adapter protein which is known to accumulate upon autophagy inhibition. Upon induction of autophagy LC3BI isoform of LC3B gets converted to LC3BII as a result of conjugation of phosphatidylethanolamine. Lower LC3BI/LC3BII ratio therefore suggests autophagy induction. LC3BII levels however, also decrease due to degradation by lysosomal enzymes upon the fusion of autophagosome to lysosome. LC3B turnover was, therefore, studied with or without treatment with chloroquine (32 µg/ ml for 1h), an inhibitor of lysosomal degradation, in order to inhibit the degradation of the LC3BII protein. Therefore, the change in the expression levels of LC3B-I and LC3B-II, before and after inhibition of the lysosomal degradation pathway

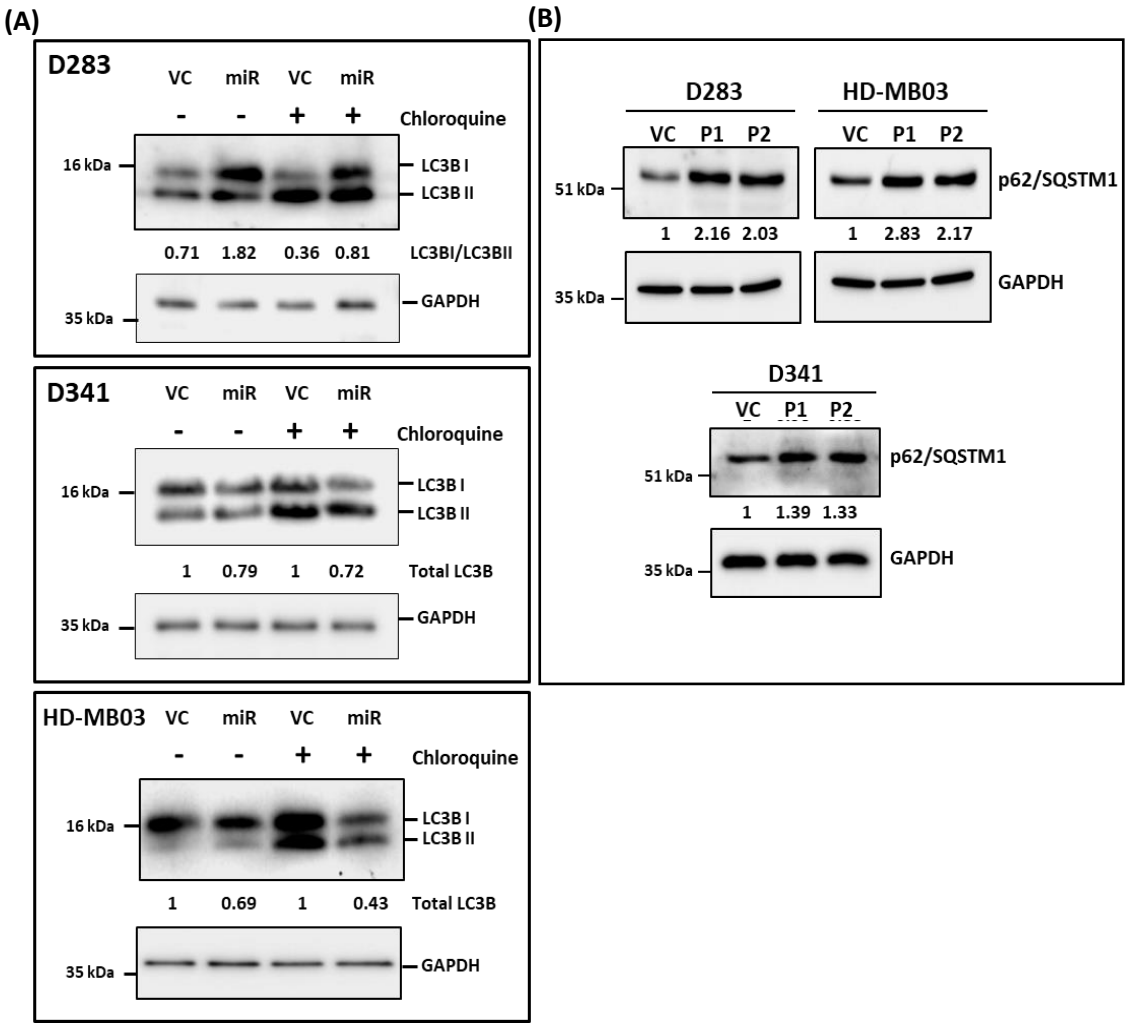

Figure 5.1.7 Effect of miR-204 expression on the autophagic potential of medulloblastoma cells. Western blot analysis showing the expression levels of autophagic marker LC3BI, LC3BII (A) and adapter protein p62/SQSTM (B) in the miR-204 expressing (miR) as compared to the vector control (VC) cells before (-) and after (+) chloroquine treatment for 1 h. Both the vector control and polyclonal populations expressing miR-204 were treated with doxycycline. The numbers below the blots indicate the fold change in LC3BI/LC3BII ratio or p62, upon miR-204 expression after normalization using the levels of GAPDH, the house-keeping control.

was studied to monitor autophagy [130]. MiR-204 expression resulted in the reduction in the total LC3BI/II levels both in the presence and absence of chloroquine in medulloblastoma cells (Figure 5.1.7 A). In the case of D283 cells (upper panel), upon

expression of mir-204, there is an increase in the level of LC3BI-form which indicates an increased LC3BI: LC3BII ratio and thus there was a reduction in the induction of autophagy both in the presence and absence of chloroquine. Further, the levels of SQSTM1/p62 adapter protein which accumulates upon inhibition of autophagy were found to increase upon miR-204 expression in all the medulloblastoma cell lines studied (Figure 5.1.7 B). Thus, miR-204 expression inhibited basal level of autophagy by targeting LC3B in medulloblastoma cells.

5.1.8 Inhibition of autophagy by knock down of ATG5 in the medulloblastoma cells

As it was observed that miR-204 inhibited basal autophagy in the medulloblastoma cells by targeting LC3B, the role of autophagy inhibition in the medulloblastoma cell growth and behavior was investigated. The objective was to determine if the inhibition of autophagy is the molecular basis of the tumor suppressive role of miR-204 in medulloblastoma cells. For autophagy inhibition, shRNA mediated knocked down of the *ATG5* gene, which is an upstream regulator of autophagy, was carried out in the three medulloblastoma cell lines- Daoy, D283 and HD-MB03.The cell lines were transduced with a shRNA targeting ATG5 gene in a doxycycline-inducible pLKO lentiviral vector. Polyclonal populations (P1, P2) stably expressing the shRNA were selected in the presence of puromycin. Fig. 5.1.8 (A) shows a reduction in the ATG5 expression levels in the polyclonal populations of the three cell lines upon doxycycline-induced shRNA expression. In order to check if autophagy was inhibited upon downregulation of ATG5, the levels of LC3B were studied by the western blot analysis as described earlier. Fig. 5.1.8 (B) shows a reduction in both LC3B-I and LC3B-II levels in the ATG5 knockdown Daoy cells, before and after treatment with chloroquine, an inhibitor of lysosomal degradation.

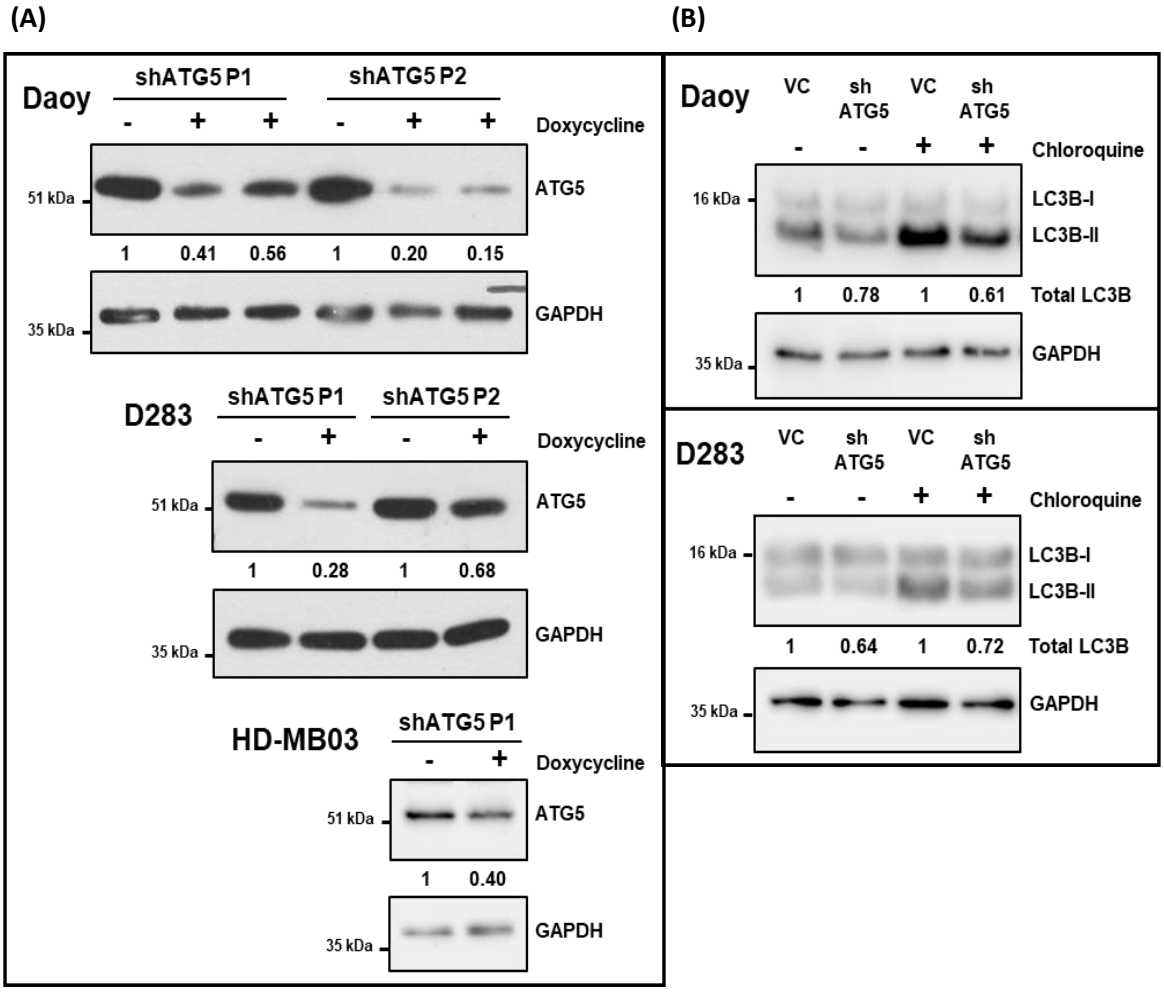

Figure 5.1.8 Inhibition of autophagy by knockdown of ATG5 in medulloblastoma cells. (A) Western blot analysis showing the levels of ATG5 in the polyclonal populations (P1 and P2) expressing shRNA against ATG5 before (-) and after (+) doxycycline induced shATG5 expression in the indicated cell lines. (B) Expression level of LC3B-I and LC3B-II isoforms in the doxycycline treated polyclonal population of the indicated cell line expressing shATG5 as compared to the parental cells expressing vector control alone, before and after treatment with chloroquine.

In D283 cells, LC3B-II levels decreased in the ATG5 knockdown cells as compared to the vector control cells, before as well as after the treatment with chloroquine. Thus, shRNA mediated knockdown of the ATG5 gene expression resulted in autophagy inhibition of the medulloblastoma cells.

5.1.9 Inhibition of autophagy did not affect the proliferation or anchorage-independent growth potential of medulloblastoma cells

The effect of autophagy inhibition upon the growth and malignant behaviour of the medulloblastoma cells expressing shRNA targeting ATG5 was studied.

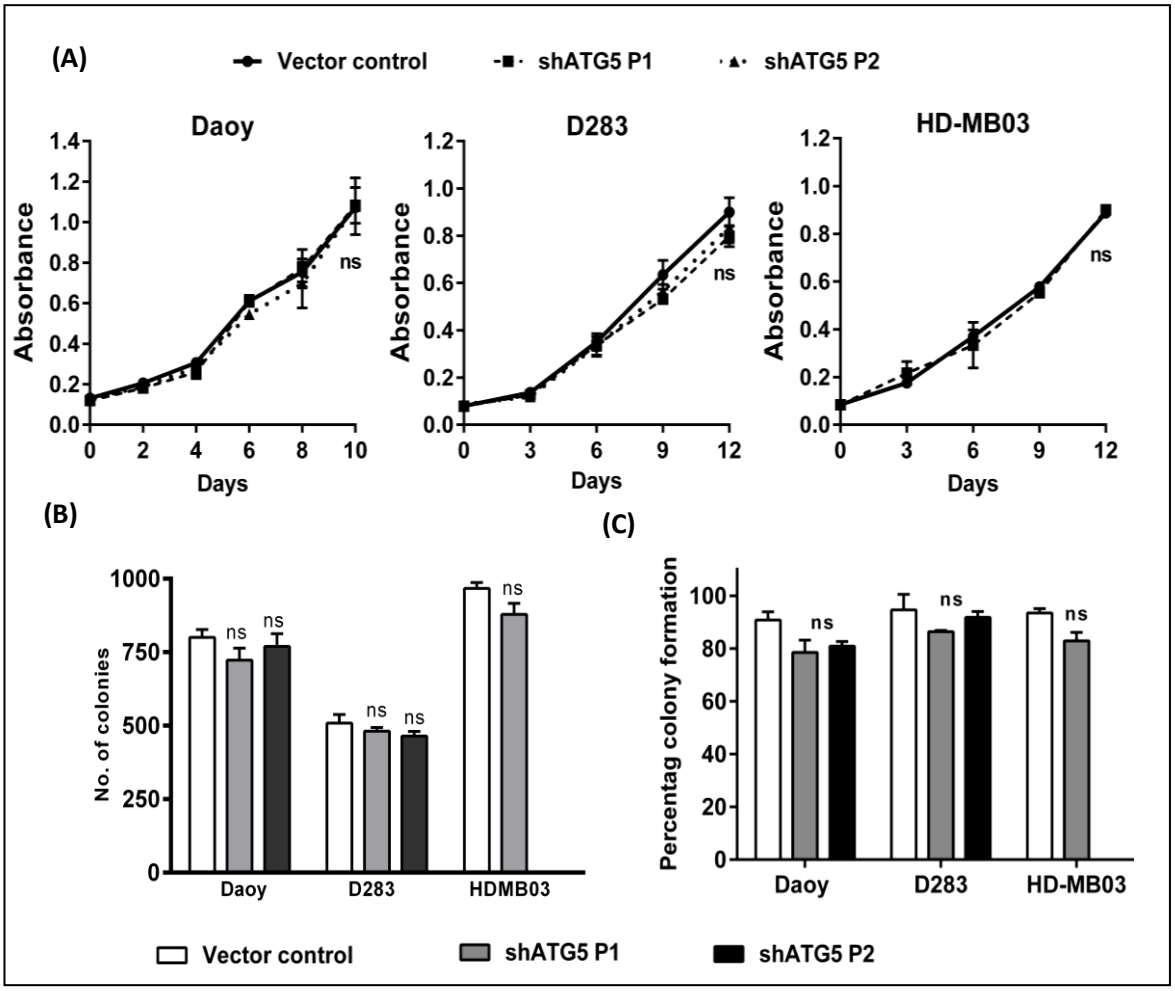

Figure 5.1.9 Effect of autophagy inhibition upon the proliferation and anchorage-independent growth of medulloblastoma cells. (A) Growth curves of the polyclonal populations (P1 and P2) expressing shATG5 and the vector control populations upon doxycycline treatment, as studied by the MTT assay. (B, C) The anchorage-independent growth potential of the polyclonal populations (P1 and P2) and their vector controls of the indicated cell line was studied by the soft agar colony forming assay. (B) Y-axis denoted the number of colonies formed by the indicated population upon doxycycline-treatment.

(C) Y-axis denotes the colony formation by the doxycycline-induced indicated population as a percentage of their un-induced counterparts. ns indicates non-significant.

The growth of Daoy, D283, and HD-MB03 polyclonal populations expressing doxycycline-induced ATG5 shRNA was studied by the MTT assay. Fig. 5.1.9 (A) shows the growth curves of the parental cell lines expressing the control vector alone and the P1, P2 populations expressing the ATG5 shRNA. The growth of the medulloblastoma cell lines did not change significantly upon autophagy inhibition by the ATG5 shRNA. The effect of autophagy inhibition on the anchorage-independent growth of the medulloblastoma cells was studied by the soft agar colony formation assay. There was no significant difference in the number in the soft agar colony-forming ability of the ATG5 knockdown cells of all three cell lines Daoy, D283, and HD-MB03 as compared to the cells expressing the control vector alone as shown in Fig 5.1.9. Thus, the downregulation of ATG5 brought about an inhibition in the autophagic potential of the medulloblastoma cells but did not affect their proliferation or anchorage-independent growth potential.

5.1.10 Inhibition of autophagy impaired the invasion potential of medulloblastoma cells:

MiR-204 expression was found to decrease anchorage-independent growth and invasion potential of medulloblastoma cells accompanied by the inhibition of basal autophagy. The invasion potential of the three medulloblastoma cell lines and their polyclonal populations expressing ATG5 shRNA was studied using the Boyden chamber invasion assay as described before. Figure 5.1.10 (A) shows microphotographs of the cells on the lower side of the membrane post-invasion through the Matrigel coated membrane. The invasion potential of the shRNA expressing Daoy, D283, and HD-MB03 cells was found to be

reduced by 50% to 80% depending upon the extent of downregulation of ATG5, and thereby inhibition of autophagy (Figure 5.1.10 B). Thus, although the autophagy inhibition did not affect the proliferative and anchorage independent growth potential of the cells, it brought about a substantial reduction in the invasive capacity of all three medulloblastoma cell lines studied.

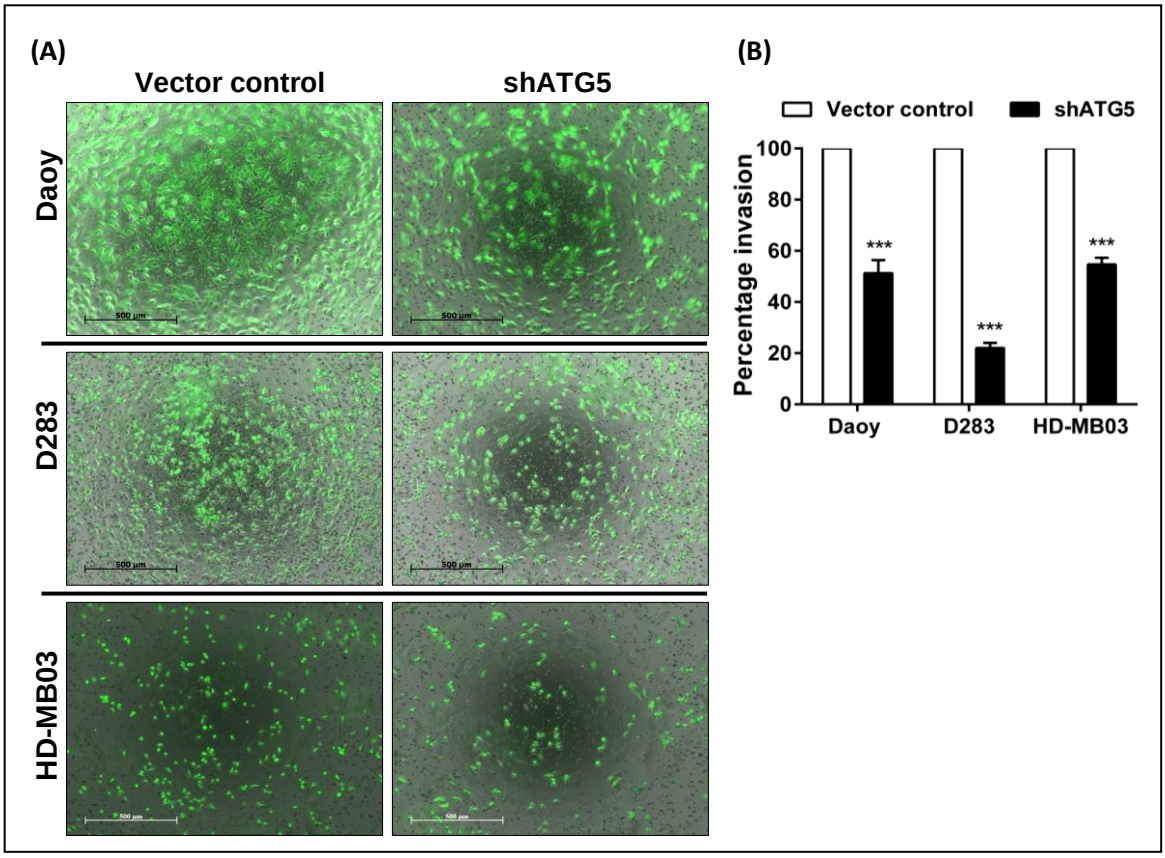

Figure 5.1.10 Effect of autophagy inhibition upon the invasion potential of medulloblastoma cells studied by the Boyden chamber assay (A) Photomicrographs of the matrigel-coated membranes post-invasion of the calcein labeled, doxycycline- induced vector control and shATG5 expressing polyclonal populations (indicated as shATG5) of the indicated cell line. (B) Y-axis denotes the invasion of shATG5 expressing cells as a percentage of the invasion of the vector control cells after normalization using the total fluorescence intensity of the cells seeded in the Boyden chamber. *** indicates $p < 0.001$ as determined by student's t-test.

Thus miR-204 appears to inhibit invasion potential of medulloblastoma cells by inhibiting the autophagic potential of the medulloblastoma cells.

5.2 Discussion

In the present study, the expression level of miR-204 was studied across the four subgroups of medulloblastoma and correlated with the incidence of metastasis and survival. Most of the WNT subgroup medulloblastomas and 75% Group 4 tumors expressed miR-204 at levels comparable to that in normal cerebellar tissues. On the other hand, almost all SHH tumors and 54% Group 3 tumors had low expression of miR-204. This finding was also validated in an independent western cohort of 763 medulloblastomas. Group 3 and Group 4 subgroups have considerable overlap in their gene expression profiles and underlying genetic alterations. Both subgroups express a set of transcription factors like OTX2, EOMES, FOXG1B. The chromosomal alterations like isochromosome 17q, a gain of chromosome 7, 18, loss of chromosome 8q, 10p, 11 also occur in both subgroups. Despite this commonality in the genomics, the two subgroups differ significantly with respect to their overall survival, with Group 3 having the worst survival of less than 50% five-year survival, while Group 4 has > 75% five-year survival rate. The molecular basis underlying the poor prognosis of many Group 3 and much better survival of most Group 4 is not understood. As a result, there is a paucity of good prognostication markers in these two subgroups.

In the present study, low levels of miR-204 expression in the combined cohort of Group 3, Group 4 medulloblastomas, as well as in Group 3 alone were found to correlate with poor survival. In the large western cohort, downregulation of miR-204 expression identified a subset of tumors having poor survival in Group 4 medulloblastomas as well. Thus, miR-204 was identified as a marker for prognostication in the two non-WNT, non-SHH

subgroups. Amplification of *MYC*, which occurs in about 15% – 20% of Group 3 tumors, is a known marker of poor prognosis in Group 3 tumors [131]. Integrated genomic analysis studies have identified several subtypes within each molecular subgroup of medulloblastomas [44, 45]. Among the three Group 3 subtypes described by Cavalli et al subtype 3γ enriched in MYC amplification and telomere maintenance pathway has the worst 5-year survival rate of 41.9%. Interestingly the subtype 3γ had the least expression of miR-204. [45]. The study by Northcott et al. [46] classified Group 3/Group 4 tumors into eight different subtypes, which eventually became the current consensus for the classification of the non-WNT, non-SHH tumors [63]. Among these eight subtypes, subtype II enriched in MYC amplification has the least miR-204 expression. Thus, the downregulation of miR-204 expression coincides with MYC amplification, the other known marker of poor prognosis in Group 3 tumors. Despite extensive subtyping of Group 4 tumors by the three integrated genomic studies, a marker for the tumors at high risk of recurrence could be not be identified in this subgroup. A study identified FSTL5 as a marker for poor prognosis in Group 3, Group 4 tumors [132]. However, almost 50% Group 3 / Group 4 tumors do not show FSTL5 expression immunohistochemically but do not necessarily display favorable clinical outcome; Thus, FSTL5 is not an accurate marker for prognosis [132]. Another study identified loss of chromosome 11 or gain of chromosome 17 as markers for better survival in Group 4 medulloblastomas [133]. These patients, irrespective of their metastasis status, showed excellent outcomes in both the discovery and the validation cohorts. However, almost 75% of Group 4 medulloblastomas do not recur. Therefore, markers are required to identify the subset of Group 4 tumors having a poor prognosis. Unlike in the SHH subgroup, *MYCN* gain or amplification had no correlation

with the poor prognosis of Group 4 tumors. Low miR-204 expression, on the other hand, identified a subset of Group 4 tumors having a poor prognosis. Thus, miR-204 is a valuable marker for prognostication in Group 4 medulloblastomas, wherein its low expression identifies a subset of tumors with poor prognosis. MicroRNAs being small in size are relatively protected from degradation during formalin fixation and hence are particularly useful in the case of FFPE tissues, which is the standard mode of processing tumor tissues for routine histopathological diagnosis. MiR-204, hence, can be introduced in routine clinical practice for risk stratification in Group 3, Group 4 medulloblastomas.

The downregulation of miR-204 expression correlating with poor survival in medulloblastoma is consistent with its tumor-suppressive, radiation sensitizing effect in medulloblastoma cells and its role in other cancers. MiR-204 is located at a fragile genomic site of chromosome 9q21.1–q22.3 that exhibits frequent loss of heterozygosity in various cancers. In a microRNA profiling study of 3312 tumors and1107 non-malignant tissues corresponding to 51 different cancer types, miR-204-211 family was found to be the top deleted microRNA family in the malignant tissues [21]. Therefore, miR-204 is likely to play a tumor-suppressive role in several types of cancers. In neuroblastoma, expression of miR-204 increased the sensitivity of the cells towards chemotherapeutic drugs such as cisplatin and etoposide by targeting *BCL2* and *NTRK2*. Furthermore, higher expression of miR-204 correlated with better overall survival in these patients [134]. MiR-204 was also identified as a promising biomarker for breast cancers wherein low level of miR-204 correlated with a poor prognosis and metastasis [135]. The downregulation of miR-204 expression has been shown to enhance glioma cell migration and stem cell like phenotype by targeting the stemness governing transcriptional factor SOX4 and the migration

promoting receptor EPHB2 [88]. MiR-204 also targets Ezrin that is overexpressed in a variety of neoplastic cells, and reduces invasion and migration of glioma cells [136]. In endometrial cancers, miR-204 has the highest difference in the expression levels between early-stage and late-stage specimens, which suggested that miR-204 might play a role in the disease progression. MiR-204 was shown to target FOXC1, thereby regulating the invasion and migration of the endometrial cells [87]. MiR-204-5p is frequently downregulated in the colorectal cancer tissues, and this downregulation correlates with a poor prognosis [137]. Upon ectopic expression, miR-204 was found to inhibit migration and invasion, increased sensitivity to chemotherapy of colorectal cancer cells, and *RAB22A,* a member of the *RAS* oncogene family, was found to be a direct target of miR-204 [137]. MiR-204 is also known to target Doublecortin, thereby controlling neuronal migration in mouse embryos [138]. Restoration of miR-204 expression in multiple established medulloblastoma cell lines belonging to Group 3 medulloblastomas was found to inhibit their proliferation potential, anchorage-independent growth, invasion potential, and tumorigenicity. It also sensitized the tumor cells towards radiation therapy. These effects of miR-204 expression is consistent with its tumor-suppressive role in various cancers including, breast cancer, colorectal cancer, endometrial cancer, neuroblastoma, and gliomas.

LC3B, a regulator of autophagy, is a known target of miR-204. MiR-204 mediated tumor-suppressive effect was accompanied by a reduction in the flux of basal levels of LC3B, indicating inhibition of basal autophagy in medulloblastoma cells. Autophagy is a process of self-degradation that leads to the lysosomal degradation of various cellular contents like damaged organelles and misfolded protein aggregates for biosynthesis and generation of

energy in times of stress or nutrient deprivation [139]. The process of autophagy is highly conserved and requires multiple steps that at first leads to the formation of the phagophore, that delivers the cargo in a double membrane-bound vesicle called the autophagosome to the lysosome. The ATG5-ATG12-ATG16L complex formation helps to in recruit LC3B-II into the growing tip of the phagophore, and once the autophagosome formation takes place, the complex gets dissociated from the membrane. Autophagosome fuses with the lysosome and gives rise to the formation of autolysosomes where the degradation of the cargo takes place by the lysosomal enzymes. Autophagy can have both a tumor suppressor or an oncogenic role in cancer [140]. It can have a tumor-suppressive role by preventing the accumulation of cellular debris and misfolded proteins. It can have an oncogenic effect by helping the tumor cells to sustain under unfavorable circumstances [141]. Mice having Beclin1 knock-out had higher incidence of lung, liver tumors and the lung tumors were considerably larger in size as compared to Beclin1 wild type mice [142]. Further, loss of ATG5/ATG7 in the liver, which is an important site for autophagy leads to hepatoma formation and accumulation of p62 adapter protein due to inhibition of autophagy further led to progression of the tumor which indicated that continuous autophagy is required for suppressing the tumorigenesis [142, 143]. Thus, inhibition of autophagy leads to oxidative stress, increased tissue damage and inflammation thereby promoting tumorigenesis. However, autophagy can also exert an oncogenic role by promoting tumorigenesis. A study performed in mutant KRAS and mutant BRAF mediated lung cancer mouse models showed that although initially the tumor formation is accelerated upon inhibition of autophagy, later on with the disease progression, the growth advantage provided by autophagy is lost and instead increased mitochondrial dysfunction in the cancer cells led to

longer survival of the autophagy deficient mice [140, 144]. One of the mechanisms in which autophagy plays its oncogenic role is by supporting the survival of the cells under condition of stress like starvation and hypoxia. Therefore, the role of autophagy inhibition in miR-204 mediated tumor-suppressive effect in medulloblastoma cells was investigated.

The expression of *ATG5*, an upstream regulator of autophagy, was downregulated using a shRNA in medulloblastoma cell lines. ATG5 downregulation inhibited autophagy as judged by the reduction in the LC3B flux and accumulation of p62 adapter protein. The autophagy inhibition did not lead to a significant decrease in the proliferation or anchorage-independent growth potential of medulloblastoma cells. However, there was a significant reduction in the invasion potential of the medulloblastoma cell line upon inhibition of autophagy. This finding suggests that miR-204 expression inhibits the invasion potential of medulloblastoma cells by inhibition of autophagy. This finding is consistent with the role of autophagy in mice breast cancer cells 4T1, where inhibition of autophagy did not inhibit the cell growth and viability but significantly led to the reduction in the metastasis of the cells to the lungs and liver [145]. The highly autophagic 4T1 cells require autophagy for the turnover of focal adhesion points in order to facilitate the motility of the cells. The autophagic regulator LC3B was found to directly interact with the focal adhesion protein Paxillin and stimulate the turnover of the focal adhesion complexes [145]. Autophagosomes are frequently associated with the focal adhesion points during disassembly, which suggests that autophagy is involved in the process of destruction of these focal adhesion complexes where the cargo protein NBR1 is known to be involved, thereby aiding in the turn-over of the focal adhesion complexes required for cell motility [146]. Studies have shown that the association of mTORC1 with the Uncoordinated 51-

like kinase 1 (ULK-1) is required for the induction of autophagy [147]. ULK1 and ULK2 have 50 % homology and are known to have compensatory roles in autophagy. Upon blocking ULK2, there was induction in autophagy as well as an increase in the migration potential of the lung cancer cells [148]. The role of autophagy in tumorigenesis has been shown to be not just by promoting cell growth under stress but also by promoting *RAS*-driven invasion in the cells [149]. Inhibition of autophagy has been reported to lead to the reduction in the secretion of the pro-migratory cytokine IL-6, the matrix metalloproteinase MMP2 and also WNT5A that is required to restore the migratory capacity of the autophagy-deficient cells [149]. The fact that autophagy inhibition led to a significant reduction in the invasion potential of the medulloblastoma cells suggests the therapeutic potential of the autophagic inhibitors in medulloblastoma. Almost one-third of medulloblastoma patients present metastasis at diagnosis. This invasive nature of medulloblastoma necessitates radiation therapy not just to the tumor bed but also to the craniospinal axis, which leads to severe toxic effects in the pediatric brain tumor patients. An autophagy inhibitor may be useful in reducing the radiation dose to the brain and spinal cord, thereby leading to reduced severity of the treatment-related side effects. Autophagy inhibitors like chloroquine, hydroxychloroquine have shown better treatment response in the clinical trials for treating various cancers [150, 151].

In summary, miR-204 expression serves as a valuable prognostication marker in the non-WNT, non-SHH medulloblastomas based on the study done in an Indian cohort and validated on a large western cohort. Its expression in multiple medulloblastoma cell lines had a tumor-suppressive effect, a finding that is consistent with its downregulation correlating with poor prognosis. MiR-204 inhibited basal autophagy in medulloblastoma

cells. Inhibition of autophagy inhibited invasion potential of medulloblastoma cells. This study for the first time has shown the role of autophagy in the invasion potential of medulloblastoma cells and thus delineates the molecular mechanism underlying the tumor-suppressive effects of miR-204 and also suggests a potential role for autophagic inhibitors as a therapeutic in medulloblastoma treatment.

Chapter – 6: SUMMARY AND CONCLUSION

Summary and Conclusions

The role of two microRNAs, miR-592 and miR-204, that are differentially expressed in the two non-WNT, non-SHH medulloblastomas was investigated in detail. Group 3 and Group 4 subgroups share genetic alterations and expression profiles but are distinct in their clinical behavior. Despite the extensive genomic analysis of these two subgroups, the molecular mechanism underlying the pathogenesis of these two tumor types is poorly understood, and there is a paucity of prognostication markers for accurate risk stratification.

The expression profiles of miR-592 and miR-204 were studied in a large cohort of 260 medulloblastomas from the Tata Memorial Centre and correlated with the clinical parameters: metastasis and overall survival. These findings were validated in an independent large western cohort of 763 medulloblastomas. Furthermore, the functional role of the two microRNAs was investigated by studying the effect of their expression on growth and malignant behavior of multiple medulloblastoma cell lines. The molecular mechanism underlying their tumor-suppressive effect on medulloblastoma cells was deciphered by identifying the genes and signaling pathways targeted by the two microRNAs. The salient findings of the study are given below.

- MiR-592 is overexpressed in 95% of the Group 4 medulloblastomas, which is almost 100-fold higher than the expression in the other subgroups and normal cerebellar tissues. Thus, it acts as a surrogate marker for Group 4 tumors, which have much better survival than Group 3 tumors.

- The expression of miR-592 brought about a reduction in the anchorage-independent growth, invasion potential, and tumorigenic potential of the Group 3 medulloblastoma cell lines, although it did not affect their proliferation, radiation sensitivity, or chemosensitivity.

- DEPTOR and EML1 genes were identified as novel direct targets of miR-592. Consistent with this finding, these genes are expressed at lower levels in Group 4 medulloblastomas as compared to Group 3 tumors, as analyzed in a large cohort of medulloblastomas.

- DEPTOR is an endogenous inhibitor of mTOR kinase. MiR-592 mediated downregulation of DEPTOR upregulated the activities of both mTORC1 and mTORC2 complexes in medulloblastoma cells. This finding is consistent with a recent phosphoproteomic study showing activation of mTOR signaling pathway in Group 4 medulloblastomas. Thus, miR-592 could contribute to the activation of mTOR pathway by targeting DEPTOR in Group 4 tumors, thereby contribute to their pathogenesis.

- MiR-592 also activated the feedback loop of mTORC1 that inhibited the activity of AKT kinase as judged by the reduction in the levels of the active form of AKT kinase and its target protein. The reduction in the AKT kinase activity is likely to decrease the malignant potential of the tumors, as is evident from the tumor-suppressive activity of miR-592 in medulloblastoma cells. MiR-592, thus, is likely to contribute to the indolent nature and much better survival rates of Group 4 medulloblastomas.

- Interestingly, miR-592 expression resulted in the upregulation of several neuronal differentiation-related genes, a characteristic of Group 4 tumors, in Group 3 medulloblastoma cell lines. MiR-592 distinguishes Group 4 tumors from Group 3 tumors,

the two tumor types that overlap in expression profile and genetic alterations. The expression of miR-592 giving Group 4 characteristics to Group 3 cell lines is consistent with the continuum of Group 3, Group 4 tumors, as has now been accepted universally.

- MiR-592 mediated activation of mTOR signaling, and MAPK signaling was found to be instrumental in upregulating neuronal differentiation-related genes in Group 3 medulloblastoma cell lines as evident from the loss of their expression upon treatment with inhibitors of mTOR and MAPK signaling.

- Thus, miR-592, a Group 4 specific microRNA, plays a crucial role in pathogenesis by targeting DEPTOR, EML1, by upregulating mTOR and MAPK kinase activity and by imparting characteristic neuronal differentiation signature to Group 4 medulloblastomas.

- MiR-204, a known tumor-suppressive microRNA, is differentially expressed in Group 3, Group 4 tumors, and downregulation of its expression correlated with poor survival in a combined cohort as well as in individual Group 3 and Group 4 medulloblastomas. These findings were validated in a large western cohort of 763 medulloblastomas as well. Thus, miR-204 is a useful prognostication marker in the non-WNT, non-SHH medulloblastomas, particularly in Group 4, which lacks markers for accurate risk stratification.

- Restoration of MiR-204 expression inhibited the anchorage-independent growth, invasion potential, and increased radiation sensitivity of medulloblastoma cells. Downregulation of miR-204 expression correlating with poor survival, therefore, is likely to be due to higher malignant potential and poor response to treatment.

- The tumor-suppressive effect of miR-204 was found to be accompanied by inhibition of basal autophagy in medulloblastoma cells by targeting LC3B, an autophagy regulator. Inhibition of autophagy upon shRNA mediated downregulation of ATG5, a key upstream regulator of autophagy, did not affect proliferation or anchorage-independent growth of medulloblastoma cells. Autophagy inhibition, however, resulted in the reduction in the invasion potential of medulloblastoma cells. Thus, miR-204 mediated inhibition of invasion potential of medulloblastoma cells is likely to be due to autophagy inhibition.

- The study, for the first time, showed the role of autophagy in the invasion potential of medulloblastoma cells and indicated the therapeutic potential of autophagy inhibitors in the treatment of medulloblastomas.

Significance of the study

- This is the first study that has correlated microRNA expression with survival in a molecularly classified two large cohorts of medulloblastomas.

- MiR-592 was identified as a molecular marker for Group 4 medulloblastoma that can be included in the routine clinical practice of molecular classification of medulloblastomas.

- The study delineated the role of miR-592 in the pathogenesis of Group 4 tumors identifying the crucial role of mTOR signaling and MAPK signaling in the biology of this tumor type.

- MiR-204 was identified as a prognostication marker for accurate risk-stratification in Group 3, Group 4 medulloblastomas, based on the clinical correlation study done on an Indian cohort and an independent large western cohort.

- The tumor-suppressive effect of restoration of miR-204 expression accompanied by inhibition of autophagy in medulloblastoma cells indicates the therapeutic potential of miR-204 and autophagy inhibitors in the treatment of medulloblastomas.

Future directions:

1. Integrated genomic analysis of Group 4 medulloblastomas has largely failed to identify the primary driver genetic alterations underlying pathogenesis of this subgroup. A recent phosphoproteomic analysis for the first time identified activation of the MAPK signaling pathway as an important driver alteration in Group 4 tumors. MiR-592, a Group 4 specific microRNA, was found to upregulate the mTOR and MAPK signaling pathway, and thereby impart the neuronal differentiation signature characteristic of Group 4 tumors to Group 3 medulloblastoma cells. Thus, the present study supports the findings from the phosphoproteomic study of Group 4 tumors indicating MAPK and mTOR signaling pathway playing crucial role in the pathogenesis of Group 4 medulloblastomas. The role of these two signaling pathways in biology of Group 4 medulloblastomas needs further investigation and validation using cell line and patient-derived xenograft (PDX) models. Cell lines have not been established from Group 4 tumors; however, PDX models are available wherein targets of these two pathways need to be identified. Whether inhibitors of the MAPK and mTOR signaling pathway could have therapeutic potential in Group 4 tumors also should be explored. Inhibitors of miR-592 may also have therapeutic potential in the treatment of Group 4 medulloblastomas.

2. MiR-204 was found to be a valuable marker for prognostication in Group 3, Group 4 medulloblastomas. This marker can be used routinely in clinics for risk stratification in these two subgroups. Group 3 patients having high miR-204 expression may not be

considered high-risk patients and thereby may be spared intense chemoradiation therapy. A clinical trial exploring this risk stratification strategy needs to be designed and explored.

3. MiR-204 was found to be tumor-suppressive in Group 3 medulloblastoma cell lines consistent with its tumor-suppressive effect in various other cancers. MiR-204 expression is downregulated in almost all SHH subgroup medulloblastomas. Its role in the pathogenesis of SHH subgroup tumors and possibly on the SHH signaling pathway remains to be studied. Lack of authentic SHH subgroup cell lines is one of the obstacles in this study. However, the studies could be carried out using PDX models and transgenic mouse models of SHH subgroup medulloblastomas. MiR-204 may have therapeutic potential in the treatment of Group 3 and SHH subgroup medulloblastomas

Chapter – 6: SUMMARY AND CONCLUSION

Summary and Conclusions

The role of two microRNAs, miR-592 and miR-204, that are differentially expressed in the two non-WNT, non-SHH medulloblastomas was investigated in detail. Group 3 and Group 4 subgroups share genetic alterations and expression profiles but are distinct in their clinical behavior. Despite the extensive genomic analysis of these two subgroups, the molecular mechanism underlying the pathogenesis of these two tumor types is poorly understood, and there is a paucity of prognostication markers for accurate risk stratification.

The expression profiles of miR-592 and miR-204 were studied in a large cohort of 260 medulloblastomas from the Tata Memorial Centre and correlated with the clinical parameters: metastasis and overall survival. These findings were validated in an independent large western cohort of 763 medulloblastomas. Furthermore, the functional role of the two microRNAs was investigated by studying the effect of their expression on growth and malignant behavior of multiple medulloblastoma cell lines. The molecular mechanism underlying their tumor-suppressive effect on medulloblastoma cells was deciphered by identifying the genes and signaling pathways targeted by the two microRNAs. The salient findings of the study are given below.

- MiR-592 is overexpressed in 95% of the Group 4 medulloblastomas, which is almost 100-fold higher than the expression in the other subgroups and normal cerebellar tissues. Thus, it acts as a surrogate marker for Group 4 tumors, which have much better survival than Group 3 tumors.

- The expression of miR-592 brought about a reduction in the anchorage-independent growth, invasion potential, and tumorigenic potential of the Group 3 medulloblastoma cell lines, although it did not affect their proliferation, radiation sensitivity, or chemosensitivity.

- DEPTOR and EML1 genes were identified as novel direct targets of miR-592. Consistent with this finding, these genes are expressed at lower levels in Group 4 medulloblastomas as compared to Group 3 tumors, as analyzed in a large cohort of medulloblastomas.

- DEPTOR is an endogenous inhibitor of mTOR kinase. MiR-592 mediated downregulation of DEPTOR upregulated the activities of both mTORC1 and mTORC2 complexes in medulloblastoma cells. This finding is consistent with a recent phosphoproteomic study showing activation of mTOR signaling pathway in Group 4 medulloblastomas. Thus, miR-592 could contribute to the activation of mTOR pathway by targeting DEPTOR in Group 4 tumors, thereby contribute to their pathogenesis.

- MiR-592 also activated the feedback loop of mTORC1 that inhibited the activity of AKT kinase as judged by the reduction in the levels of the active form of AKT kinase and its target protein. The reduction in the AKT kinase activity is likely to decrease the malignant potential of the tumors, as is evident from the tumor-suppressive activity of miR-592 in medulloblastoma cells. MiR-592, thus, is likely to contribute to the indolent nature and much better survival rates of Group 4 medulloblastomas.

- Interestingly, miR-592 expression resulted in the upregulation of several neuronal differentiation-related genes, a characteristic of Group 4 tumors, in Group 3 medulloblastoma cell lines. MiR-592 distinguishes Group 4 tumors from Group 3 tumors,

the two tumor types that overlap in expression profile and genetic alterations. The expression of miR-592 giving Group 4 characteristics to Group 3 cell lines is consistent with the continuum of Group 3, Group 4 tumors, as has now been accepted universally.

- MiR-592 mediated activation of mTOR signaling, and MAPK signaling was found to be instrumental in upregulating neuronal differentiation-related genes in Group 3 medulloblastoma cell lines as evident from the loss of their expression upon treatment with inhibitors of mTOR and MAPK signaling.

- Thus, miR-592, a Group 4 specific microRNA, plays a crucial role in pathogenesis by targeting DEPTOR, EML1, by upregulating mTOR and MAPK kinase activity and by imparting characteristic neuronal differentiation signature to Group 4 medulloblastomas.

- MiR-204, a known tumor-suppressive microRNA, is differentially expressed in Group 3, Group 4 tumors, and downregulation of its expression correlated with poor survival in a combined cohort as well as in individual Group 3 and Group 4 medulloblastomas. These findings were validated in a large western cohort of 763 medulloblastomas as well. Thus, miR-204 is a useful prognostication marker in the non-WNT, non-SHH medulloblastomas, particularly in Group 4, which lacks markers for accurate risk stratification.

- Restoration of MiR-204 expression inhibited the anchorage-independent growth, invasion potential, and increased radiation sensitivity of medulloblastoma cells. Downregulation of miR-204 expression correlating with poor survival, therefore, is likely to be due to higher malignant potential and poor response to treatment.

- The tumor-suppressive effect of miR-204 was found to be accompanied by inhibition of basal autophagy in medulloblastoma cells by targeting LC3B, an autophagy regulator. Inhibition of autophagy upon shRNA mediated downregulation of ATG5, a key upstream regulator of autophagy, did not affect proliferation or anchorage-independent growth of medulloblastoma cells. Autophagy inhibition, however, resulted in the reduction in the invasion potential of medulloblastoma cells. Thus, miR-204 mediated inhibition of invasion potential of medulloblastoma cells is likely to be due to autophagy inhibition.

- The study, for the first time, showed the role of autophagy in the invasion potential of medulloblastoma cells and indicated the therapeutic potential of autophagy inhibitors in the treatment of medulloblastomas.

Significance of the study

- This is the first study that has correlated microRNA expression with survival in a molecularly classified two large cohorts of medulloblastomas.

- MiR-592 was identified as a molecular marker for Group 4 medulloblastoma that can be included in the routine clinical practice of molecular classification of medulloblastomas.

- The study delineated the role of miR-592 in the pathogenesis of Group 4 tumors identifying the crucial role of mTOR signaling and MAPK signaling in the biology of this tumor type.

- MiR-204 was identified as a prognostication marker for accurate risk-stratification in Group 3, Group 4 medulloblastomas, based on the clinical correlation study done on an Indian cohort and an independent large western cohort.

- The tumor-suppressive effect of restoration of miR-204 expression accompanied by inhibition of autophagy in medulloblastoma cells indicates the therapeutic potential of miR-204 and autophagy inhibitors in the treatment of medulloblastomas.

Future directions:

1. Integrated genomic analysis of Group 4 medulloblastomas has largely failed to identify the primary driver genetic alterations underlying pathogenesis of this subgroup. A recent phosphoproteomic analysis for the first time identified activation of the MAPK signaling pathway as an important driver alteration in Group 4 tumors. MiR-592, a Group 4 specific microRNA, was found to upregulate the mTOR and MAPK signaling pathway, and thereby impart the neuronal differentiation signature characteristic of Group 4 tumors to Group 3 medulloblastoma cells. Thus, the present study supports the findings from the phosphoproteomic study of Group 4 tumors indicating MAPK and mTOR signaling pathway playing crucial role in the pathogenesis of Group 4 medulloblastomas. The role of these two signaling pathways in biology of Group 4 medulloblastomas needs further investigation and validation using cell line and patient-derived xenograft (PDX) models. Cell lines have not been established from Group 4 tumors; however, PDX models are available wherein targets of these two pathways need to be identified. Whether inhibitors of the MAPK and mTOR signaling pathway could have therapeutic potential in Group 4 tumors also should be explored. Inhibitors of miR-592 may also have therapeutic potential in the treatment of Group 4 medulloblastomas.

2. MiR-204 was found to be a valuable marker for prognostication in Group 3, Group 4 medulloblastomas. This marker can be used routinely in clinics for risk stratification in these two subgroups. Group 3 patients having high miR-204 expression may not be

considered high-risk patients and thereby may be spared intense chemoradiation therapy. A clinical trial exploring this risk stratification strategy needs to be designed and explored.

3. MiR-204 was found to be tumor-suppressive in Group 3 medulloblastoma cell lines consistent with its tumor-suppressive effect in various other cancers. MiR-204 expression is downregulated in almost all SHH subgroup medulloblastomas. Its role in the pathogenesis of SHH subgroup tumors and possibly on the SHH signaling pathway remains to be studied. Lack of authentic SHH subgroup cell lines is one of the obstacles in this study. However, the studies could be carried out using PDX models and transgenic mouse models of SHH subgroup medulloblastomas. MiR-204 may have therapeutic potential in the treatment of Group 3 and SHH subgroup medulloblastomas

Thesis Highlight

Name of the student: Raikamal Paul **Enrolment No.:** LIFE09201304012

Name of the CI/OCC:

Thesis Title: Role of miR-592 and miR-204 in medulloblastoma pathogenesis

Discipline: Life Sciences **Sub Discipline:** Cancer Biology

Date of viva voce: 30.12.2020

Medulloblastoma is a common malignant brain tumor in children consisting of four different subgroups, namely, WNT, SHH, Group 3 and Group 4. Group 3 and Group 4 medulloblastomas have an overlap in their expression profile and genetic alterations, but differ significantly in their clinical characteristics with Group 3 having the worst overall survival of ~ 45%. Therefore, there is a dire need to understand the biology of Group 3, Group 4 tumors and look for potential molecular markers in them that would be essential for accurate risk stratification. This is the first study that has correlated microRNA expression with survival in a molecularly classified two large cohorts of medulloblastomas. MiR-592 was identified as a molecular marker for Group 4 medulloblastoma that can be included in the routine clinical practice of molecular classification of medulloblastomas. The study delineated the role of miR-592 in the pathogenesis of Group 4 tumors identifying the crucial role of mTOR signaling and MAPK signaling in the biology of this tumor type. MiR-592 expression brought about the neuronal differentiation related signature that was characteristic of group 4 medulloblastomas. Thus mir-592 expression could contribute to the pathogenesis as well as the indolent nature of the group 4 tumors. On the other hand, MiR-204 was identified as a prognostication marker for accurate risk-stratification in Group 3, Group 4 medulloblastomas, based on the clinical correlation study done on an Indian cohort and an independent large western cohort. The tumor-suppressive effects of restoration of miR-204 expression accompanied by inhibition of autophagy in medulloblastoma cells indicates the therapeutic potential of miR-204 and autophagy inhibitors in the treatment of medulloblastomas. Further, inhibition of autophagy itself was shown to inhibit the invasion potential of the medulloblastoma cells, indicating the role of autophagy in medulloblastoma cell invasion for the first time. Thus, the study significantly contributed in understanding the biology of medulloblastoma.

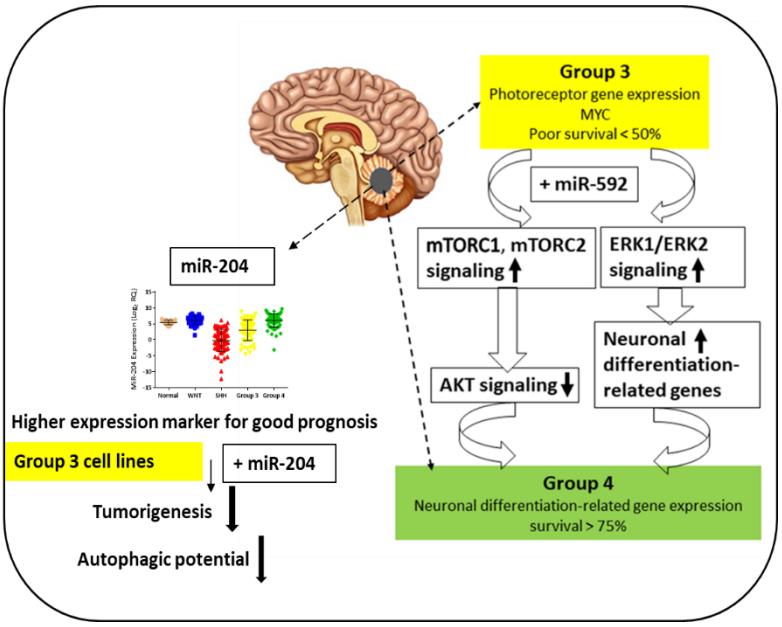

Figure 1: Role of miR-204 and mi592 in the disease pathogenesis of medulloblastoma